UNIVERSITE 8 MAI 1945 GUELMA
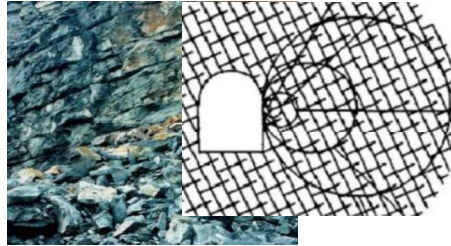جامعة 8 ماي 1945 قالمة

Faculté des Sciences et de la Technologie

Département de : **Génie Civil & Hydraulique**

Polycopié de cours

ROCK MECHANICS

Destiné aux étudiants en 2ème Année Master Spécialité Géotechnique

Elaboré par : Dr BENAMARA Fatima Zohra

Année 2024

Preface

Rock mechanics is a principal discipline for students pursuing a Master's degree, particularly in the field of Geotechnical Engineering. This course aims to provide an in-depth understanding of the mechanical behavior of rocks under external forces and environmental conditions.

The course support "Rock Mechanics" is intended for students of Master II specialized in Geotechnics. The content of the subject is developed in accordance with the official program of the Ministry of Higher Education and Scientific Research.

The document contains the information needed to perform practical calculations in terms of principles, methods, formulas, tables and abacuses. The handout covers all the chapters of the official program. The interested party is invited to explore the different concepts in more depth by consulting a bibliographic list provided at the end of the book.

At the end of the course, students will have acquired a good knowledge of the specificities of the field of rock mechanics and its applications; in particular, they will have been able to understand the determining factors in the design of structures carried out in rock masses.

They will also have acquired the basic notions of rock mechanics applied in the field of civil engineering. They will also have been able to acquire the practice of rock mass classification calculations and the pre-dimensioning of underground structures by the mperic and analytical methods (convergence-confinement). Finally, I will be grateful to the reader for his editorial corrections, his remarks, as well as his suggestions.

Table of Contents

Chapter II: Mechanical behavior of rocks and rock masses   39

Chapter III: Slope Stability   83

Introduction

The objectives of learning rock mechanics are essential for various engineering applications, particularly in fields such as civil engineering, mining, and geotechnical engineering. The first objective is to determine the properties of rocks and rock masses, including physical, mechanical, hydraulic, and thermal characteristics. This involves both laboratory testing of intact rock samples and field measurements of rock mass properties to inform engineering decision

Students learn to model and predict how rock masses will behave under different loading conditions associated with construction or excavation projects. This includes understanding stress distributions, deformation patterns, and potential failure mechanisms in rock masses

A significant aim is to apply knowledge of rock mechanics to design safe and effective engineering solutions. This includes developing support systems for tunnels, assessing slope stability, and ensuring the integrity of foundations built on or within rock

Students are trained to use various rock mass classification systems (like RMR and Q systems) which aid in evaluating the quality and stability of rock masses for different engineering applications

Understanding how rocks respond to excavation is essential for designing safe underground structures. Rock mechanics provides the tools to analyze and predict rock behavior under different conditions, including stress distributions and potential failure modes, which is crucial for maintaining stability during construction

In many underground scenarios, particularly in brittle rock, stress-driven failure processes can dominate behavior. Understanding these processes allows engineers to anticipate challenges such as shallow unravelling or strainbursting, which can complicate construction efforts and threaten safet

Knowledge of the rock mass behaviour in general, the failure process and the strengthin particular, is important for the design of all kinds of underground excavations.

One of the most common ways of estimating the rock mass strength is by using a failure criterion.

Rock mass classification is also useful because the variety of factors affecting rock behaviour can be accommodated in a mathematical expression, thus providing an index value for rock quality.

This Course handout provides guidance in the description and engineering classification of intact rock and rock masses, the types, applications and analyses of rock property tests, the evaluation of intact rock and rock mass properties, and the selection of design parameters for project structures founded on rock.

Rock mass characterization refers to the compilation of information and data to build a complete conceptual model of the rock foundation in which all geologic features that might control

the stability of project structures, as well as the physical properties of those features, are identified and defined.

Estimating rock mass strength using a failure criterion involves a systematic approach that integrates geological data, classification systems, and empirical relationships. The Hoek-Brown criterion serves as a practical tool for engineers to assess rock behavior under stress

Rock mass failure criteria are generally stress dependent and often include classification systems to represent the rock mass properties

The document is organized into four chapters presented as follows:

In the first chapter, we present the generalities on rocks such as the physical and thermal properties of rocks, the discontinuities of rock masses: typology, description and geometric representation of joints,

The second chapter describes the mechanical behavior of rocks as well as the failure criteria and the different methods of classification of rock masses according to the empirical methods "RQD, RMR, QS and GSI

The third chapter is devoted to the study of the stability of rock slopes, the failure modes, as well as the stabilization techniques.

The fourth chapter is devoted to the study of the stability of rock cavities and the analytical methods used in this context.

CHAPTER I

GENERAL INFORMATION ABOUT ROCKS AND ROCK MASSES

Chapitre I

General Information About Rocks and Rock Masses

I. 1 Introduction

Rock mechanics is a discipline that uses the principles of mechanics to describe the behavior of rocks. Rock mechanics is an interdisciplinary field that integrates principles from geology, engineering, and physics to address practical challenges related to rock behavior. Understanding these principles is essential for ensuring safety and efficiency in projects involving rock materials. By applying advanced testing methods and theoretical frameworks, engineers can make informed decisions regarding design and construction practices in rocky environments.

Rock mechanics is a crucial field within geomechanics that focuses on understanding the mechanical behavior of Rock mechanics is defined as the theoretical and applied science of the mechanical behavior of rock materials. It examines how rocks respond to stresses, strains, and other forces acting upon them. This includes understanding failure mechanisms, deformation characteristics, and the stability of rock structures

I.2 The main types of rocks

The study of the processes and phenomena of formation and erosion that constantly take place on the Earth's crust has led scientists to classify rocks into three large types. These three types of rocks are both very distinct but they are also very linked. Distinct by their mineralogical and physicochemical characteristics, and linked by their belonging to the same cycle of formation and transformation of rocks in the lithosphere.
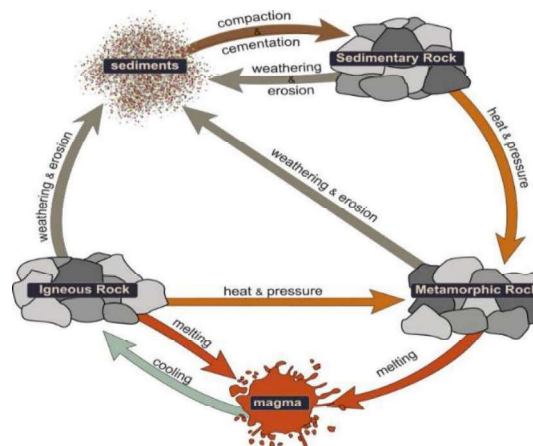
Figure I.1 *The rocks cycle[47]*

➢ Magma is at the origin of the formation of the Earth's crust by cooling, at the level of oceanic ridges, subduction zones, hot spots, etc.

> ➢ **The first phase of the cycle**: is made up of the cooling and crystallization of magma. We are talking about igneous rocks, which come from fire. When they are brought to the surface of the globe by internal geodynamic processes (plate tectonics, formation of mountain ranges, etc.), igneous rocks are quickly attacked by external geodynamic processes (erosion). Igneous rocks weather and disintegrate over time to give particles of different sizes.

> ➢ **The second phase:** the particles are transported and modified to be deposited in the form of loose deposits (soils, gravel, sand, mud, etc.). These sediments can consolidate over time under the accumulation of other sediments to gradually give rise to a more or less solid rock. This type of rock and these sediments form another type of rock called sedimentary rocks, "rocks that have been deposited".

> ➢ **The third phase:** under the effect of high temperature and pressure all types of rocks can change (chemical and mineralogical formula) to give rise to a third type of rocks called metamorphic rocks "rocks having changed shape". [38]

I.2.1 Igneous rocks

Igneous rocks come from the cooling or crystallization of magma as it escapes from the asthenosphere. We also speak of magmatic rocks. However, the cooling of magma depends on the conditions of the environment in which it takes place, at depth or on the surface. If cooling takes place slowly, i.e. in the depths of the lithosphere, it is called fractional crystallization.

I.2.1.1 Fractional crystallization [41]

he minerals that make up igneous rocks crystallize (solidify, freeze) at a range of different temperatures. This explains why cooling magma can have some crystals within it and yet remain predominantly liquid. The sequence in which minerals crystallize from a magma as it cools is known as **Bowen's reaction series** Igneous rocks can be divided into four categories based on their chemical composition: felsic, intermediate, mafic, and ultramafic. The diagram of Bowen's reaction series [42]
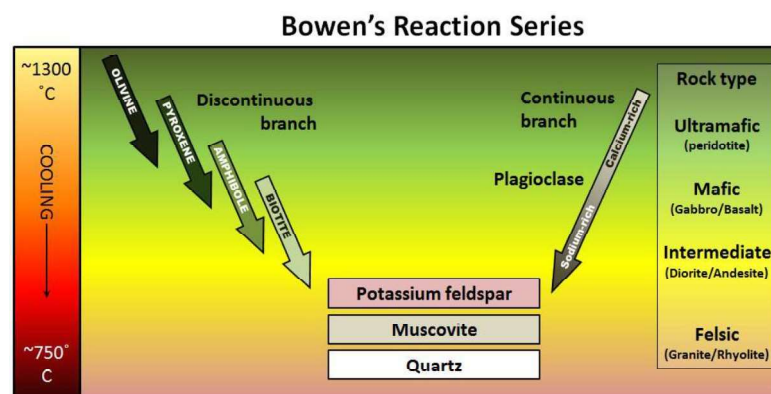
Figure I.2 *The Bowen sequence and the four corresponding types of igneous rocks.* [42]
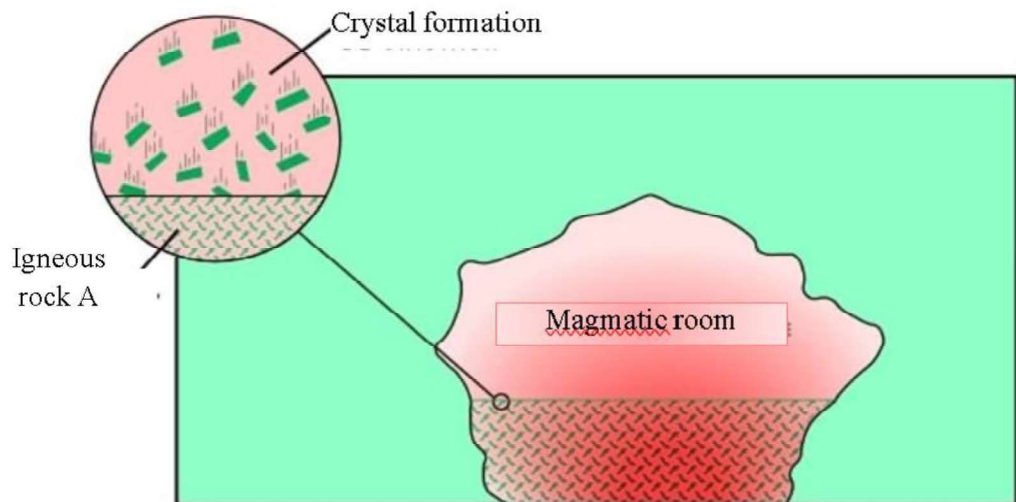
Figure I.3 Cooling of magma in a magma room, formation of magma minerals High temperature: mafic
or ultramafic rocks.[43]

According to Bowen's principle, the first crystals to form are those of high temperature, olivine first, pyroxenes and amphiboles second, these crystals will agglomerate and settle at the bottom of the chamber to form a rock rich in olivine, pyroxene and amphibole. We speak of mafic or ultramafic igneous rock depending on the proportions of the crystals present. A gabbro or a peridotite. The remaining liquid is then depleted of these minerals; It is a magma of a different composition from its initial composition, called intermediate composition.
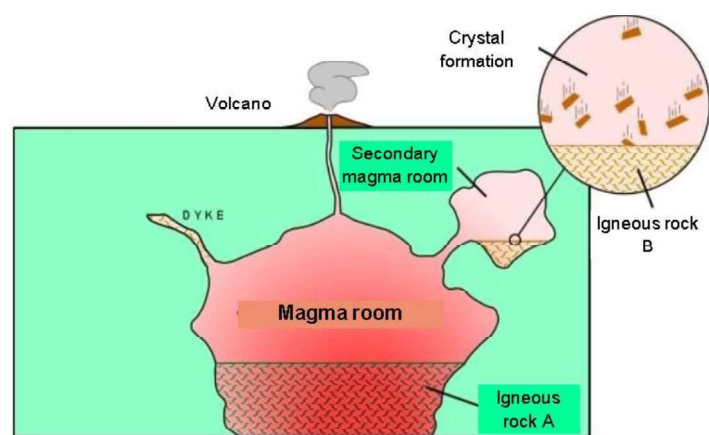
Figure I.4 Cooling of magma in a magma room; formation of intermediate-temperature minerals:
intermediate rocks. .[43]

In conclusion, we can see that one and the same magma gives rise to different mineralogical associations. That is, igneous rocks that differ depending on the cooling conditions.

I.2.1.2 Classification of Igneous Rocks

Igneous rocks are formed when magma cools and solidifies. They are classified by using grain size. Winch reflects the depth at which molten rocks form within the Earth. Classification of igneous rocks can be based on their predominant grain size. Three types of rock can be identified:

Extrusive igneous rocks: The magma (1200°C) arrives at the surface (20°C) of the lithosphereit cools very quickly: the crystals do not have time to form and develop. They are then microscopic or non-existent. The rock has a glassy appearance. This is called **VOLCANIC magma:** The rocks that come from this process are called: **EFFUSIVE MAGMATIC ROCKS or VOLCANIC ROCKS.** They are also called **EXTRUSIVE ROCKS**. They have cooled in the open air or under water; in the form of lava flows. Example of volcanic rocks: basalt, rhyolite, andesite... They are low in silica and rather dark in colour.

Intrusive igneous rocks (**PLUTONIC rocks**): cool very slowly before reaching the surface. They are found in the form of large masses called batholiths or thin veins such as and sills. These veins are formed when magma rises to the surface. Intrusions of igneous rocks can be concordant or discordant. The former fill in existing cracks or fractures in the rocks, unlike discordant ones which are so powerful that they cause new fractures. In summary, a simplified classification of igneous rocks is given in Table 1.1

Table I.1 simplified classification of igneous rocks .[43]

]	Intrusive	Extrusive
Other names given	Plutonic	Effusive Volcanic
Cooling speed	Slow	Fast
Cooling location	Inside the Earth	On the Earth's surface
Thickness of the crystals formed	Big	Small
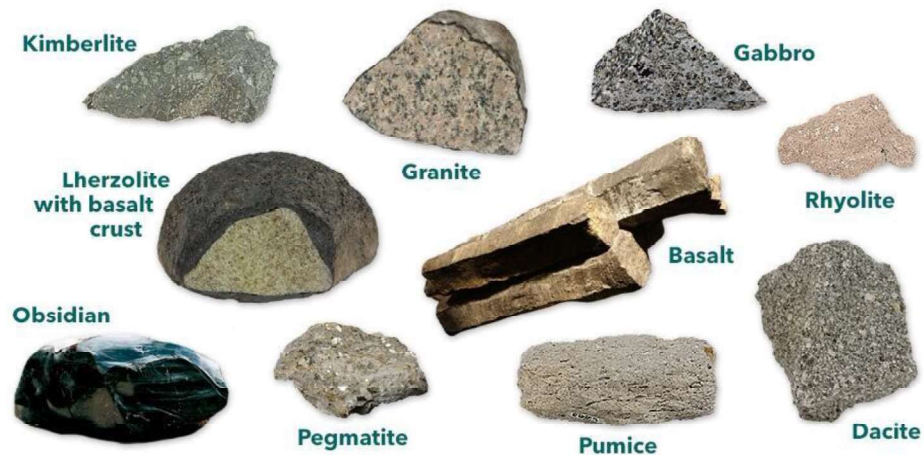
Figure I.5 Exemples of igneous rocks [43]

I.2.2 Sedimentary rocks

Sedimentary rock formed at or near Earth's surface by the accumulation and lithification of sediment (detrital rock) or by the precipitation from solution at normal surface temperatures (chemical rock). Sedimentary rocks are the most common rocks exposed on Earth's surface but are only a minor constituent of the entire crust, which is dominated by igneous and metamorphic rocks. Sedimentary rocks are produced by the weathering of preexisting rocks and the subsequent transportation and deposition of the weathering products. This complex process is composed of four main phases

a. production of particles: by erosion and surface alteration of crustal rocks,

b. transport of these particles: mainly by water, wind or ice

c. sedimentation and deposition: in a favourable environment for the formation of a sediment

d. diagenesis: physicochemical process (compaction, chemical cementation, biochemical cementation, etc.) that transforms powdery sediments into sedimentary rock. *.[43]*
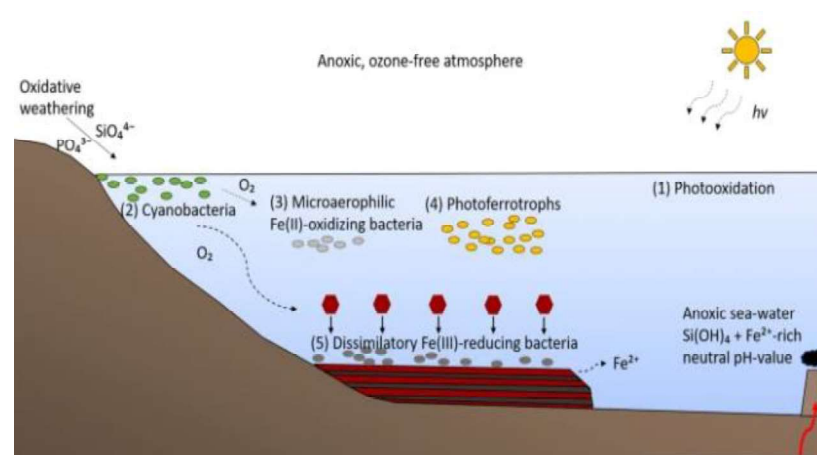
Figure I.6 The main phases of sedimentary rock formation [48]

I.2.2.1 Diagenesis

Diagenesis is the process that describes physical and chemical changes in sediments first caused by water-rock interactions, microbial activity, and compaction after their deposition. Diagenesis is the process by which sedimentary rocks are altered after they are deposited, but before they are buried and lithified (turned into rock). This process involves physical, chemical, and biological changes that can affect the mineralogy, texture, and other properties of the sedimentary rock. Diagenesis can occur at relatively low temperatures and pressures, usually within the upper few kilometers of the Earth's crust. It can involve a variety of processes, such as compaction, cementation, dissolution, recrystallization, and the formation of new minerals

 Sedimentary deposits can reach tens, hundreds or even thousands of meters of material. The processes of diagenesis are varied and complex: they range from the simple compaction of the sediment (under the effect of overload) to its cementation (by the addition of a natural binder), through phases of dissolution, recrystallization or replacement of certain minerals.

The diagenetic process that is primarily responsible for the transition from sediment to rock is cementation

> ➢ Cementation: This is a relatively simple process. The water that circulates in the voids of a sediment, for example sand, is supersaturated compared to certain minerals (carbonates). It precipitates these minerals which are deposited on the grains of sand and end up welding them together; A sedimentary rock is then obtained, which in this case is called a sandstone (limestone cement sand). Depending on the amount of minerals deposited, the degree of cementation can be low, so we have a friable rock. It can be very pushed, and we have a very solid rock.
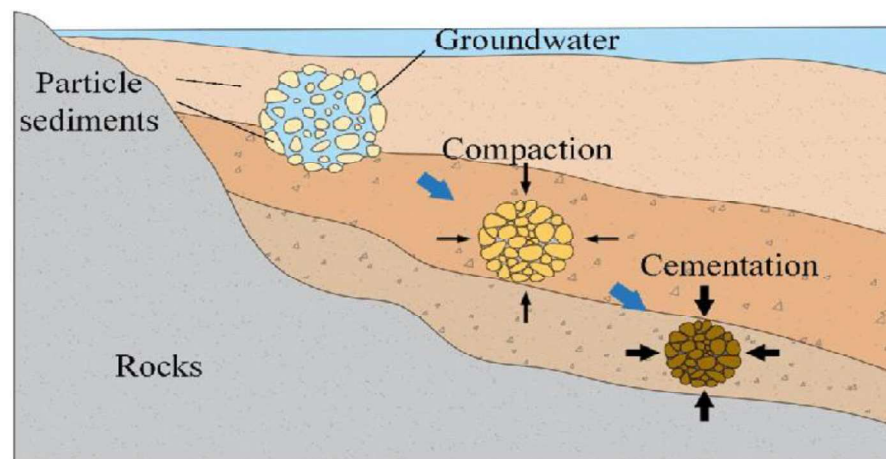
Figure I.7 Diagenesis process: cementation and compaction [49]

I.2.2.2 Classification of sedimentary rocks.

It is possible to classify sedimentary rocks into three main genetic classes:

Clastic sedimentary rock (also called 'detrital' sedimentary rock) consists of sediment pieces that come from weathered bedrock, cemented together to make a new rock.

a. Clastic (or detrital) rock is classified and named based on the size and composition of the clasts.

b. They form nearly 85% of all sedimentary rocks.

c. They are formed of mineral particles resulting from the alteration of pre-existing rocks.

d. They are generally classified according to the grain size of their constituents (conglomerates, sandstone, siltstone, argillite); [49]

Biochemical sedimentary rock is formed from shells and bodies of underwater organisms (such as coral). The living organisms extract chemical components from the water and use them to build shells and other body parts.

Biochemical sedimentary rocks are commonly composed of calcite, from a wide variety of sea life, or silica, largely from the single-celled microorganisms called radiolarian.

Organic sedimentary rock contains the remains of organic material that has undergone the lithification process. The source materials are plant and animal remain that are transformed through burial and heat, and end up as coal, oil, and methane (natural gas)

a. They constitute about 15% of sedimentary rocks.

b. In some cases, organisms use carbonates, phosphates, silicates to make their shells or bones and it is their remains that constitute sedimentary rocks.

c. Plants accumulate carbonaceous materials by photosynthesis and are directly responsible for charcoal.

d. Other types of carbonaceous sediments such as oil shales, petroleum, etc. are generated by bacteria.

Chemical sedimentary rock

Chemical sedimentary rocks form by chemical precipitation that begins when water traveling through rock dissolves some of the minerals. These minerals are carried away from their source and eventually redeposited, or precipitated, when the water evaporates away.

a. of relatively low importance (around 1%).

b. Chemical weathering contributes the dissolved ions in water that ultimately form the various rock types.

c. result from the precipitation (purely physico-chemical) of minerals in a supersaturated medium.

d. Evaporites (anhydrite, salt, gypsum, sylvite, …) are the best example: they are formed by the evaporation of brines (water very rich in salts);

I.2.2.3 Naming of sedimentary rocks

The naming of sediments and sedimentary rocks is based on two main criteria:

➢ Particle size,

➢ Mineralogical composition.

Particle size (in terrigenous and allochemical animals is used as a classification criterion. Two sizes are important to remember: 0.062 and 2 mm (Table I.2).

Table I. 2 *Naming of sedimentary rocks[46]*

Figure I.8 *Exemples of sedimentary rocks [45]*

I.2.3 Metamorphic rocks

Metamorphic rocks are the result of the transformation of rocks (igneous or sedimentary) under the effect of temperature T and/or high pressures P. Two main types of metamorphisms exist:

a) Contact metamorphism

b) Regional metamorphism

I.2.3.1 Contact metamorphism

When magma at a temperature above 1200°C comes into contact with the rocks of the lithosphere (cold), Contact metamorphism is the one that occurs in the host rock in a aureole in contact with intrusive magma. When the introduced magma is still hot in a sequence of cold rocks, there is heat transfer (arrows) and cooking of the host rock on the contact limit. The width of the aureole is a function of the size of the intrusive mass varying from a few millimeters to several hundred meters, even going a few kilometers in the case of a very large intrusive mass.
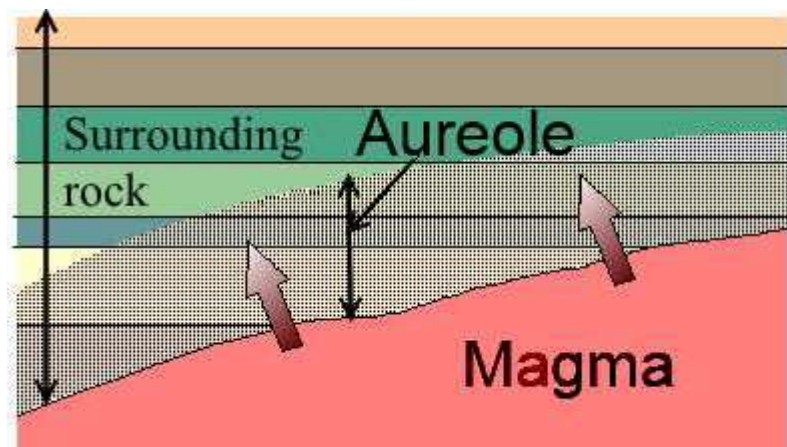
Figure I.9 *Contact metamorphism [52]*

I.2.3.2 Regional metamorphism

Regional metamorphism is a geological process that alters large volumes of rock under conditions of high temperature and pressure, typically occurring deep within the Earth's crust. This type of metamorphism is most commonly associated with convergent plate boundaries, where tectonic forces cause significant burial and deformation of rocks, often leading to the formation of mountain ranges. Regional metamorphism produces three major transformations:

Conditions: The process involves a combination of heat, pressure, and fluids acting on pre-existing rocks (protoliths), resulting in significant changes in mineralogy and texture.[49]

Foliation: The intense directed pressures lead to the development of foliation, a texture characterized by the alignment of platy minerals. Common examples include slate, schist, and gneiss. The diagram below shows how mountains are built when continents collide.
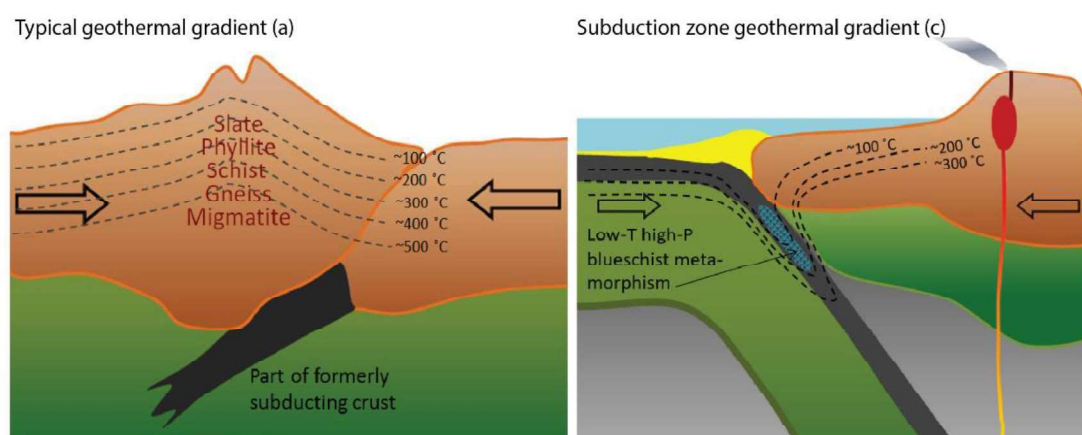
Figure I.10 *Building. Mountains [49]*

Prentice HallIn the "roots" of the mountain belt, rocks may be buried to depths of 20 km or so. They get very hot (500oC or more) and so re-crystallise to form new minerals and textures. Rocks metamorphosed

at depth may later be pushed up along faults, bringing them closer to the surface. As the mountains are eroded away by glaciers and rivers, these rocks become exposed for us to see.

In quantitative terms, metamorphic rocks of regional type are much more important than those of contact type.
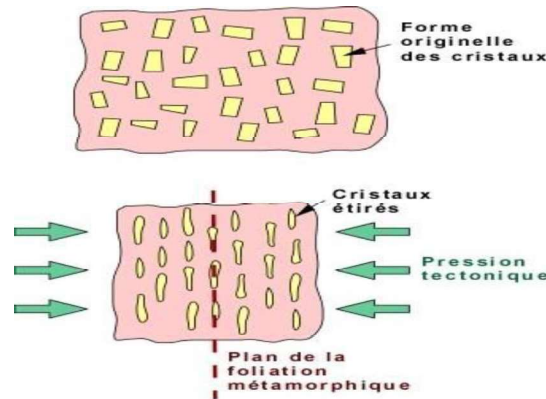
Figure I.11   Metamorphic foliation [43]

I.2.3.3 Naming of metamorphic rocks

As a result of the metamorphism that rocks undergo, specific minerals develop at each degree of metamorphism. These minerals are therefore used as indicators of the degree of metamorphism undergone by the rock studied.

These minerals can tell us, for example, about the conditions of T and P that existed during the formation of the rock. And from there, deduce the depth at which it was found. In the same way as for igneous and sedimentary rocks, metamorphic rocks have been given a name. Figure I.12 below shows the original rocks (left) and the result of their metamorphism (right) as well as the degree of metamorphism (arrows were drawn from it).
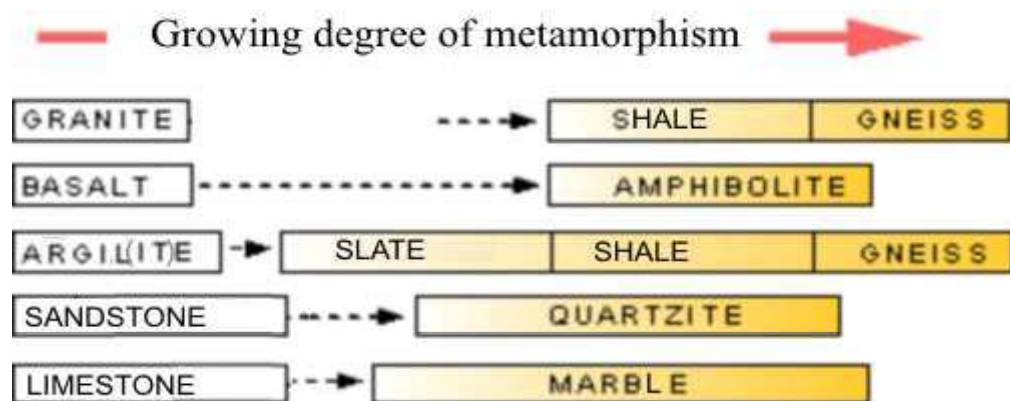
Figure I.12 Naming of the metamorphic rocks (left: rock of origin; right: resulting metamorphic rock. Length of the arrow = degree of metamorphism) [43]

Figure I.13 *Exemples of metamorphic rocks [39]*

I.2.4 Loose Rocks

Loose rocks refer to fragmented or unconsolidated materials found on the surface of the earth or within geological formations. Loose rocks are independent grains, resulting in rocks with some instability on slopes, as well as high porosity but variable permeability. The size of these rocks is between 0 and 125 mm (sand and gravel), which allows its use in the construction of roads and buildings.

The initial stage in the formation of loose rocks involves the weathering of solid rock into smaller fragments. This can occur through various means:

I.2.4.1 Physical Weathering

Processes such as freeze-thaw cycles cause water to seep into cracks in the rock. When temperatures drop, the water freezes and expands, exerting pressure that can fracture the rock further

I.2.4.2 Chemical Weathering

Chemical reactions, including those caused by acid rain or biological activity (such as lichen growth), can dissolve minerals and weaken rock structures, contributing to fragmentation

I.2.4.3 Transport and Accumulation

Once broken down, these fragments are transported by gravity, water, wind, or ice to lower elevations where they accumulate. This process is termed **sedimentation**, which is essential for forming sedimentary rocks from loose material

I.2.4.4 Consolidation

Over time, as more material accumulates, the weight of overlying debris compresses the lower layers. This process leads to **compaction** and eventual cementation, transforming loose sediments into solid sedimentary rocks

Figure I.14 *Loose Rocks [50]*

I.2.4.5 Soft rocks and hard soils

Sedimentary rocks are formed from sediments (soils) through a long process of compaction and cementation. The process can be stopped before the sediment has been completely solidified. The materials could then be strongly consolidated, but not fully solidified.

Typically, these materials have low strength and high deformability, and when placed in contact with water, they can often be dissolved. Once dry, they behave like a weak rock and in the water they collapse. Depending on the degree of solidification, such materials can be described and treated accordingly, with the principles of soil mechanics or the principles of rock mechanics.

I.2.4.6 Swelling rock

Some rocks have the power to swell; when exposed to water, they swell. This is mainly due to the swelling behaviour of the minerals making up the rock, typically the clay mineral montmorillonite. Rocks and soils that contain a high amount of montmorillonite minerals will have swelling and shrinkage characteristics. In practice, swelling is a complex problem that is likely to produce excessive deformations when the rock is exposed to it.[21]

I.2.4.7 Fractured and crushed rock

Due to the different geological processes, rocks can be highly fractured and sometimes crushed. The characteristics of fractured and crushed rocks are quite different from those of massive rocks. They behave like granular materials or in the form of blocks whose mechanical properties depend on their geometry and friction. When such materials are encountered in construction, they must be considered separately.

Figure I.15   Examples of highly fractured and crushed rocks[21]

I.3 Physical properties of rocks

Rocks possess various physical properties that are essential for understanding their behavior in geological processes and engineering applications. The physical properties of rocks are density, specific gravity, water content, degree of saturation, porosity, and pore number. Whereas mechanical properties are obtained from destructive testing. Mechanical properties obtained from laboratory testing include compressive strength and tensile strength tests.

I.3.1 General appearance of rocks

The general appearance of rocks is characterized by several key features that reflect their formation processes and mineral content. These features include texture, color, grain size, and structure, all of which provide insights into the rock's history and classification.

I.3.1.1 Texture

Rock textures describe the size, shape, and arrangement of mineral grains or crystals within a rock, which can provide valuable information about the rock's history and formation process. Texture describes the physical arrangement and size of mineral grains within a rock. It can be classified into several types:

- Phaneritic: Large, visible crystals typical of intrusive igneous rocks, indicating slow cooling (e.g., granite) [40].

- Aphanitic: Small crystals that are not visible to the naked eye, common in extrusive igneous rocks formed by rapid cooling (e.g., basalt) [25].

- Porphyritic: A mix of large and small crystals, suggesting a complex cooling history where some minerals crystallized before the rest (e.g., porphyritic andesite)[41].

- Glassy: Lacks a crystalline structure, resulting from extremely rapid cooling (e.g., obsidian), which often appears smooth and shiny .

- Vesicular: Contains numerous gas bubbles, giving it a spongy appearance (e.g., pumice) [40].

I.3.1.2 Color

Though many rocks are some shade of gray, some rocks can be very colorful. The color of a rock is determined by its chemical composition. For example, the green in some rocks comes from the presence of minerals such as chlorite, while the red in other rocks comes from the presence of minerals such as hematite. Rocks can also be a combination of colors, while some may even change color when exposed to the air or when heated.[5]

Color is influenced by the mineral composition of the rock. For instance:

- Igneous Rocks: Can range from light-colored (granite) to dark-colored (basalt), depending on the presence of minerals like quartz or olivine.

- Sedimentary Rocks: Often display layered colors due to different sedimentation processes; for example, sandstone can show variations based on its mineral content [27].

-Metamorphic Rocks: May exhibit banding or foliation due to pressure and temperature changes, often resulting in streaks of different colors (e.g., gneiss) .

Other examples of igneous rocks along with their features are listed below in the table:

Table I.3 *Examples of igneous rocks along with their features* [27].

Rock Name	Colour	Texture
Diorite	Medium coloured	Course
Rhyolite	Light coloured (pastel)	Pastel
Obsidian	Dark coloured	Glass
Tuff	Fine-grained ash	Ash particles

I.3.1.3 Grain Size

Grain size provides critical information about the cooling history and environment of formation:

- Coarse-grained: Grains are large enough to be seen without magnification, indicating slow cooling (e.g., diorite)[42].

- Medium-grained: Grains are visible but smaller than coarse grains (e.g., some sandstones) .

- Fine-grained: Grains are microscopic, typical of rapidly cooled volcanic rocks .

I.3.1.4 Structure

The structure refers to larger-scale features that may be visible in hand specimens or outcrops:

- Bedding: Layers found in sedimentary rocks that reflect deposition over time [26].

- Foliation: A planar arrangement of mineral grains in metamorphic rocks due to directed pressure.

I.3.1.5 Coherence of Rocks

Coherence in the context of rocks refers to the physical and chemical properties that allow different mineral particles to bond together, forming a solid mass. This concept is important in geology, engineering, and environmental science, as it influences the strength, stability, and behavior of rock materials. A rock is coherent if the elements that make it up are related to each other. You can't separate them with your fingers.

I.3.1.6 Hhardness

Hardness in rocks is a property that indicates their resistance to scratching and abrasion. This property is commonly assessed using the Mohs Scale of Hardness, developed by the German mineralogist Friedrich Mohs in 1812. The scale ranks ten minerals from softest to hardest, providing a relative measure of hardness based on scratch resistance. the hardness of a rock is estimated by comparing it to that of other materials. Talc is the softest mineral with a hardness of 1. It can be easily scratched with a fingernail. Gypsum is a little harder with a hardness of 2 and can be scratched with a copper penny. And calcite is harder still with a hardness of 3 and can be scratched with a knife blade.

At the other end of the scale, diamond is the hardest mineral, with a hardness of 10. It can only be scratched by another diamond.

So, depending on the rock's chemical composition and texture, its hardness can range from very soft to very hard. Metamorphic rocks are hard, sedimentary rocks are much softer, and igneous rocks can be either hard or soft depending on their composition.
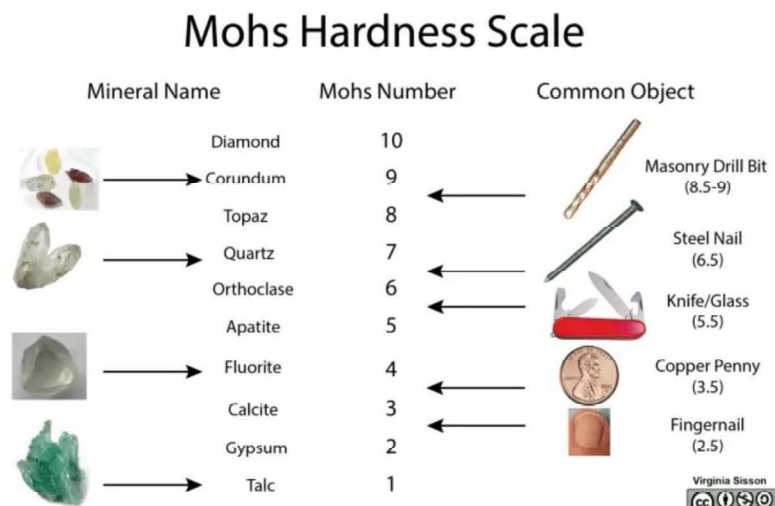
Figure I.16 *Relative Hardness Scale of Minerals, Mohs Scale [28]*

I.3.1.7 Luster

Luster is the way a rock's surface reflects light and is an important characteristic for identifying a rock. Rocks can have two types of luster: metallic and non-metallic.

Metallic luster is shiny and looks like metal. Non-metallic luster is duller and can range from being pearly to looking like glass.

Most rocks have a non-metallic luster, but some, like gold and silver, have a metallic luster. [5]

I.3.1.8 Streak

The streak of a rock is its color in powder form. It is obtained by scratching the rock on an unglazed porcelain plate and rubbing the resulting powder on a white tile. The color of the powder is then compared to a chart of streak colors.

Surprisingly, two rocks can have the same color but different streak colors. For example, a rock that is green in color may have a white or pale green streak.

I.3.1.9 Cleavage

A rock's cleavage is the way it breaks when struck. Some rocks have a well-defined cleavage, while others do not. Cleavage is determined by the arrangement of atoms in a rock's crystalline structure. When a rock has a well-defined cleavage, it means that its atoms are arranged in sheets that can easily slide past each other.

Rocks with a well-defined cleavage will break along these sheets, resulting in smooth, flat surfaces. Rocks without a well-defined cleavage will break in an irregular pattern.

One way to test for cleavage is to strike the rock with a hammer and observe the shape of the resulting pieces.

Cleavage in one direction. Example: MUSCOVITE

Cleavage in two directions. Example: FELDSPAR

Cleavage in three directions. Example: HALITE

Cleavage in two directions. Example: CALCITE
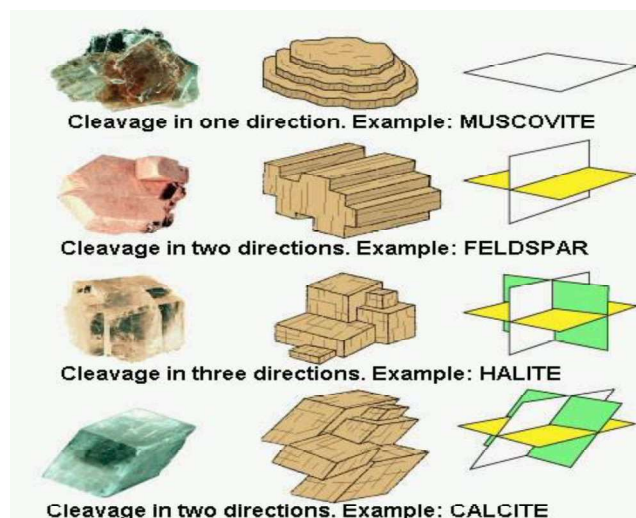
Figure I.17 *Cleavage planes [29]*

I.3.2 Physical propreties of Rocks

I.3.2 .1 Phase relationships

Rocks like soils are three phase materials. They consist of solid particles such as grains and crystals with void space in between. The void space can be occupied by air or water or both. As for soil, the components of a rock can be represented by a phase diagram and several parameters can be defined such as porosity, specific gravity, water content, degree of saturation and density.

- **Density**

Density is a critical property defined as the mass per unit volume of a rock, typically expressed in grams per cubic centimeter (g/cm³) or kilograms per cubic meter (kg/m³). The density of rocks varies significantly depending on their mineral composition and porosity:

- **Bulk Density**: This is the overall density of the rock, including both solid material and pore spaces. It can be affected by the presence of fluids in the pores. The bulk density, ρ is equal to

$$\rho = \frac{(M_w + M_s)}{V} \qquad (I.1)$$

For rocks, the bulk density varies between 2.5 and 3.0 g/cm³. Values for different rock types. In general, low density rocks are highly porous. The dry density ρ_d is the value of the bulk density when the rock is dry, i.e. Mw =0 (Sr =0%). On the other hand, when the rock is saturated (Sr =100%), the bulk density is defined as ρ_{sat}. The following relationships exist between densities and other physical properties introduced before:

$$\rho_d = (1 - n).\rho_s = (1 - n).G_s.\rho_w \qquad (I.2)$$

And

$$\rho_{sat} = \rho_d + n.\rho_w \qquad (I.3)$$

Typical density ranges for common rock types are as follows:

Granite: 2.63 - 2.75 g/cm³

Limestone: 1.55 - 2.75 g/cm³

Shale: 2.06 - 2.67 g/cm³

Sandstone: 2.00 - 2.60 g/cm³

- Porosity

Porosity is defined as the ratio of the volume of voids (pores) to the total volume of the rock, expressed as a percentage. It indicates how much fluid a rock can hold and significantly influences its density and mechanical behavior: The porosity, n, (expressed in percent) is defined as follows [5]

$$n = \frac{V_v}{V}.100\% \qquad (I.4)$$

It represents the relative proportion of solid grains and voids in the rock. It is also a measure of the interconnected pore space. Note that the pore phase may not be completely continuous in a rock and fluid may not permeate to all the pores.

The apparent porosity is the measure of the volume of interconnected pores and cracks linked to the external surface of the rock. On the other hand, the total porosity is a measure of the volume of all the cracks and

pores and includes those interconnected to the external surface and those having no connection to the external surface of the rock. Porosity values for different rock types are given in Table I.4

Porosity is generally low for crystalline rocks, e.g., granite (<5%) and can be high for clastic sedimentary rocks, e.g., sandstone (up to 50%). Porosity affects permeability.

The porosity is of the order of one hundredth for some marbles and quartzites, one tenth for many sedimentary rocks, and it can reach 0.5 for some chalks and tuffs.

***TablI I.4** Porosities for Different Rock Types*

Rock Type	Porosity %
Granite	0.4-4.0
Andesite	0.1-11
Gabbro,Diorite, Diabase	0.1-1.0
Basalt	0.2-22
Limestone	0.2-4.4
Sandstone	1.6-26
Chert	4
Gneiss	0.3-2.2
Marble	0.3-2.1
Quartzite	0.3-0.5
Slate	0.1-1.0

Total Porosity: This includes all pore spaces within the rock.

Effective Porosity: This considers only interconnected pores that contribute to fluid flow.

Porosity values can range widely among different rock types:

Sandstone: Up to 30% or more

Shale: Typically, lower, around 8% to 20%

Limestone: Varies widely depending on composition and cementation

- **Permeability**

Permeability is a measure of a material's ability to transmit fluids. It is obtained by Darcy's law, demonstrated by a very simple experiment in which Darcy showed that the volume flow **Q** through a sand column of length **L** is proportional to the section **A** of the column and to the hydraulic load gradient **Δh/L**. The hydraulic head h (or piezometric height) is a function of the altitude *z*, the fluid pressure **P**, the density of the fluid ρand the gravity **g**.

$$\frac{Q}{S} = \frac{k\Delta h}{L} \quad with \quad h - z + \frac{P}{\rho g} \qquad (I.5)$$
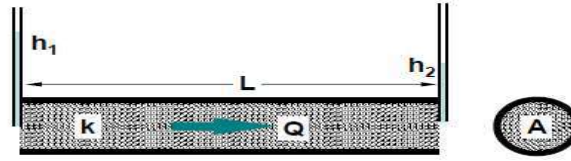
The proportionality factor k is called the coefficient of permeability or hydraulic conductivity. The dimension of k is that of a velocity (m/s).

Permeability is homogeneous to a surface: its SI unit is therefore m2. In practice, the Darcy is often used as a unit, with the equivalence 1 *Darcy* = 0.987 10 ^{12} m2. By comparison we see that $k = (\rho g/\mu)k$ and therefore for water at 20°C, we have the following correspondence 1 *Darcy* = 0.96 10^{-5} m/s.

Most rocks have very low permeabilities. The permeability of the rock is governed by porosity. Porous rocks such as sandstone usually have high permeability while granites have low permeability. Except for porous rocks, the permeability of frequently encountered rocks is very low, in the order of 10^{-10} to 10^{-12} m/s, exceptionally up to 10^{-5} m/s for very porous rocks. If the discontinuities are open and empty, and the flow regime is laminar, fluid mechanics can estimate the permeability coefficient kf

$$k_f = \frac{\gamma e^2}{12\mu} \tag{I.6}$$

With γ and μ the density weight and viscosity coefficient of the liquid, and the thickness of the fracture.

- **Hardness and Abrasiveness**

Hardness is the characteristic of a material to resist permanent deformation. The hardness of the rock depends on several factors, including mineral composition and density. A typical measurement is the Schmidt rebound hardness number. Schmidt hardness can be correlated with the strength of the rock.
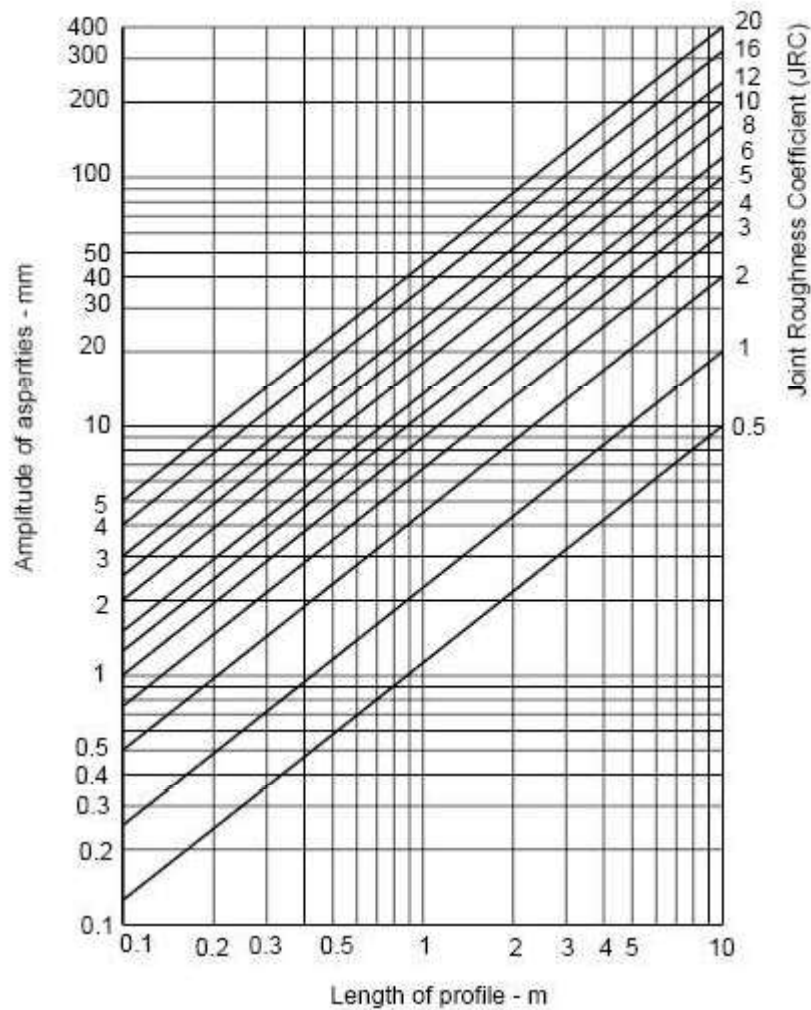
Figure I.18 Alternative method for estimating *JRC* from measurements of surface roughness amplitude from a straight edge [5]

Abrasiveness measures the abrasion of rock compared to other materials, e.g. steel. The abrasiveness is strongly influenced by the percentage of quartz in the rock. A high quartz content leads to greater abrasiveness. Abrasiveness is measured by tests, e.g. the Cerchar test which gives the Cerchar Abrasiveness Index (CAI).

Table I.5 *Cerchar Abrasiveness Index (CAI) [5]*

Granite	4.5 – 5.3
Diorite	4.2 – 5.0
Andésite	2.7 – 3.8
Basalte	2.0 – 3.5
Grès	1.5 – 3.5, 2.8 – 4.2
Schiste argileux	0.6 – 1.8
Calcaire	1.0 – 2.5
Gneiss	3.5 – 5.3
Ardoise	2.3 – 4.2
Quartzite	4.3 – 5.9

I.4 Acoustic properties of rocks

The characterization of rock materials by ultrasonic methods is commonly used. The study of the propagation of compression and shear waves in a dry and saturated material makes it possible to evaluate the physical properties of the material such as its porosity, its cracking state and its elastic properties (Young's modulus, Poisson's ratio). The analysis of ultrasonic signals in terms of attenuation was mainly exploited en physique des roches pétrolière.

This parameter is particularly interesting for the analysis of the anisotropy of a material, either structural or related to microcracking. Classical rock physics is concerned with the propagation of Pet S volume waves, characterized by their velocities (first and second, depending on the order in which they are received) and their attenuation. For a P wave, the vibratory movement takes place along the direction of propagation and affects the volume of the rock. Vp is therefore the speed of a compression wave (or longitudinal wave). Vs is the velocity of a shear wave (or shear wave), whose vibratory motion takes place in a plane normal to the direction of propagation. They are slower than P waves and do not propagate in water.

Since Vp and Vs are expressed as a function of the Lamé coefficients, the measurement of the propagation time of an ultrasonic wave in a rock makes it possible to go back to the elastic modulicities. In the case of an isotropic material, the calculation of the Poisson's ratio υ and the Young's modulus E is as follows:

The wave velocity is related to the degree of compactness (density and porosity) of the rock. Well-compacted rock usually has a high velocity as long as the grains are in contact and the waves can pass through the solid grains. [(]

The P wave velocity of igneous rocks, gneiss and quartzite is 5000-7000 m/s, for shales, sandstone and conglomerates, the velocity is 3000-5000 m/s.

Since Vp and Vs are expressed as a function of the Lamé coefficients, the measurement of the propagation time of an ultrasonic wave in a rock makes it possible to go back to the elastic modulicities. In the case of an isotropic material, the calculation of the Poisson's ratio ν and the Young's modulus E is as follows:

Module élastique Es = ρv_p^2 (GPa), (g/cm^3), (km/s)

$$E = \rho \frac{Vp^2(1+v)(1-2v)}{(1-v)}$$ (I. 7)

Shear modulus Gs = ρv_s^2 (GPa), (g/cm^3), (km/s)

Coefficient de Poisson

$$v = \frac{1/2-\left(V_s/V_p\right)^2}{1-\left(V_s/V_p\right)^2}$$ (I. 8)

The Vp/Vs ratio is interesting to use and allows a clear distinction between sandstone and limestone, because the Poisson's ratio of calcite is very different from that of quartz.

***Table I.6** Physical and mechanical properties of the main minerals [23]*

Minéraux	ρ_s (g/cm^3)	E (GPa)	v	Vp (m/s)
Quartz	2,65	96,4	0,08	6 050
Olivine	3,2-3,6	216	0,24	8 770
Augite	3,2-3,6	14 3	0,24	7 330
Amphibole	2,9-3,2	110	0,29	6 800
Muscovite	2,7-3	80	0,25	5 880
Biotite	2,8-3,1	67	0,30	5 360
Orthose	2,5-2,6	63	0,29	5 680
Plagioclase	2,6-2,8	77	0,29	6 220
Magnétite	4,4-5,2	218	0,19	7 410
Calcite	2,7	84	0,28	6 320
Dolomie	2,8-3,1			7 900
Halite	2,1-2,6	36		4 320
Gypse	2,3-2,4			5 200

I. 4.1 Degree of fissuring

The degree of intact rock fissuring can be characterized through direct observation using the microscope. It can also be characterized through simple tests such as measurement of sonic velocity or permeability. Permeability will be discussed in another set of lecture notes. The sonic velocity method (or pulse method) consists of propagating waves in intact samples of rock. Transmitters and receivers transducers and an oscilloscope are used to measure the time that longitudinal and transverse elastic waves propagate through an intact rock sample

As discussed by Goodman [23], if we know the mineral composition of the rock, the theoretical longitudinal velocity V_l* that the sample would have without fissures and pores can be written as

$$\frac{1}{V_l^*} = \sum_{i=1}^{N} \frac{C_i}{V_{il}}$$ (I. 9)

where N is the number of mineral constituents in the rock, V_{il} and C_i are the theoretical longitudinal velocity and concentration of the ith mineral. Values of V_{il} for some common minerals are given in Table I.6 .

The ratio between the measured value Vl and the theoretical value $V_l *$ can serve as an index to describe the degree of rock fissuring

$$I_f = \frac{V_l}{V_l^*} \, . \, 100\%$$ (I. 10)

The degree of fissuring is affected by the temperature

I.4.2 wave propagation in an elastic medium

Classical rock physics is concerned with the propagation of P-volume waves and S, characterized by their velocities (first and second, according to the order of them

The velocity of the P waves varies with the **porosity** of the pores, but decreases even more sharply with the porosity of the cracks. To estimate the relative share of pore porosity or crack in rocks of different lithology,

the **continuity index IC** is used, defined as the ratio of the wave velocity P measured in the sample to the wave velocity calculated Vp^* from the mineralogical composition. Vp^* is the weighted arithmetic average of the Vi-wave velocities of each mineral constituting the rock, the weighting coefficients being the contents **ci** of the rock in each mineral:

$$IC(\%) = 100 \frac{V_p}{V_p^*} \ avec \ V_p^* = \sum c_i x V_i \tag{I.11}$$

We can write according to the porosity of the pore's np and the porosity of the cracks n_f:

$$IC = 100\left(1 - A \, n_p - B \, n_f\right) \ avec \ n_f + n_p = n_{totale} \ et \ n_f \ll n_p \tag{I.12}$$

In the case of exclusively porous rocks (ntotal=np), there is an experimental relationship between the continuity index IC = ICp and the porosity n:

$$IC_p = 100\left(1 - 1 - 1,4 \, n_p\right) \tag{I.13}$$

In the most common case of a porous and fissured rock, the total porosity n total is approximately equal to np, which makes it possible to evaluate what the value of the ICp continuity index of the porous medium corresponding to the rock would be if it were affected only by pores:

$$IC_p = 100(1 - 1,4 \, n) \tag{I.14}$$

The difference between the value of the measured continuity index IC and this ICp value corresponds to the existence of cracks; it is expressed in a relative way by the Degree of Cracking DF:

$$DF = 1 - \frac{IC}{IC_p} \tag{I.15}$$
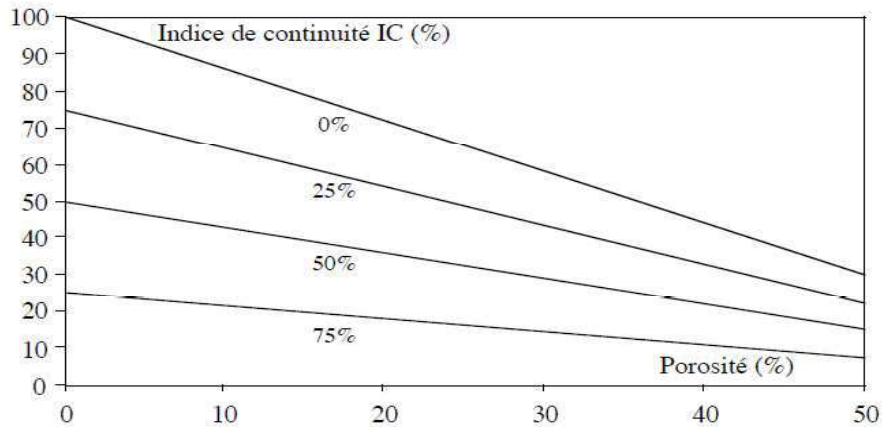
Figure I.19 Determination of the degree of cracking with the continuity index [23]

So, any rock, regardless of its porosity n, can be affected by a degree of cracking varying between 0 and 100%, with DF expressed in percent. In the plane (IC-Porosity), the lines of equal value of the degree of cracking form a bundle (figure) located below the line of the uncracked media. It is therefore possible, from the measurement of the porosity, the velocity of the Vp waves, and the calculation of the IC continuity index, to estimate the cracking density of a rock.

I. 5 Properties of rock discontinuities

Properties of rock discontinuities govern the overall behaviour of the rock masses. Rock discontinuities include joints, fractures, faults and other geological structures. Rock joints are by far the most common discontinuity encountered in rock masses. Rock fractures are random features. Rock faults and folds are major but localised geological structures and therefore are dealt individually.

I.5.1 Geometrical Characteristics of Rock Joints

I.5.1.1 Joint Sets and Length: Joints and Fractures, Set Number, and Persistence

As discussed early in the chapter dealing with rock formation, joints are generally in sets, i.e., parallel joints. The number of joint sets can vary from 0 to as many as 5 (Table I.7). Typically, one joint set cuts the rock mass into plates, two perpendicular sets cut rock into column and three into blocks, and more sets cut rocks into mixed shapes of blocks and wedges, as shown in Figure I.20

Table I.7 ISRM suggested description of joint sets [1]

I	Massive, occasional random fractures
II	One joint set
III	One joint set plus random fractures
IV	Two joint sets
V	Two joint sets plus random fractures
VI	Three joint sets
VII	Three joint sets plus random fractures
VIII	Four or more joint sets
IX	Crushed rock, earth-like
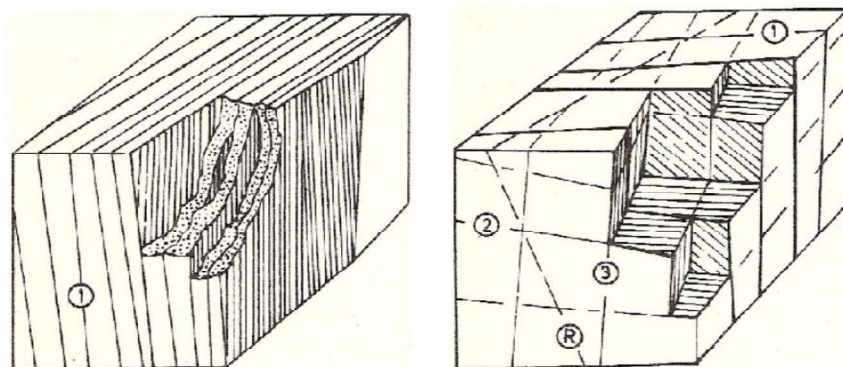
Figure I.20   Rock masses showing one and three joint sets

Rock mass quality is influenced by the number of rock fractures and they are usually considered in the overall degree of fracturing of a rock mass, in term of joint spacing and RQD,

Persistence is the areal extent or size of a discontinuity, and can be crudely quantified by observing the trace lengths of discontinuities on exposed surfaces. The persistence of joint sets controls large scale sliding or 'down-stepping' failure of slope, dam foundation and tunnel excavation. Figure *I.21* gives diagrams showing persistence of various joint sets, while Table 6 presents the classification of persistence commonly adopted.

Table 8 ISRM classification of discontinuity persistence [46]

Description	Surface Trace Length (m)
Very low persistence	< 1
Low persistence	1 – 3
Medium persistence	3 – 10
High persistence	10 – 20
Very high persistence	> 20
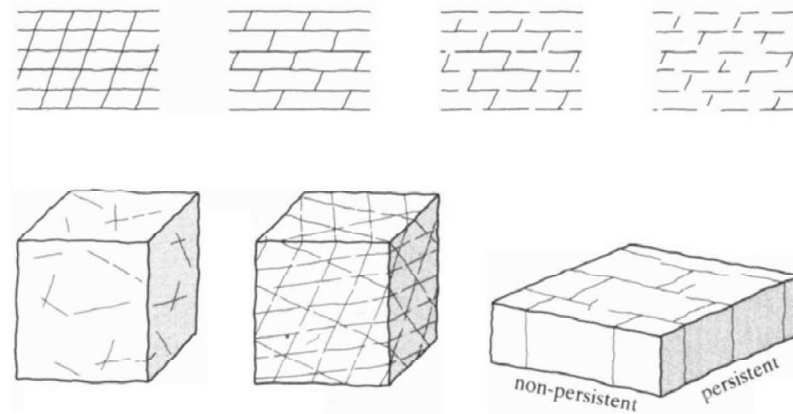
Figure I.21   Sketches indicating persistence of various joint sets [9]

I.5.1.2 Joint Orientation

Orientation of a discontinuity is described by its dip and dip direction or its dip and strike. The orientation of major joint set relative to an engineering structure largely controls the possibility of unstable conditions or excessive deformations developing. The mutual orientation of discontinuities will determine the shape of the individual blocks and beds comprising the rock mass.

Orientation of a plane is measured by the degree of inclination and the direction of facing of the plane. It does not fix its position. Therefore, two parallel planes have the same orientation. In rock mechanics and engineering geology, the orientation of a plane is generally defined by dip angle (inclination), dip direction (facing) or strike (running), as illustrated in Figure I.22. *[1]*
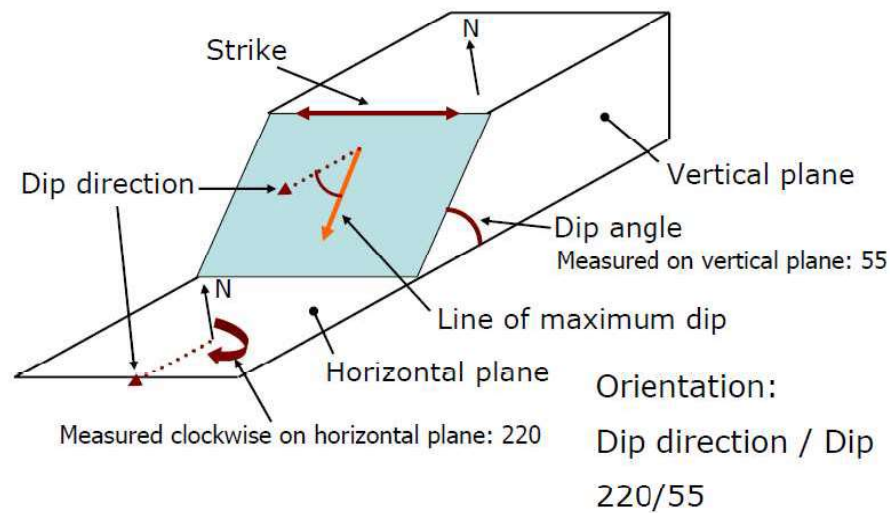
Figure I.22   Representation of joint plane orientation [2]

Dip or dip angle represents the degree of inclination. It is the acute angle between the plane and the horizontal plane. It is also the acute angle between a line with maximum dip in the inclined plane and its horizontal projection. Dip angle is generally expressed by an acute angle between 0° and 90°.

Dip direction represents the facing direction. It is the bearing measured clockwise from the north (0°) of the line with maximum dip in the inclined plane. Dip direction is generally expressed by a direction angle of 0° to 360°.

Dip direction and strike direction are always perpendicular. In rock mechanics, dip direction/dip format is generally used, e.g., 210/35, or 030/35, where dip directions always have 3 digitals. Sometime, when strike is used instead of dip direction, the general direction of plane dip must be given, otherwise, it could mean two possible planes, e.g., dip/strike 120/35 would be either dip direction/dip 210/35, or 030/35.

Therefore, correctly it should be presented as strike/dip 120/35SW which is the plane in dip direction/dip 210/35, or 120/35NE which is the plane in dip direction/dip 030/35.

I.5.1.3 Joint Spacing: Joint Spacing, Frequency, Block Size, and RQD

The spacing of adjacent joints largely controls the size of individual blocks of intact rock It controls the mode of failure. A close spacing gives low mass cohesion and circular or even flow failure. It also influences the mass permeability. Joint spacing for a particular pair of joint is the perpendicular distance between the two joints. For a joint set, is usually expressed as the mean spacing of that joint set. However, when the expose is limited, often the apparent spacing is measured. *Figure I.23* shows the relationship between spacing of individual joint set, apparent spacing and average spacing.
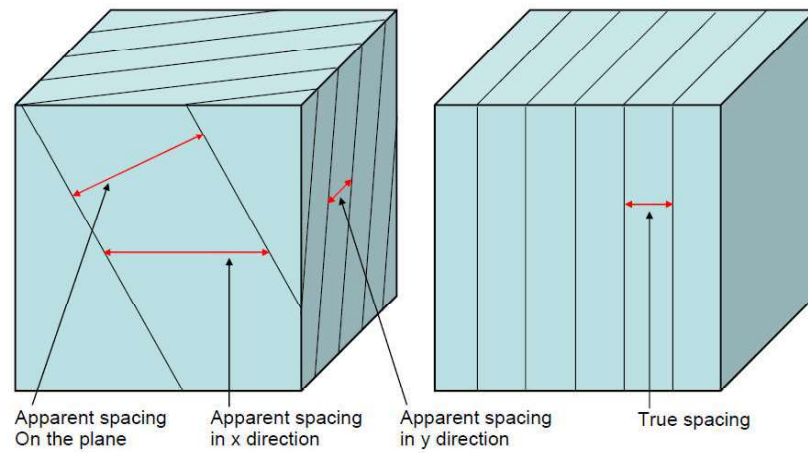
Figure I.23 *Joint spacing, apparent spacing and true spacing [1]*

ISRM recommends the use of the terms in Table I.9 to describe joint spacing. The description ranges from extremely close spacing to extremely wide spacing.

Table I.9 *Classification of discontinuity spacing [1]*

Description	Joint Spacing (m)
Extremely close spacing	< 0.02
Very close spacing	0.02 − 0.06
Close spacing	0.06 − 0.2
Moderate spacing	0.2 − 0.6
Wide spacing	0.6 − 2
Very wide spacing	2 − 6
Extremely wide spacing	> 6

Joint frequency (λ), is defined as number of joint per metre length. It is therefore simply the inverse of joint spacing (sj),

Another measure of fracturing degree is the Rock Quality Designation (RQD). Is is defined as the percentage of rock cores that have length equal or greater than 100 mm over the total drill length (Figure I.24).

Figure I.24 Example of measuring RQD from core logging

I.5.1.4 Joint Roughness

Roughness is a measure of the inherent surface unevenness and waviness of the discontinuity relative to its mean plane. The wall roughness of a discontinuity has a potentially important influence on its shear strength, especially in the case of undisplaced and interlocked features (e.g. unfilled joints). The importance of roughness declines with increasing aperture, filling thickness or previous shear displacement.

When the properties of discontinuities are being recorded from observations made on either drill core or exposures, it is usual to distinguish between small-scale surface irregularity or **unevenness** and larger-scale undulations or waviness of the surface

Table I.10 Classification of discontinuity roughness [2]

Class	Description
I	rough or irregular, stepped
II	smooth, stepped
III	slickensided, stepped
IV	rough or irregular, undulating
V	smooth, undulating
VI	slickensided, undulating
VII	rough or irregular, planar
VIII	smooth, planar
IX	slickensided, planar

Descriptive terms may also be used particularly in the preliminary stages of mapping. For example, the ISRM

Commission (1978a) suggests that the terms listed in Table I.10 and illustrated in Figure I.25 may be used to describe roughness on two scales – the small scale (several centimetres) and the intermediate scale (several metres). Large-scale waviness may be superimposed on such small- and intermediate-scale roughness (Figure I.25). *[2]*
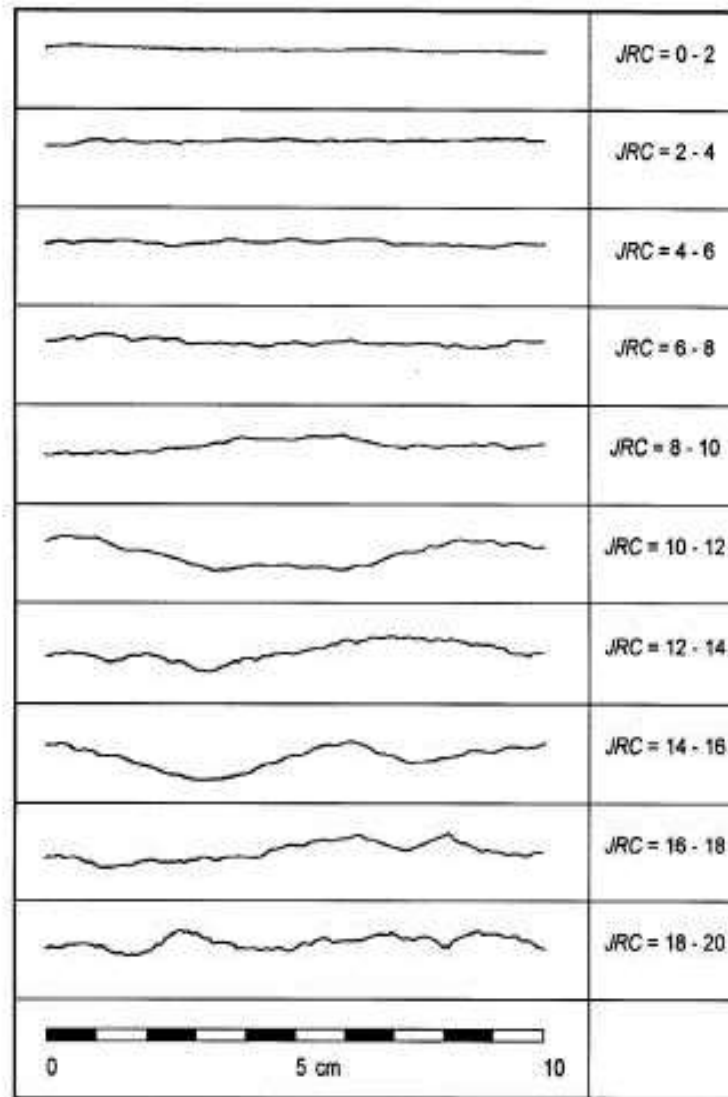
Figure I.25 Typical roughness profiles and suggested nomenclature. Profile lengths are in the range 1 to10 m; vertical and horizontal scales are equal [2]

I.5.1.5 Joint Aperture

Aperture is the perpendicular distance separating the adjacent rock walls of an open discontinuity in which the intervening space is filled with air or water. Aperture is thereby distinguished from the width of a filled discontinuity (Figure I.26).

Large apertures can result from shear displacement of discontinuities having appreciable roughness, from outwash of filling materials (e.g. clay), from solution or from extensile opening. In most subsurface rock masses, apertures will be small, probably less than half a millimetre.
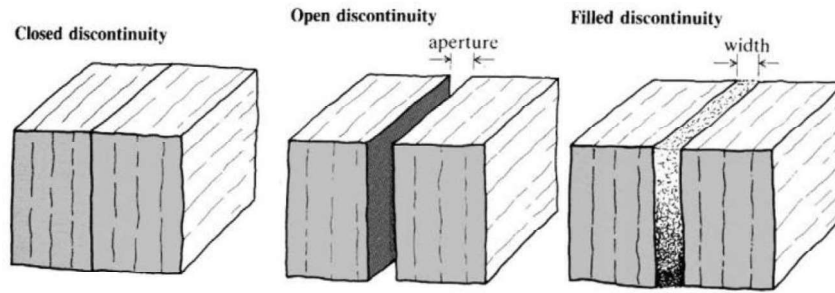
Figure I.26 *Suggested definition of the aperture of open discontinuities and the width of filled [4]*

CHAPTER II

MECHANICAL BEHAVIOUR OF ROCKS AND ROCK MASSES

Chapter II

Mechanical behaviour of rocks and rock masses

II. 1 Introduction

For the purpose of design and to evaluate the stability of underground structure, mechanical properties of the rock must be known. It provides the knowledge of material deform or fail, under the action of applied force. The mechanical properties are tensile strength, compressive strength, shear strength, creep or time properties and strain or deformation properties. The mechanical properties can be determined by static testing which includes uniaxial (unconfined) compressive, tensile, shear and flexural strength, triaxial compressive, shear strength etc. and also elastic constants, i.e., modulus of elasticity and Poisson's ratio obtained from uniaxial, triaxial stress-strain relationship.

it is important to understand the course of these experiments, to be able to read and interpret the results and to assess the effect of certain parameters on the deformation (deformation rate, T, P, etc.). In fact, these experiments attempt to simulate the deformations of the Earth's crust to better understand the physical processes behind the development of different geological structures, such as faults and folds.[9]

II. 2 In-situ and laboratory characterization

The mechanical behaviour of rocks is studied through mechanical tests in the laboratory, which take place either in simple compression or in a triaxial cell. In these tests, cylindrical or cubic specimens are subjected to a known stress state while varying various parameters such as temperature, confinement pressure, strain rate.

These tests allow us to simulate in the laboratory brittle deformation, which will result in the development of a discontinuity plane in the sample, a fracture for example, accompanied or not by slippage on the discontinuity plane, or ductile deformation, which will be accommodated by the distortion and/or expansion of the material without rupture or loss of cohesion. [6]

Mechanical behavior is classified into two types depending on whether the stress-strain relationships are reversible or not. It is therefore necessary to carry out an unloading-reloading cycle to make this first classification.

II.2.1 Elastic deformation -plastic
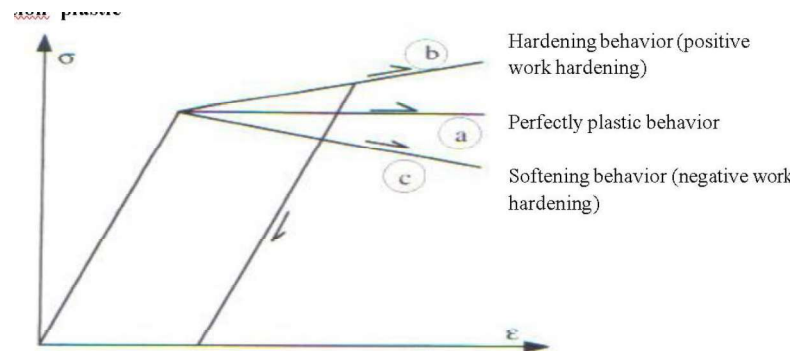
Figure II.1 *Types of elastoplastic behavior .[10]*

Elastic behaviour: reversible rock deformation

- linear relationship between σ and ε

- Elastic materials accumulate deformation that they give back when the stress is released

Plastic behaviour: non-reversible deformation of the rock

- no linear relationship between σ and ε

- Plastic materials do not return to deformation after stress relaxation

- The behavior is perfect elastoplastic if the yield strength does not depend on the history of stresses and strains. In other words, the axial stress-strain curve has a plateau (curve a).

- If the slope of the axial stress-strain curve is positive, this behaviour is referred to as hardening or positive work hardening (curve b).

- If the slope of the axial stress-strain curve is negative, it is a softener or negative work hardening behaviour (curve c).

- When the behavior depends on time, the behavior is elasto-viscoplastic. *[31]*

II.2.2 Brittle and ductile deformation

Brittle rock: deforms elastically or even a little plastically before breaking

- Discontinuous, cold and rapid deformation

- characterized by a direction and direction of movement

Ductile rock: undergoes large deformations without rupture

- Continuous and hot deformation.

- characterized by the movement of blocks at the boundaries of the domain

Ductile-brittle rock: some rocks have a ductile behaviour before fracture so the temperature, pressure and rate of deformation vary the brittle/ductile limit.

The brittle–ductile transition stress in the rock mass is crucial in understanding its mechanical behavior under varying conditions. Rocks exhibit two primary modes of deformation: brittle and ductile. In the brittle regime, rocks tend to fracture and fail through the propagation of cracks and fractures. This is characterized by a sudden release of stored elastic energy, resulting in a relatively rapid failure. In the field of rock mechanics, several researchers have characterized brittleness as a material's propensity to fracture when subjected to stress, such as tension or compression, without undergoing significant or lasting deformation. This definition emphasizes that a brittle material can break suddenly, often with little warning, because it lacks the ability to absorb energy and deform plastically before failure. Such behavior is contrasted with ductile materials, which can undergo considerable deformation before fracturing. Brittleness is a critical factor in understanding how rocks and other materials will behave under different loading conditions, making it essential in various engineering and geological applications
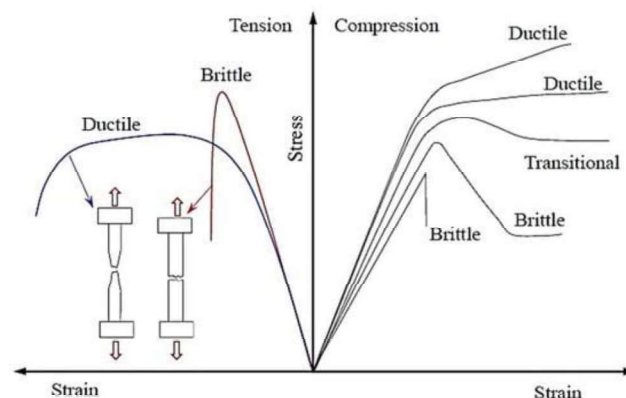
*Figure II.2 Brittle and ductile behavior under tension (**left**) and compression (**right**). The right side illustrates the rock's behavior under varying confining pressures [31]*

II.2.3 Physical Parameters

The behavior of rocks depends on 3 physical parameters: **-** Temperature, Pressure, Deformation rate

   a) **Pressure**
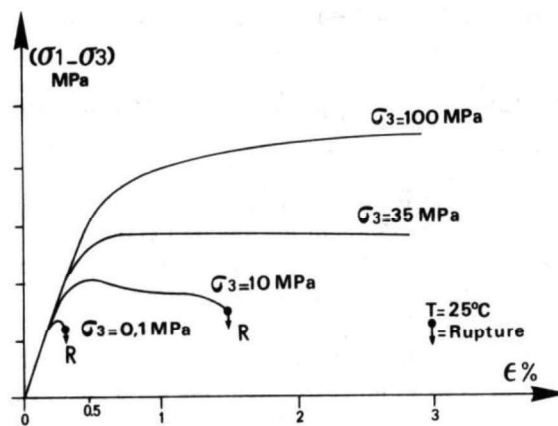
Figure II.3 Effect of pressure on rock behaviour

- delayed fracturing due to increased containment pressure.

- If the containment pressure reaches high values above 30 MPa, the rupture no longer exists deformation by shortening by 3 to 20%.

- If the fluid pressure is high, there will be brittle deformation at any depth

b) Temperature
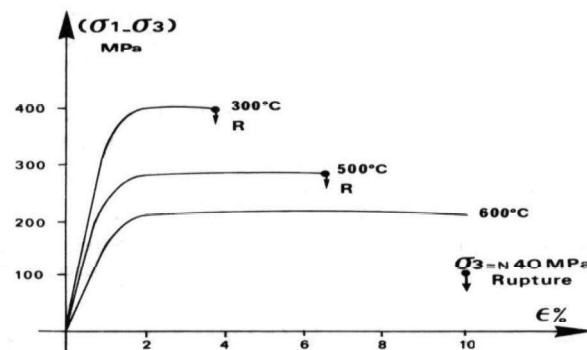
Figure II.4 Effect of temperature on rock behaviour

- If the temperature increases, the plastic creep threshold decreases and the rock softens and deforms before failure, so the hydrostatic pressure delays the failure. The combined effect of pressure and temperature extends the ductile domain of the rock.

c) Strain rate
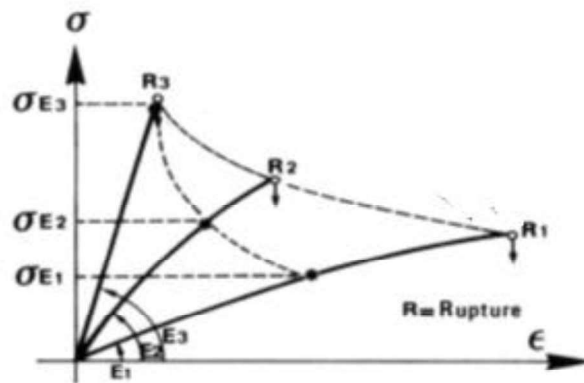
Figure II.5 *Effect of deformation rates on rock behaviour* [24]

For increasing deformation rates, the plastic domain decreases and the elastic domain increases, so for increasing deformation rates, the plastic domain decreases and the rock becomes brittle.

    - Brittle behavior up to 4000 meters deep with T≈150°C and P ≈100 MPa

    - ductile behaviour if normal geothermal gradient (9000 metres and T≈ 300 °C

II. 3 Laboratory tests on intact rock

The basic tests involve three types of stresses:

- traction: indirect traction (or Brazilian test);

- uniaxial (or monoaxial or simple) compression;

- triaxial compression (isotropic and deviatoric).

II. 3.1 Uniaxial Compression Test

Uniaxial compressive strength is the ultimate stress of a cylindrical rock sample under axial loading. It is the most important of the mechanical properties of rock, used in design, analysis and modelling.

The specimens are typically 50 mm in diameter and 100 to 120 mm high. The stresses along the compression axis are denoted σ_1[24]

In parallel with load measurement, axial and radial deformations are also measured.

Figure III.6 *Uniaxial compression test on a granite*
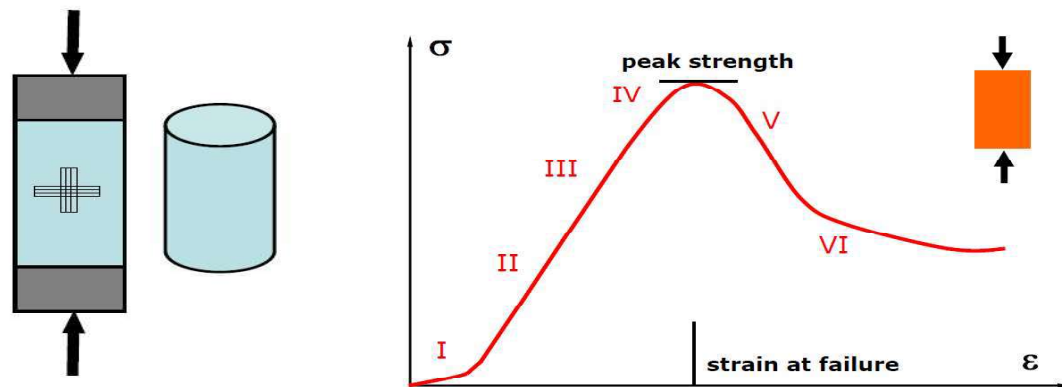
Figure II.7 *Uniaxial test on rock (a) Uniaxial compression test. (b) Stress-strain curve of uniaxial test [16]*

Stage 1- The rock is initially loaded. In connection with the deformation, the existing micro-cracks close, resulting in an initial nonlinearity of the curve.

Stage 2- The rock has a linearly elastic behavior with a linear stress-strain curve, axially and radially.

Stage 3- The rock behaves almost linearly. The axial stress-strain curve is quasilinear and is almost reversible.

Stage 4- The rock undergoes a rapid acceleration of micro-cracking and volume increase.

Stage 5- The rock has passed the peak stress, but is still intact, even though the internal structure is heavily disturbed. The specimen undergoes a softening of the deformations (failure).

Stage 6- The rock breaks into several blocks rather than an intact structure. [14]

II.3.1.1 Characteristic curves
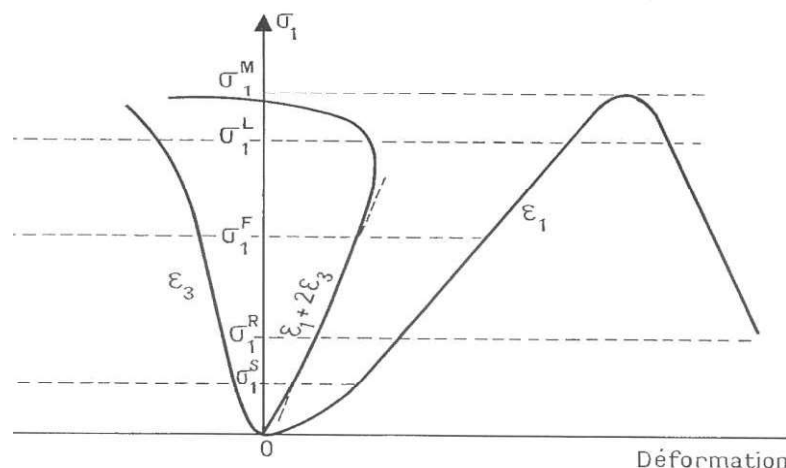
Figure II.8 *Unaxial Compressive test curve* [14]

A first phase called tightening is observed, where the internal cracks and micro-cracks oriented orthogonally to the direction of loading close, we observe a quasi-linear phase (from $\sigma_1 S$ to σ_1^F).

We then define a Young E modulus and a Poisson coefficient **ν**. The range of variation of **E** is very large, ranging from a few thousand MPa for marls to more than 100 GPa for some siliceous sandstones. The Poisson ratio is taken to be equal to 0.2 or 0.3.

On the stress-strain curve, the linear phase continues up to σ_{1L} but the volume strain curve **($\varepsilon v = \varepsilon_1 + 2\varepsilon_3$)** is no longer so. This phase corresponds to the creation and opening of micro-cracks, by buckling parallel to the axis of the specimen. Overall stability is always assured. Above σ_{1L}, the rock behaves unstably, with an increasing volume (expansion or dilation) and cracks that propagate rapidly. In the case of a uniaxial test, the fracture is brittle and the post-peak curve is only obtained with a deformation-controlled press. The stress σ_{1M} is the simple compressive strength, also denoted **σc**.

σ_c peut prendre des valeurs très différentes : de quelques MPa pour une roche très altérée à plus de300 MPa pour certains basaltes ou quartzites.[14]

II.3.2 Triaxial compressive and shear strengtht Test

This test is carried out on cylindrical specimens prepared in the sam manner as those used for uniaxial compression tests. The specimen is placed inside a pressure vessel (FiguresII.9) and a fluid pressure is σ3 applied to its surface. A jacket, usually made of a rubber compound, is used to isolate the specimen from the confining fluid which is usually oil.

The axial stress, σ1, is applied to the specimen via a ram passing through a bush in the top of the cell and hardened steel end caps. [23]

At depth, the rock is subjected to axial and radial (triaxial) stresses, and the compressive strength is higher under triaxial conditions.

The true triaxial compression state means 3 different principal stresses. It is often admitted for simplify that the 2 radial stresses are equal to the minor principal stress (axisymmetric triaxial test).
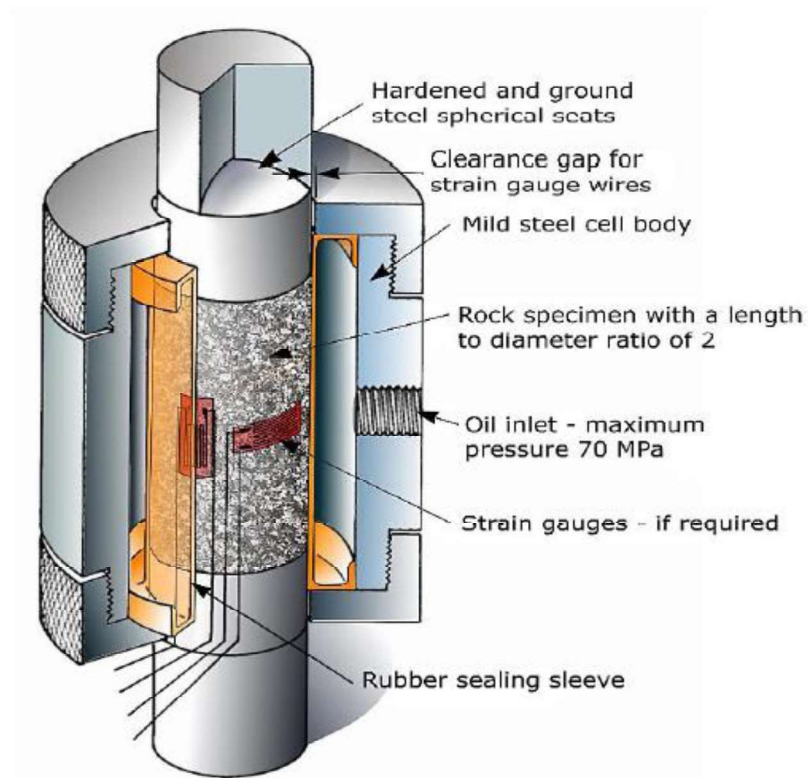
Figure II.9 Cut-away view of the triaxial cell designed [11]
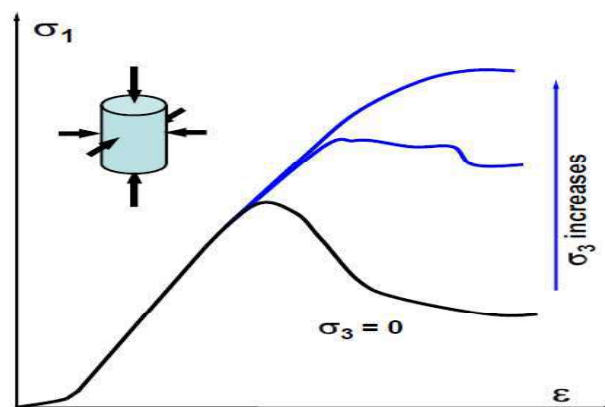
Figure II.10 Triaxial Compression Test curve [8]

The behaviour of the rock in triaxial compression changes with increasing confinement pressure:

(a) Maximum resistance increases;

(b) The behaviour after the peak gradually changes from brittle to ductile.

In the elastic domain, the stress-strain behavior is the same as in uniaxial compression.
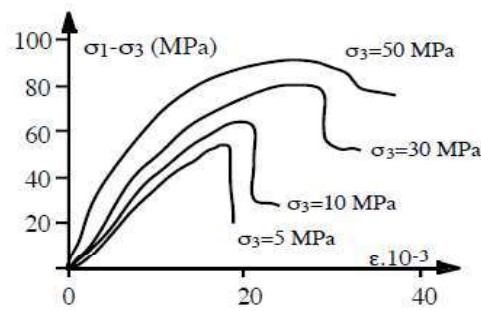
Figure II.11 *effet of containment pressure on the behaviour of a marl in function of containment pressure* [9]
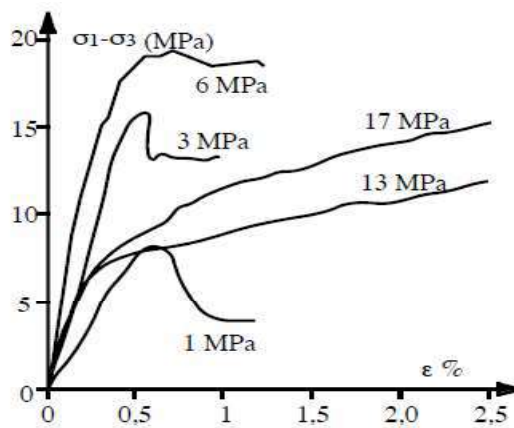
Figure III.12 *Effect of Confinement Pressure on the Behavior of a Chalk as a Function of Confinement Pressure*

Shear strength by triaxial tests. From a series of triaxial tests, the max stresses (σ_1) are obtained for different lateral stresses (σ_3).

By drawing the Mohr circles, we define the intrinsic curve and obtain the cohesion and the internal angle of friction.
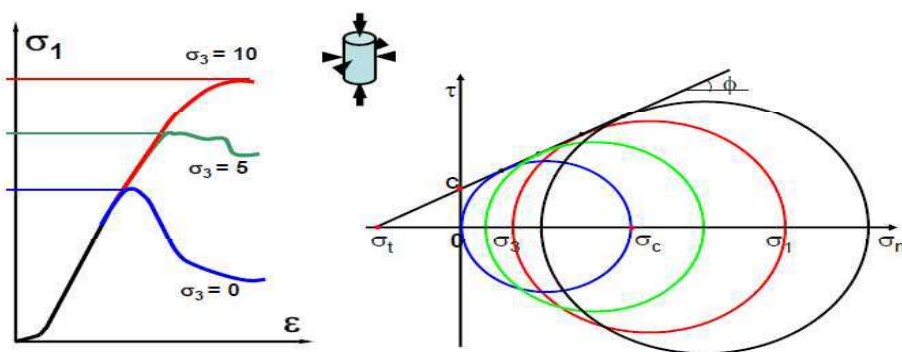
Figure II.13 *Triaxial Shear Test [23]*

II.3.3 Tensile Strength of Rock

Rocks usually have a low tensile strength, due to pre-existing microcracks. The existence of these microcracks can also be the cause of the sudden rupture of the tensile rock under low stress.

The tensile strength of the rock can be obtained from several types of tests. The most well-known tensile test is the Brazilian test. [15]

The tensile strength is measured by loading a cylindrical specimen in tension to its failure. The indirect methods such as Brazilian test and flexural strength or bending test are also used to measure tensile strength.

a) Brazilian Test

The specimen is cut out of a cylindrical core by a diamond saw. The length to the diameter ratio is usually 0.5. The periphery of the specimen should be smooth. The specimen is placed under compression testing machine. Compressive load (normally 220 kgf/s) is applied slowly till failure take place (Fig II.13).

$$T_o = \frac{2F_c}{\pi DL}$$

$(II.1)$

Fc = applied failure load in kg along the length of the specimen

D = diameter of specimen in cm

L = length of the specimen in cm

To = uniform tensile strength in kg/cm^2
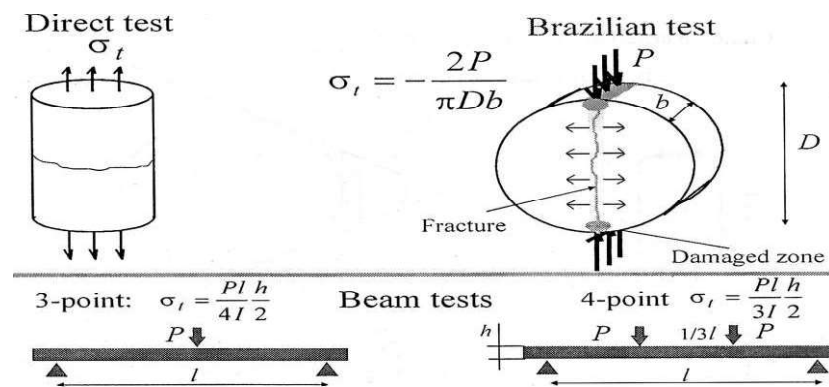
Figure II.14 Brazilian Test for Tensile Strength of Rock [21]

II.3.4 Direct shear test

The rock resists the shear force by two internal mechanisms, cohesion and internal friction. Cohesion is a measure of the internal bonding of the rock. Internal friction results from the contact between the particles, and is defined by the angle of internal friction.

A direct shear test also known as shearbox test is a laboratory or field test used by geotechnical engineers to measure the shear strength properties of soil or rock material, or of discontinuities in soil or rock masses. The test is performed on three or four specimens from a relatively undisturbed soil sample.

A specimen is placed in a shear box which has two stacked rings to hold the sample; the contact between the two rings is at approximately the mid-height of the sample.
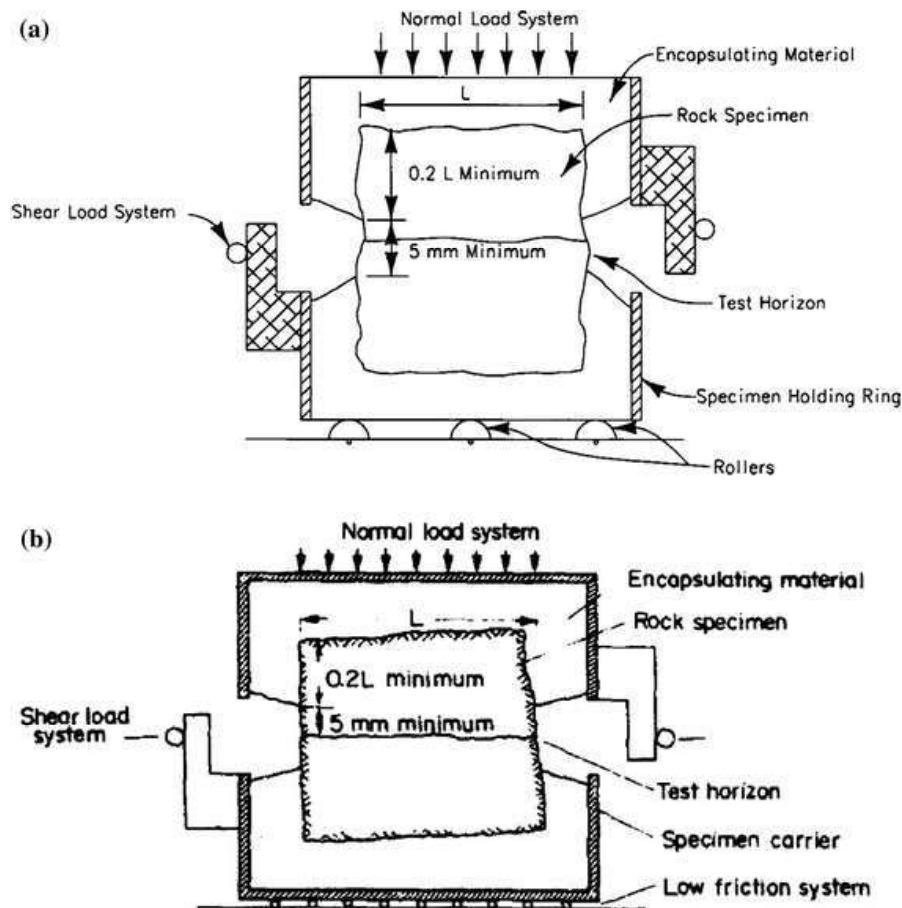
Figure II.15 *Schematic representation of direct shear test under constant normal stress (CNL [32]*

Shear strength is a function of, among other things:

- Of the rubbing of hanging wall,
- The roughness of the hanging rocks,
- Of their degree of interweaving
- Of their alteration.

II.3.5 In Situ Shear Tests

The conditions of friction along interfaces are extremely important for many construction projects in rock. The direct shear test is the established method for determining peak and residual friction because it directly produces a relationship between normal and shear forces and between the corresponding normal and tangential displacements. A further important advantage of direct shear tests is that generally they also permit large shearing displacements.

A large number of tests has shown that Coulomb's law can be applied for determining the frictional resistance ts of plane interfaces as a function of normal stress sn. Any irregularities, such as are found at most rock interfaces, will lead however to lifting processes and - under higher normal stresses - shearing processes which exert a decisive effect on the conditions of friction. In such cases it is necessary to consider bilinear or exponential laws of friction.

The mechanical behaviour of interfaces is often complicated in addition by the presence of a rock vein. Where the thickness (t) of the rock vein is small in relation to the amplitude of roughness (T), the shear strength is still determined by the interface characteristics.

To conduct the test, a block measuring around 300 mm high is etched out of the in-situ rock and surrounded with a square steel frame (dimensions 1000 x 1000 x 300 mm). The joint between the steel frame and the specimen is filled with cement mortar to ensure a close-fitting connection between the frame and the specimen. The surface of the specimen is levelled off with a layer of cement and a pressure distribution plate is placed on top. A steel-reinforced abutment is cast likewise in cement on the side facing the shear force cylinder. The front side of the abutment slopes at an angle of 75 °. When the cement has hardened, the steel abutments for the shear force cylinder are positioned (see Fig. II.16).[2]
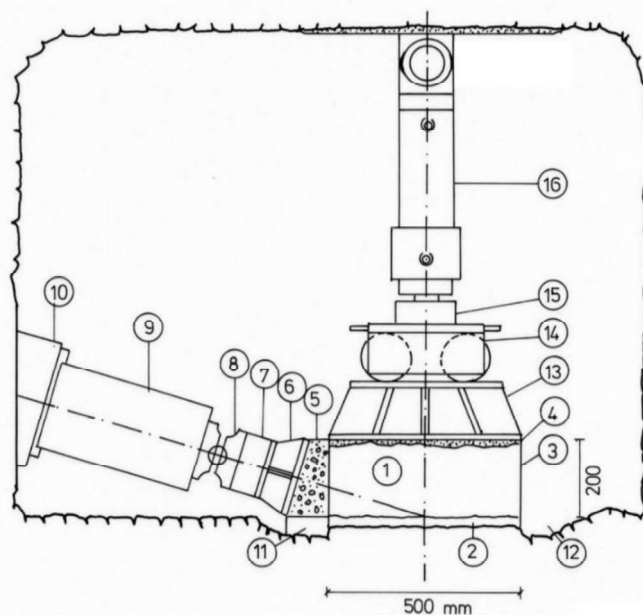
Figure II. 16 *In-situ shear test on a specimen of 500 x 500 x 200 mm or 1000 x 1000 x 300 mm* [23]

1 Test block	9 Jack for 1 MN
2 Shear joint	10 Abutment
3 Jacket made of steel sheet	11 Styrene
4 Levelling mortar	12 Drainage ditch
5 Abutment	13 Load distribution plate
6 Load distribution plate	14 Roller bearing

7 Load cell   15 Load cell

8 Ball joint   16 Jack for 0.2 MN or 1 MN

II.3.6 The point load test

Sometimes the facilities required to prepare specimens and carry out uniaxial compression tests to the standard described above are not available. In other cases, the number of tests required to determine the properties of the range of rock types encountered on a project may become prohibitive. There may be still further cases, in which the uniaxial compressive strength and the associated stress–strain behaviour need not be studied in detail, with only an approximate measure of peak strength being required. In all of these instances, the point load test may be used to provide an indirect estimate of uniaxial compressive strength. In this test, rock specimens in the form of core (the **diametral** and **axial** tests), cut blocks (the **block** test) or irregular lumps (the **irregular lump** test) are broken by a concentrated load applied through a pair of spherically truncated, conical platens.

The compressive strength of rock depends upon shape, surface quality of loading system, rock specimen surface, porosity and moisture content of the rock, rate of loading and specimen size. The compressive strength of the rock decreases with increase in its porosity. Water in rock pores reduces the magnitude of internal friction of rock thereby reducing the rock strength. Usually, wet sample has its strength 1/3 of that of a dry sample (Figure II.17). The load should be applied at least 0.5D from the ends of the specimen in diametral tests, where D is the core diameter, and equivalent distances in other tests).

From the measured value of the force, P, at which the test specimen breaks, an Uncorrected Point Load Index, Is, is calculated as

$$I_s = \frac{P}{D_e^2} \qquad\qquad (II.2)$$

where De, the equivalent core diameter, is given by the core diameter, D, for diametral tests, and by 4A/_ for axial, block and lump tests, where A is the minimum cross-sectional area of a plane through the specimen the platen contacts points.[30]

The index, Is, varies with De and so size correction must be applied in order to obtain a unique point load strength index for a particular rock sample for use for strength classification.

Wherever possible, it is preferable to carry out diametral tests on 50–55 mm diameter specimens. The size-corrected **Point Load Strength Index,** *is* (50), is defined as the value of Is that would have been measured in a diametral test with D = 50 mm. The results of several series of tests carried out by a number ofinvestigators show that the value of Is determined in a test of equivalent diameter, De, may be converted to an *is* (50) value by the relation

$$I_{s(50)} = I_s \; x \; \left(\frac{D_e}{50}\right)^{0.45} \qquad\qquad (II.3)$$

A number of investigators have developed correlations of the Point Load Index with the uniaxial compressive strength, σc. The most commonly used correlation is

$$\sigma_c \approx (22 - 24)I_{s(50)} \qquad\qquad (II.4)$$
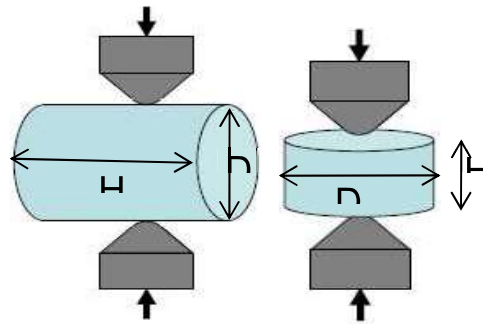
(a)*Diamétral test*   (b) *axial test*

Figure II. 17 *Principle of the point resistance test* [23]

Where De the equivalent diameter of the cylindrical specimen is given by:

De² = D²   for the diametrical test;

      = 4 A/π   for axial test;

A=HD=Minimum Section Area of a Plane through Load Points

The point resistance is corrected in relation to the point resistance corresponding to an equivalent specimen with a diameter equal to 50 mm.

For ≠ 50 mm, the size correction factor is:

$$F = (D_e/50)^{0.45} \qquad\qquad (II.5)$$

The corrected point resistance index Is(50) is given by: Is(50) = F Is

Table II.1 *Typical values of the point resistance index is [3]*

Granite	5 − 15
Gabbro	6 − 15
Andesite	10 − 15
Basalte	9 − 15
Grès	1 − 8
Mudstone	0.1 − 6
Calcaire	3 − 7
Gneiss	5 − 15
Schiste	5 − 10
Ardoise	1 − 9
Marbre	4 − 12
Quartzite	5 − 15

Correlation between the point resistance index and resistances.

$$\sigma_c \approx 22\ I_{s(50)} \qquad\qquad (II.6)$$

The correction factor can vary between 10 and 30.

$$\sigma_t \approx 1.25\, I_{s(50)} \qquad\qquad\qquad (II.7)$$

$I_{s(50)}$ should be used as an independent resistance index.

II. 4. Types of strength criterion

A peak strength criterion is a relation between stress components which will permit the peak strengths developed under various stress combinations to be predicted. Similarly, a residual strength criterion may be used to predict residual strengths under varying stress conditions. In the same way, a yield criterion is a relation between stress components which is satisfied at the onset of permanent deformation. [12]

Given that effective stresses control the stress–strain behaviour of rocks, strength and yield criteria are best written in effective stress form. However, around most mining excavations, the pore-water pressures will be low, if not zero, and so $\sigma'_{ij} \cong \sigma_{ij}$. For this reason, it is common in mining rock mechanics to use total stresses in the majority of cases and to use effective stress criteria only in special circumstances.

The data presented in the preceding sections indicate that the general form of the peak strength criterion should be

$$\sigma_1 = f(\sigma_2\, \sigma_3) \qquad\qquad\qquad (II.8)$$

The strength limit is defined by the stress at which the material begins to deform plastically. This usually represents an upper limit to the load that can be applied.

A limit strength (failure) criterion is an assumption that concerns the stress limit under any stress state. This is usually described by three main constraints.

II.4.1 Coulomb's shear strength criterion

In one of the classic papers of engineering science, Coulomb postulated that the shear strengths of rock and of soil are made up of two parts − a constant cohesion and a normal stress-dependent frictional component. (Actually, Coulomb presented his ideas and calculations in terms of forces; the differential concept of stress that we use today was not introduced until the 1820s.) Thus, the shear strength that can be developed on a plane such as *ab* in Figure II.18 is

$$\tau = c + \sigma_n\, tan\varphi \qquad\qquad\qquad (II.9)$$

where c = cohesion and φ = angle of internal friction.
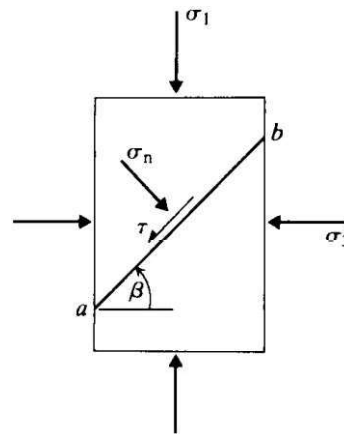
Figure II.18 *Shear failure on planeab*
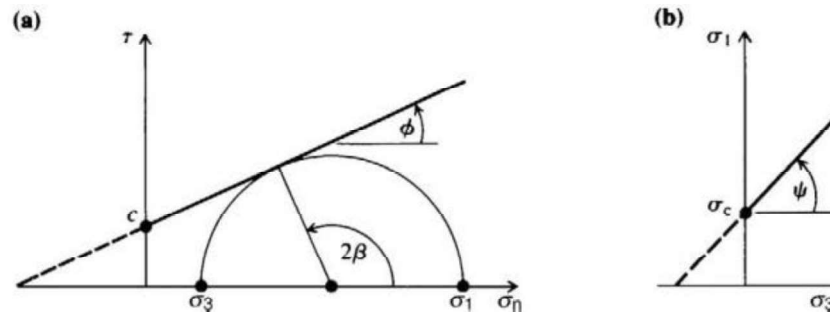
Figure II.19 *Coulomb strength envelopes in terms of (a) shear and normal stresses, and (b) principal stresses A* [23]

Applying the stress transformation equations to the case shown in Figure II.19 Gives

$$\sigma_n = \tfrac{1}{2}(\sigma_1 + \sigma_3) + \tfrac{1}{2}(\sigma_1 - \sigma_3)\cos 2\beta \tag{II.10}$$

And

$$\tau = \tfrac{1}{2}(\sigma_1 - \sigma_3)\sin 2\beta \tag{II.11}$$

Substitution for σn and τ in equation 4.11 and rearranging gives the limiting stress condition on any plane defined by β as

$$\sigma_1 = \frac{2c + \sigma_3[\sin 2\beta + \tan\phi\,(1 - \cos 2\beta)]}{\sin 2\beta - \tan\phi\,(1 + \cos 2\beta)} \tag{II.12}$$

There will be a critical plane on which the available shear strength will be first reached as σ₁ is increased. The Mohr circle construction of Figure 19a gives the orientation of this critical plane as

$$\beta = \frac{\pi}{4} + \frac{\phi}{2} \tag{II.13}$$

For the critical plane, sin 2β = cos φ, cos 2β= −sinφ and equation II.12 reduces

$$\sigma_1 = \frac{2c \cos \phi + \sigma_3(1 + \sin \phi)}{1 - \sin \phi}$$

(II.14)

This linear relation between σ3 and the peak value of σ1 is shown in Figure II.19b.

Note that the slope of this envelope is related to φ by the equation to

$$\tan \psi = \frac{1 + \sin \phi}{1 - \sin \phi}$$

(II.15)

and that the uniaxial compressive strength is related to *c* and φ by

$$\sigma_c = \frac{2c \cos \phi}{1 - \sin \phi}$$

(II.16)
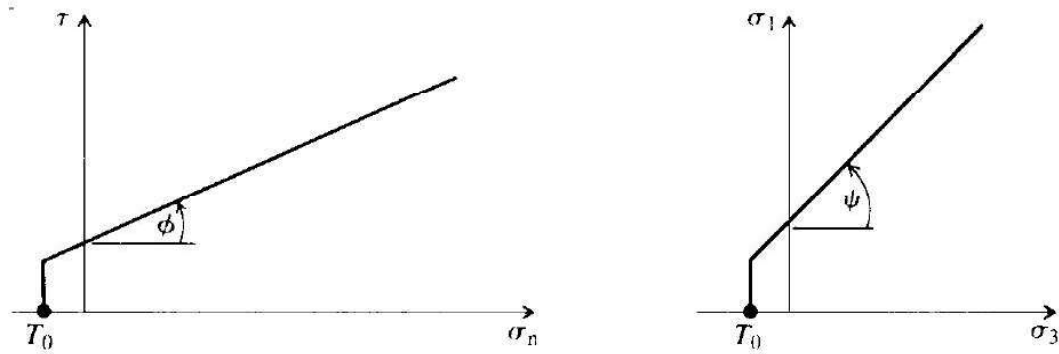
Figure II.20 *Coulomb strength envelopes with a tensile cut-off* [23]

If the Coulomb envelope shown in Figure II.19b is extrapolated to σ1 = 0, it will intersect the σ₃ axis at an apparent value of uniaxial tensile strength of the material given by

$$\sigma_T = \frac{2c \cos \phi}{1 + \sin \phi}$$

(II.17)

The Mohr–Coulomb criterion can also be represented in a σ1–σ3 graph. In this case we have:

$$\sigma_1 = \sigma_c + \sigma_3 \tan\psi$$

(II.18)

$$\tan\psi = \frac{1 + \sin\phi}{1 - \sin\phi}$$

(II.19)

$$\sigma_1 = \sigma_c + \sigma_3 \frac{1 + \sin\phi}{1 - \sin\phi}$$

(II.20)
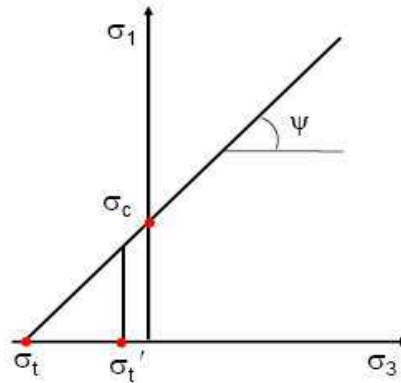
Figure II.21 *Mohr-Coulomb envelope in terms of principal stresses [54]*

The Mohr-Coulomb criterion is only valid for the weak containment domain. At a high level of confinement, he overestimates resistance. It also overestimates tensile strength. In most cases, rock mechanics deals with superficial problems and low confinement, so this criterion is widely used, thanks to its simplicity and success.

II.4.2 Griffith crack theory

In 1921, Griffith postulated that fracture of brittle materials, such as steel and glass, is initiated at tensile stress concentrations at the tips of minute, thin cracks (now referred to as Griffith cracks) distributed throughout an otherwise isotropic, elastic material. Griffith based his determination of the conditions under which a crackwould extend on his energy instability

A crack will extend only when the total potential energy of the system of applied forces and material decreases or remains constant with an increase in crack length.

In 1924 , Griffith extended his theory to the case of applied compressive stresses. Neglecting the influence of friction on the cracks which will close under compression, and assuming that the elliptical crack will propagate from the points of maximum tensile stress concentration (*P* in Figure II.21), Griffith obtained the following criterion for crack extension in plane compression:
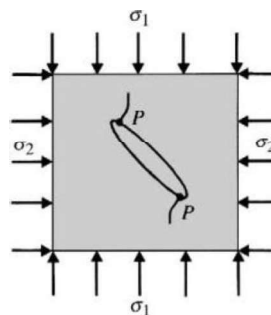
Figure II.22 *Griffith crack model for plane compression [54]*

$$(\sigma_1 - \sigma_2)^2 - 8T_0(\sigma_1 + \sigma_2) = 0 \quad \text{if } \sigma_1 + 3\sigma_2 > 0$$
$$\sigma_2 + T_0 = 0 \quad \text{if } \sigma_1 + 3\sigma_2 < 0$$

$$\text{(II.21)}$$

where $T0$ is the uniaxial tensile strength of the uncracked material (a positive number). This criterion can also be expressed in terms of the shear stress, and the normal stress, σn acting on the plane containing the major axis of the crack:

$$\tau^2 = 4T_0(\sigma_n + T_0)$$

<div align="right">(II.22)</div>

The envelopes given by equations II.21 and II.23 are shown in Figure II.22. Note that this theory predicts that the uniaxial compressive stress at crack extension will always be eight times the uniaxial tensile strength.
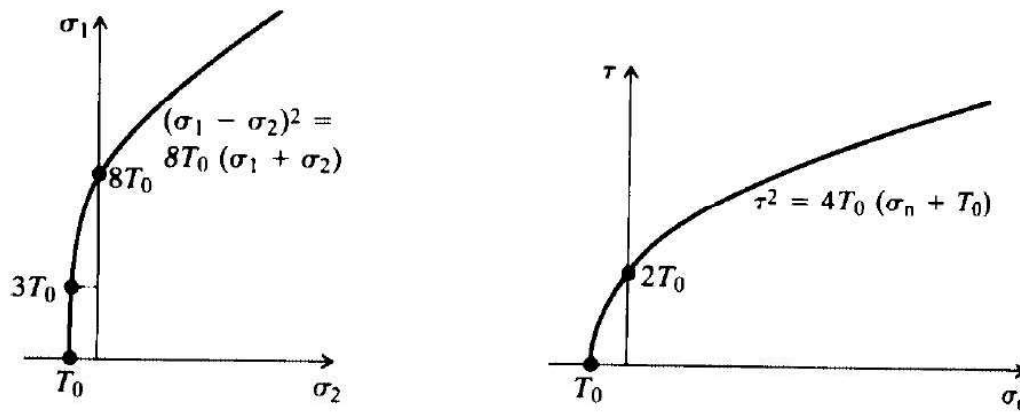
Figure II.23 *Griffith envelopes for crack extension in plane compression [54]*

Griffith's plane compression theory does not give a very good model for the maximum strength of the rock under multiaxial compression. This only gives a good estimate of tensile strength, and underestimates compressive strength, especially under high lateral stresses. A number of modifications to Griffith's solution were introduced, but today they are not used.

II.4.3 Hoek and Brown criterion

In 1980, Hoek and Brown, two Anglo-Saxon engineers, proposed a new criterion of plasticity, empirical but respecting the "optimal" shape of the parabola in the plane of the principal stresses. It is written as follows :

<div align="center">$\sigma_1 = \sigma_3 + (m_b\,\sigma_3\,\sigma_{ci} + s\,\sigma_{ci}^2)^a$ (II.23)</div>

where σ_1 the major principal stress, σ_3 the minor principal stress, σ_c the uniaxial compressive strength of the intact rock, and *m* and s are constants for a specific rock type.

Although the constants *m* and s arise from the curve-fitting procedure, there is an element of physical interpretation associated with them which is helpful for the engineer to consider.

The parameter s relates to the degree of fracturing present in the rock sample: it is a representation of the cohesion of the rock. For completely intact rock, it takes the value 1 (which can be demonstrated by substituting *o3* = 0 into the criterion: $\sigma_1 = s\,\sigma_c^{0.5}$ *and* hence s = 1, noting that *0,* is the intercept on the σ_c

axis in Fig. **6.20**) and, for rock which is highly fractured, it reduces in value and tends towards zero as the strength is reduced from peak to residual.
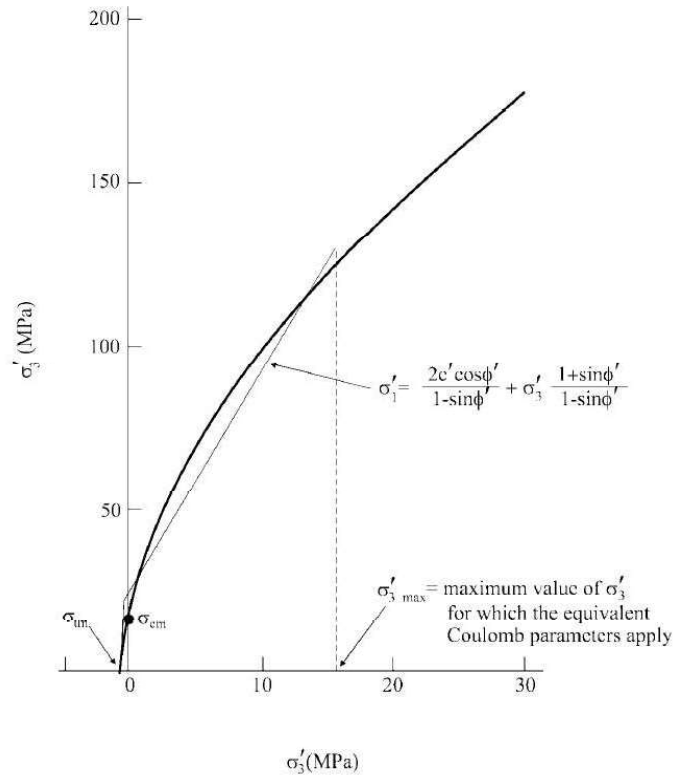
Figure II.24 *Hoek-Brown peak strength envelope for a diorite rock mass with σc = 100 MPa,mi = 25 and GSI 65 and the equivalent Coulomb shear strength parameters [10]*

σ1 is the strength of the solid for a confinement stress σ_3.

σci is the uniaxial compressive strength of the intact rock in the rocky massif.

The parameter a is usually 0.5.

Lab test results indicate that the failure envelop is nonlinear. Hoek et al. (2002) have developed a simple empirical law based on the analysis of a huge number of lab tests and have proposed the following relation:

$$\sigma_1' = \sigma_3' + \sigma_c \left(m_b \frac{\sigma_3'}{\sigma_c} + s \right)^a .$$

(II.24)

Typical values for intact rock are a = 0.5 and s = 1). According to equation (II.24), which is the formulation of the Hoek-Brown failure criterion for intact rock, m_i is an intact rock parameter:

$$\sigma_1' = \sigma_3' + \sigma_c \left(m_i \frac{\sigma_3'}{\sigma_c} + 1 \right)^{1/2}$$

(II.25)

The constants m_b and s are parameters that change with the type of rock and the quality of the massif.

Table II.2 *Approximate relations between rock mass quality and the material constants in the Hoek-Brown failure criterion[37]. Undisturbed values are in italics*

Approximate relationship between rock mass quality and material constants					
Disturbed rock mass m and s values *(EMPIRICAL FAILURE CRITERION)* $\sigma_1 = \sigma_3 + \sqrt{m\sigma_c\sigma_3 + s\sigma_c^2}$ σ_1 = major principal stress σ_3 = minor principal stress σ_c = uniaxial compressive strength of intact rock, and m and s are empirical constants.		CARBONATE ROCKS WITH WELL DEVELOPED CRYSTAL CLEAVAGE *dolomite, limestone and marble*	LITHIFIED ARGILLACEOUS ROCKS *mudstone, siltstone, shale and slate (normal to cleavage)*	ARENACEOUS ROCKS WITH STRONG CRYSTALS AND POORLY DEVELOPED CRYSTAL CLEAVAGE *sandstone and quartzite*	FINE GRAINED POLYMINERALLIC IGNEOUS CRYSTALLINE ROCKS *andesite, dolerite, diabase and rhyolite*	COARSE GRAINED POLYMINERALLIC IGNEOUS & METAMORPHIC CRYSTALLINE ROCKS – *amphibolite, gabbro gneiss, granite, norite, quartz-diorite*
INTACT ROCK SAMPLES *Laboratory size specimens free* *from discontinuities* CSIR rating: RMR = 100 NGI rating: Q = 500	m s m s	7.00 1.00 7.00 1.00	10.00 1.00 10.00 1.00	15.00 1.00 15.00 1.00	17.00 1.00 17.00 1.00	25.00 1.00 25.00 1.00
VERY GOOD QUALITY ROCK MASS *Tightly interlocking undisturbed rock* *with unweathered joints at 1 to 3m.* CSIR rating: RMR = 85 NGI rating: Q = 100	m s m s	2.40 0.082 4.10 0.189	3.43 0.082 5.85 0.189	5.14 0.082 8.78 0.189	5.82 0.082 9.95 0.189	8.56 0.082 14.63 0.189
GOOD QUALITY ROCK MASS *Fresh to slightly weathered rock, slightly* *disturbed with joints at 1 to 3m.* CSIR rating: RMR = 65 NGI rating: Q = 10	m s m s	0.575 0.00293 2.006 0.0205	0.821 0.00293 2.865 0.0205	1.231 0.00293 4.298 0.0205	1.395 0.00293 4.871 0.0205	2.052 0.00293 7.163 0.0205
FAIR QUALITY ROCK MASS *Several sets of moderately weathered* *joints spaced at 0.3 to 1m.* CSIR rating: RMR = 44 NGI rating: Q = 1	m s m s	0.128 0.00009 0.947 0.00198	0.183 0.00009 1.353 0.00198	0.275 0.00009 2.030 0.00198	0.311 0.00009 2.301 0.00198	0.458 0.00009 3.383 0.00198
POOR QUALITY ROCK MASS *Numerous weathered joints at 30-500mm,* *some gouge. Clean compacted waste rock* CSIR rating: RMR = 23 NGI rating: Q = 0.1	m s m s	0.029 0.000003 0.447 0.00019	0.041 0.000003 0.639 0.00019	0.061 0.000003 0.959 0.00019	0.069 0.000003 1.087 0.00019	0.102 0.000003 1.598 0.00019
VERY POOR QUALITY ROCK MASS *Numerous heavily weathered joints spaced* *<50mm with gouge. Waste rock with fines.* CSIR rating: RMR = 3 NGI rating: Q = 0.01	m s m s	0.007 0.0000001 0.219 0.00002	0.010 0.0000001 0.313 0.00002	0.015 0.0000001 0.469 0.00002	0.017 0.0000001 0.532 0.00002	0.025 0.0000001 0.782 0.00002

With: **s** a parameter defining the degree of cracking =1 for an intact sample and 0 for a completely granular material);

– m_i a parameter related to the nature of the rock (notion of cohesion, typically from 0.1 to 5).

The Hoek-Brown Resistance Envelope is not a straight line. It's a curve. At a high level of stress, the envelope curves downwards, and thus give a lower strength evaluation than that of the Mohr-Coulomb envelope.

Relationship between the quality of the rock mass and the Hoek-Brown constants

The development and application of the Hoek-Brown criterion leads to a better definition of the parameters mb and s. For a given GSI, we can calculate m_b,

$$m_b = m_i \exp{[(GSI-100)/28]} \qquad\qquad (II.26)$$

II.5 Mechanical and Hydraulic Properties of Rock Joints and Fractures

II.5.1 Normal Stiffness and Displacement

Normal deformation characteristics and normal stiffness of rock joints are important parameters for analysis and design. As discussed in an earlier chapter, a joint represents a discontinuity of stress and displacement. A natural joint always has opening aperture of less than 1 mm to a few mm. With increasing normal stresses, the opening closes,

and contact areas of the joint surfaces increase. Therefore, as shown in Figure II.25, the normal stress – normal displacement curve can be highly non-linear. The normal stiffness, slope of the curve, is therefore not a constant.
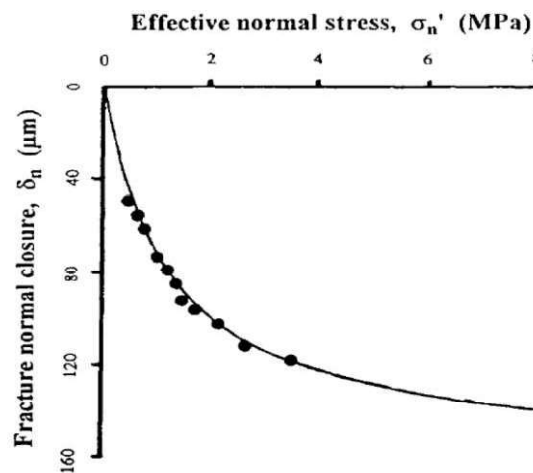

Figure II.25 Normal stress - normal displacement relation of joints in a granite

There are several mathematical models describing the normal stress – displacement relationship. In developing a joint element finite element model, [30] used a hyperbolic relation between normal stress, σn, and normal displacement, dn,

$$\frac{\sigma_n - \sigma_{ni}}{\sigma_{ni}} = A \left(\frac{d_n}{d_{max} - d_n}\right)^t$$

(II.27)

where d_{max} is the maximum possible closure, σ_{ni} = a seating pressure defining the initialnormal stress conditions for measuring normal displacement, and A and t are experimentally determined constants.

Based on a great number of laboratory experiments on matched rock fractures in dolorite, limestone, siltstone and sandstone, a hyperbolic function was proposed to express the normal effective stress-closure relation of a matched fracture. Assuming positive signs for compression and fracture closure and negative signs for tension and fracture opening, the normal effective stress-closure relation is,

$$\sigma_n = \frac{k_{ni}\, d_n}{1 - (d_n/d_{max})}$$

(II.28)

II.5.2 Shear Strength of Rock Joints and Fractures

Shear behaviour of rock joints is perhaps one of most important feature in civil engineering rock mechanics. Conditions for sliding of rock blocks along existing joints and faults at slope or excavation opening are governed by the shear strengths developed on the sliding rock discontinuities. As seen in Figure II.26a, in slope, shear is subjected to a constant normal load generated by the weight of the blocks; while in tunnel, shear is subjected to constant stiffness due to the constraints of lateral displacement.
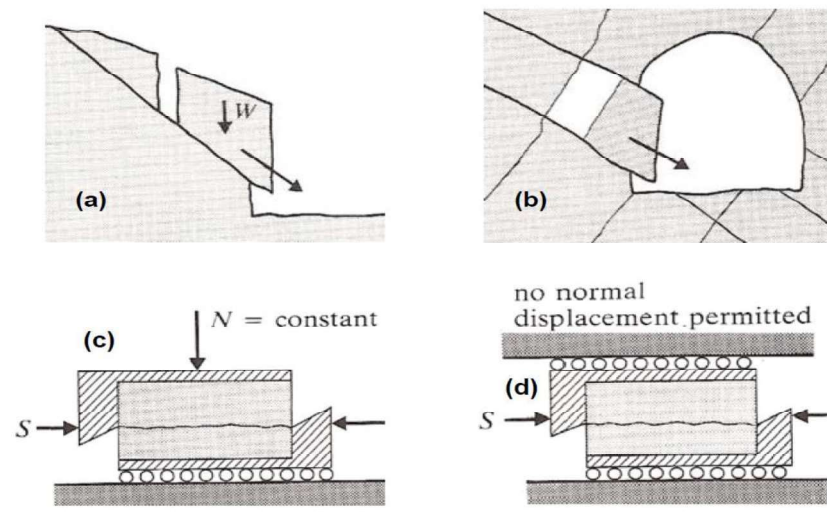
Figure II.26 *Controlled normal load (a, c) and controlled normal displacement (b, d) shearing modes and tests [54]*

The shear properties are usually determined by direct shear test shown in Figure II.26C. Detailed description of test preparation and methodology is given in a later section.

Sliding between two smooth horizontal contact surfaces gives the relationship between the friction angle φ, the normal force (N) and shear force (Fs), as Fs = N $\tan\varphi$.

It is therefore not surprised that shear tests carried out on smooth, clean fracture surfaces at controlled normal load condition generally give shear strength (s) - effective normal stress (σn) curve (Figure II.28) and it follows the simple Coulomb law:

$$\tau = \sigma_n \tan \varphi_b \qquad\qquad\qquad (II.29)$$

where φ is the effective angle of friction of the fracture surfaces. For the case shown in Figure II.26c, $\varphi = 35°$, a typical value for quartz-rich rocks.
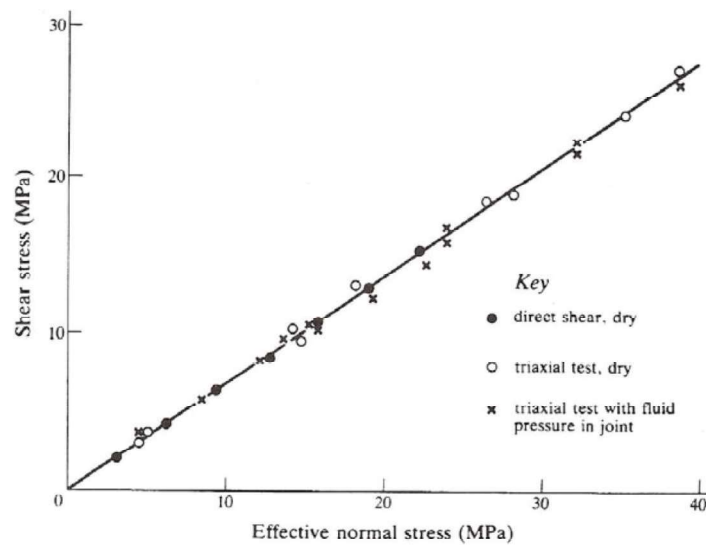
Figure II.27 Shearing of smooth quartzite surfaces under various conditions

Naturally occurring discontinuity surfaces are far from being smooth. Figure II.27 is typical of the results obtained for clean, rough fractures. As observed in the tests, shear stress quickly mobilised and reaches a peak. When shearing is progressed, the shear strength stablised to a residual level. The peak is usually term as the peak shear strength and the residual is the residual shear strength. For rough joints, peak shears strength is significantly higher than the residual strength.
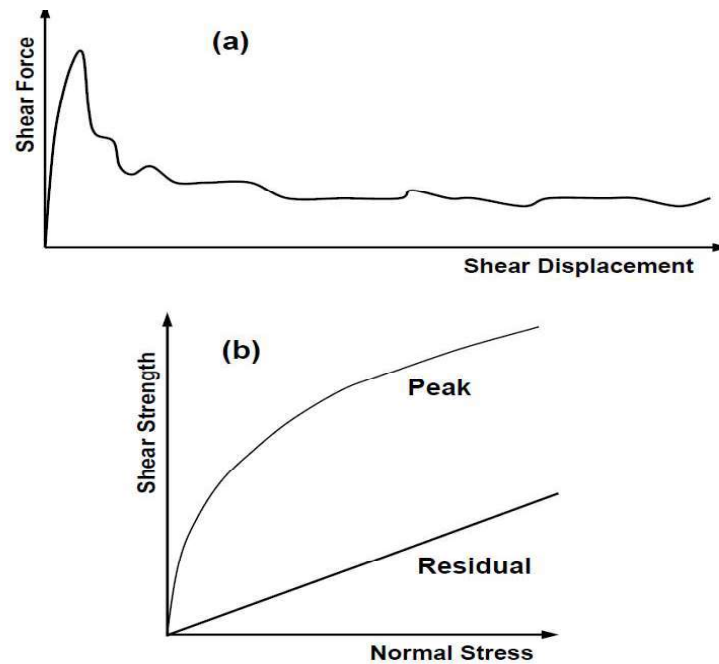
Figure II.28 Results of a direct shear test on a clean rough rock joint [10]

Observations of shear test results show that residual strength follows the linear friction law

$$\tau_r = \sigma_n \tan \varphi_r. \tag{II.30}$$

On the other hand, peak shear strength does not follow the linear fiction law. The peak strength for rough joints does not linearly proportional to normal stress. The gradient of the peak shear strength – normal stress decreases with increasing normal stress.

For idealized rough fracture models shown in Figure II.29, it is similar as sliding between two contact surfaces at an inclination.

Therefore, at low normal stress and at relatively short shear distance, shear strength is also influenced by the inclination angle,

$$\tau = \sigma_n \tan(\phi + i) \tag{II.31}$$

It was found that when the normal stress is increased above a critical value, shear stress can eventually be developed so high that it causes shear failure through the asperities.

When such shearing through asperity occurs, the shear strength is somehow related to the shear strength of the materials of the asperities. Comparing to rock joint, rock materials have higher cohesion and internal friction angle of generally around 30°.

Figure II.29 *Idealized surface roughness models and bilinear peak strength envelope*

Therefore, shear strength for a rough fracture could exhibit two features, a lower portion representing shearing by climbing th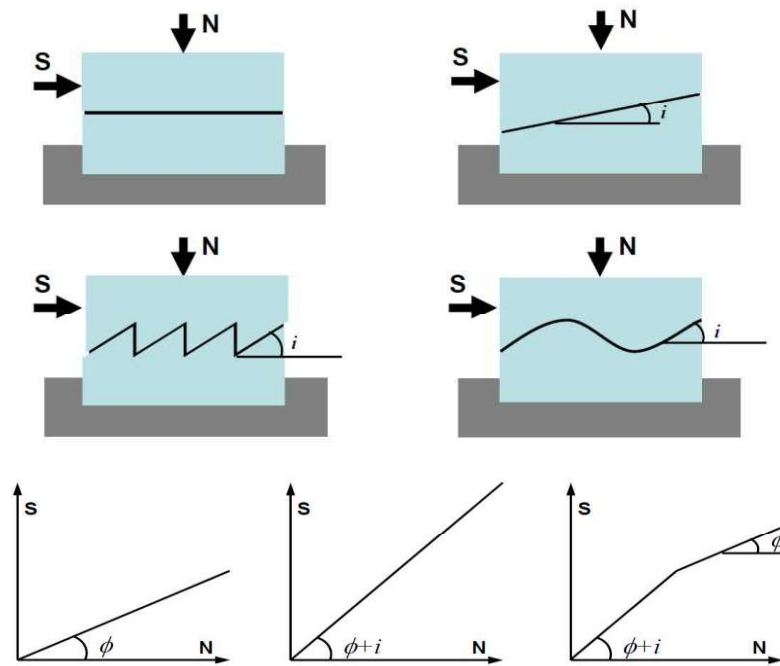e asperity angle, and an upper portion representing shearing off the asperities. This leads to a bilinear shear strength model shown in Figure II.29, and is expressed by the equations below. In the equation, σ_n' is the critical normal stress when shearing of asperity is assumed to start.

$$\tau = \sigma_n \tan(\varphi+i) \qquad \text{For } \sigma_n \leq \sigma_n' \qquad (II.32)$$

$$\tau = c + \sigma_n \tan\varphi \qquad \text{For } \sigma_n \geq \sigma_n' \qquad (II.33)$$

However, in reality, there is not clear boundary between shearing by climbing the asperity angle and shearing off the asperities. With increasing normal stress, asperity shearing off increases progressively. Therefore, the actual shear stress − normal stress relation is represented by a curve, as shown in Figure II.29. [54]

Based on extensive test results and noticing the progressive damage of asperities, Barton [36] proposed that the peak shear strengths of joints could be represented by the empirical relation below,

$$\tau = \sigma_n \tan[JRC \log_{10}(JCS/\sigma_n) + \varphi_r] \qquad (II.34)$$

where σ_n = effective normal stress, JRC = joint roughness coefficient on a scale of 1 for the smoothest to 20 for the roughest surfaces, JCS = joint wall compressive strength, and φ_r = drained residual friction angle.

II.5.3 Other Factors Affecting Joint Shear Behaviour

Roughness effect can cause shear strength to be a directional property. Figure II.30 a illustrates a case in which rough discontinuity surfaces were prepared in slate specimens.

Directional effects are not just in foliated rocks, but rather universal. As discussed in the geometrical properties, surface profile is a 3D feature while shearing is a directional activity. Surface profile along a particular direction would be different along another direction and hence gives different shear strength.
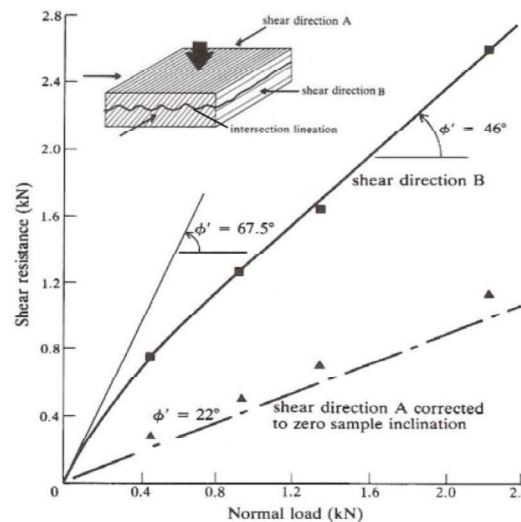
Figure II.30 *Effect of shearing direction on the shear strength of a joint in a slate* [12]

The natural discontinuities normally suffered weathering and alteration, which in term, also change the degree of matching of the discontinuity surfaces. It was found that the mismatched discontinuities generally have much lower shear strength than matched (interlocked) ones (Figure II.31).
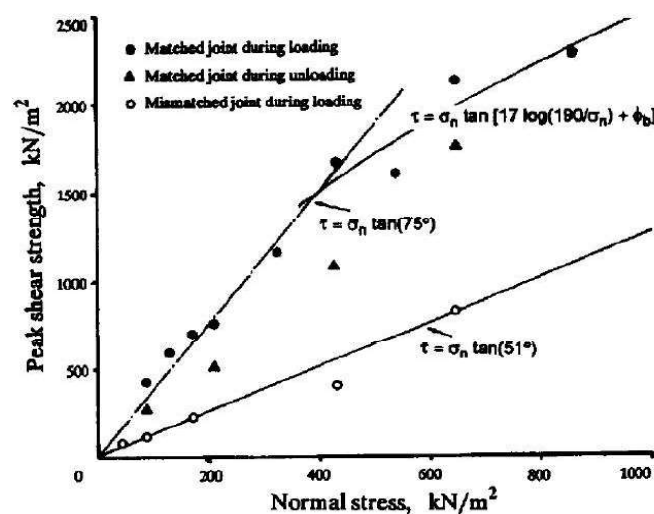
Figure II.31 *Shear strength of matched and mismatched fractures in a granite*

When a joint is wet, it has generally a lower friction angle than a dry joint. The shear strength of a wet joint is calculated use the wet friction angle. If the joint is subjected to groundwater pressure, the normal stress in the shear strength equation is the effective normal stress, i.e., total stress − water pressure.

II.5.4 Flow and Permeability of Rock Joints

From the early chapter on mechanics, it showed that flow in parallel plates is governed by the cubic flow law. The parallel plates theory is applicable to flow in rock joints. Therefore, flow and permeability of a rock joint are given as,

$$Q = \frac{w \, i \, g \, d_e^3}{12 \, v}$$

(II.35)

$$k = \frac{g \, d_e^2}{12 \, v}$$

(II.35)

where g = acceleration due to gravity, v = kinematic viscosity of the fluid, w = width of the joint, and d = aperture of smooth plates or equivalent hydraulic aperture of the rough joint.

The parallel plates theory is assumed for smooth plates and laminar flow. When it is applied to actual rock joints with rough surfaces, which are far from smooth, the equation does not truly represent the real case. The original equation therefore, does not account for the deviations from the ideal conditions due to the joint surface geometry and other effects. Somehow, modification has to be introduced to reflect the effects of joint roughness and flow path. Therefore, in the above equation, instead of the aperture of smooth plates, in natural rock joints, equivalent hydraulic aperture is used. The equivalent hydraulic aperture of a rock joint (d_e)is estimated

$$d_e = f \, d$$

(II.36)

where d is the actual aperture of the rock joint, and f is a factor that accounts for deviations from the ideal conditions that are assumed in the parallel smooth plate theory, and $f \leq 1$.

II.5.5 Correlations between Geometrical, Mechanical and Hydraulic Properties

II.5.5.1 Joint Surface Profile and Normal Stiffness

It was observed that closure under load was more complete in smooth joints than in rough joints. Conversely, rough joints in strong rocks close least under normal stress. The initial normal stiffness and maximum closure were dependent on roughness (JRC) and wall strength (JCS).

The effect of joint surface mismatch was noticed. when mismatch occurs the number of contact points may reduce, although the individual areas of contacting asperities may become larger.

II.5.5.2 Joint Surface Profile and Permeability

Many studies have been conducted on strength, deformation and conductivity coupling of rock joints in an attempt to relate these to the joint surface roughness. A relationship between equivalent hydraulic aperture and real joint aperture based on the Joint [12]

Roughness Coefficient (JRC):

$$d_e = \frac{JRC^{2.5}}{(d/d_e)^2}$$

(II.37)

where de is the equivalent hydraulic aperture and d is the real aperture of a joint.

II.5.5.3 Joint Closure and Permeability

The permeability and hydraulic aperture of rock joints changes with effective normal stress. As shown in Figure II.32, joint permeability reduces asymptotically and approaches to zero with increasing effective normal stress.
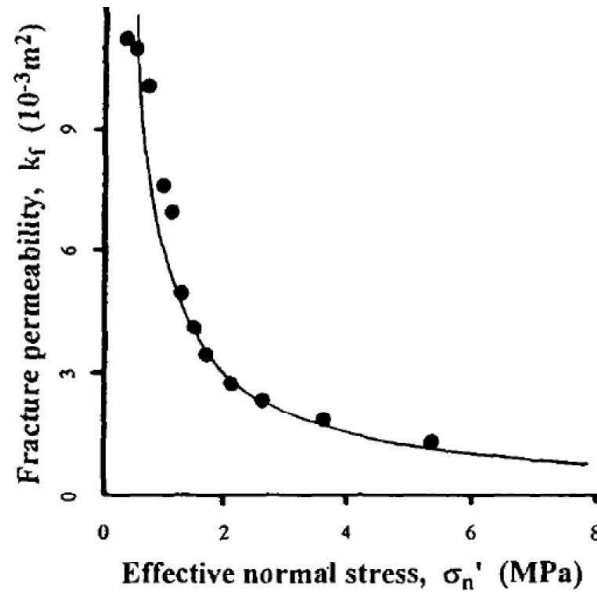

Figure II.32 *Changes of permeability with effective normal stress of rock joints in a granite*

$$\frac{k_j}{k_r} = [1 - B \, Ln \, (\frac{\sigma_n{'}}{\sigma_r{'}})]^2$$

(II.38)

where kr = the rock joint permeability at a reference effective normal stress σr', and B is a parameter dependent on surface properties of the joint.

II.5.5.4 Joint Shear, Aperture and Permeability

For an originally matched and closed joint, shear will start to general separation of the joint surface and creating larger aperture and high permeability, as illustrated in Figure II.32. As seen from the figure, when shear occurs, dilation occurs due the climbing effects. The climbing effects may be less obvious if the joint is under high normal stress. In this case, the asperities would be crashed and crashed particles may be filled in the joint. This may still result in increasing of permeability but not as significant as in the previous case.
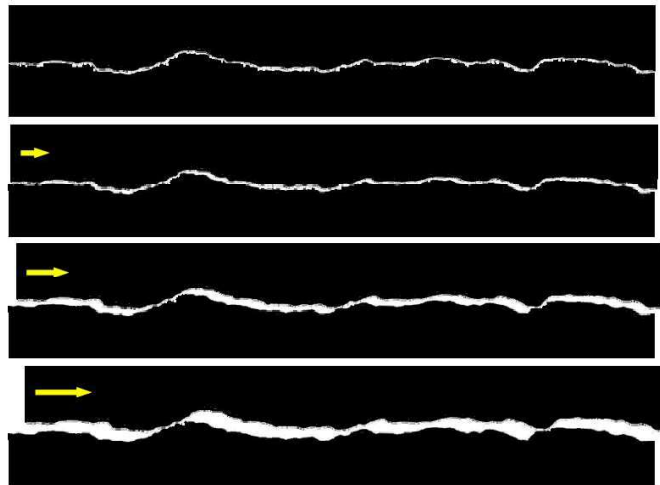

Figure II.33 Change of aperture with shear displacement of a matched joint [12]

II. 6 Rock mass classification

Rock mass classification schemes have been developing for over 100 years since [] attempted to formalise an empirical approach to tunnel design, in particular for determining support requirements. While the classification schemes are appropriate for their original application, especially if used within the bounds of the case histories from which they were developed, considerable caution must be exercised in applying rock mass classifications to other rock engineering problems.

Most of the multi-parameter classification schemes Bieniawski [25] and [22] were developed from civil engineering case histories in which all of the components of the engineering geological character of the rock mass were included; Different classification systems place different emphases on the various

Rock quality designation index (RQD) The Rock Quality Designation index (RQD) was developed by Deere [23] to provide a quantitative estimate of rock mass quality from drill core logs. RQD is defined as the percentage of intact core pieces longer than 100 mm in the total length of core. The core should be at least NW size (54.7 mm in diameter) and should be drilled with a double-tube core barrel. The correct procedures for measurement of the length of core pieces and the calculation of RQD are summarised in Figure II.33.
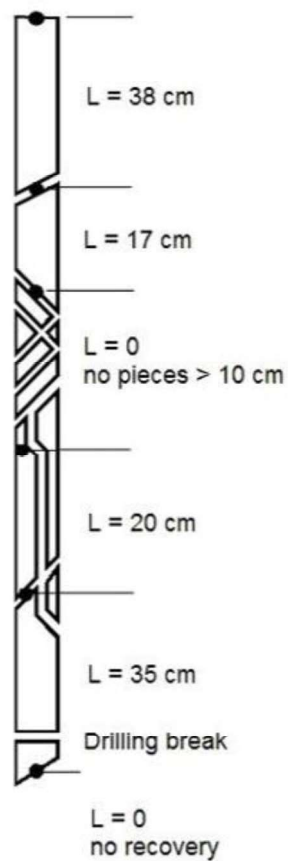
$$Total\ length\ of\ core\ run = 200cms \qquad\qquad (II.39)$$

$$RQD = \frac{\sum length\ of\ core\ pieces > 10\ cm\ length}{Total\ length\ of\ core\ run} x100 \qquad (II.40)$$

$$RQD = \frac{38 + 17 + 20}{200}\ x\ 100 = 55\% \qquad\qquad (II.41)$$

Figure II.33 *Procedure for measurement and calculation of RQD [14]*

Table II.3 Rock mass quality classification according to RQD [14]

RQD	Rock Mass Quality
< 25	Very poor
25 − 50	Poor
50 − 75	Fair
75 − 90	Good
99 − 100	Excellent

RQD has been widely accepted as a measure of fracturing degree of the rock mass. His parameter has been used in the rock mass classification systems, including the RMR and the Q systems.

The RQD may be estimated from the number of discontinuities per unit volume. The suggested relationship for clay-free rock masses is:

$$RQD = 115 - 3.3 \, Jv \qquad\qquad (II.42)$$

where Jv is the sum of the number of joints per unit length for all joint (discontinuity) sets known as the volumetric joint count. The use of the volumetric joint count can be quite useful in reducing this directional dependence.

II.6.1 Rock Mass Rating (RMR) system

Geomechanics Classification Bieniawski [25] published the details of a rock mass classification called the Geomechanics Classification or the Rock Mass Rating (RMR) system. Over the years, this system has been successively refined as more case records have been examined and the reader should be aware that Bieniawski has made significant changes in the ratings assigned to different parameters. The following six parameters are used to classify a rock mass using the RMR system:

1. Uniaxial compressive strength of rock material.
2. Rock Quality Designation (RQD).
3. Spacing of discontinuities.
4. Condition of discontinuities.
5. Groundwater conditions.
6. Orientation of discontinuities.

The Rock Mass Rating system is presented in Table II.4, giving the ratings for each of the six parameters listed above. These ratings are summed to give a value of RMR. The following example illustrates the use of these tables to arrive at an RMR value.

Table II.4 Rock Mass Rating System [25]

(a) Five basic rock mass classification parameters and their ratings									
1.	Strength of intact rock material	Point load strength index (MPa)	> 10	4 – 10	2 – 4	1 – 2			
		Uniaxial compressive strength (MPa)	> 250	100 – 250	50 – 100	25 – 50	5 – 25	1 – 5	< 1
	Rating		15	12	7	4	2	1	0
2.	RQD (%)		90 – 100		75 – 90	50 – 75	25 – 50		< 25
	Rating		20		17	13	8		3
3.	Joint spacing (m)		> 2		0.6 – 2	0.2 – 0.6	0.06 – 0.2		< 0.06
	Rating		20		15	10	8		5
4.	Condition of joints		not continuous, very rough surfaces, unweathered, no separation	slightly rough surfaces, slightly weathered, separation <1 mm	slightly rough surfaces, highly weathered, separation <1 mm	continuous, slickensided surfaces, or gouge <5 mm thick, or separation 1–5 mm		continuous joints, soft gouge >5 mm thick, or separation >5 mm
	Rating		30	25	20	10		0
5.	Groundwater	inflow per 10 m tunnel length (l /min), or	none	< 10	10 – 25	25 – 125		> 125
		joint water pressure/major in situ stress, or	0	0 – 0.1	0.1 – 0.2	0.2 – 0.5		> 0.5
		general conditions at excavation surface	completely dry	damp	wet	dripping		flowing
	Rating		15	10	7	4		0

adjustment made to account for joint orientation, a final RMR rating is obtained, it can be also expressing in rock mass class, as shown in Table II.5. The table also gives the meaning of rock mass classes in terms of stand-up time, equivalent rock mass cohesion and friction angle.

Table II.5 Rating adjustment for joint orientations[25]

Strike and dip orientation of joints		very favourable	favourable	fair	unfavourable	very unfavourable
Rating	tunnels	0	– 2	– 5	– 10	– 12
	foundations	0	– 2	– 7	– 15	– 25
	slopes	0	– 5	– 25	– 50	– 60

Table II.6 Effects of joint orientation in tunneling [25]

Strike perpendicular to tunnel axis				Strike parallel to tunnel axis		Dip 0° – 20°
Drive with dip		Drive against dip				
Dip 45° – 90° very favourable	Dip 20° – 45° favourable	Dip 45° – 90° fair	Dip 20° – 45° unfavourable	Dip 45° – 90° very unfavourable	Dip 20° – 45° fair	irrespective of strike fair

Table II.7 Rock mass classes determined from total ratings and meaning

RMR Ratings	81 – 100	61 – 80	41 – 60	21 – 40	< 20
Rock mass class	A	B	C	D	E
Description	very good rock	good rock	fair rock	poor rock	very poor rock
Average stand-up time	10 year for 15 m span	6 months for 8 m span	1 week for 5 m span	10 hours for 2.5 m span	30 minutes for 0.5 m span
Rock mass cohesion (KPa)	> 400	300 – 400	200 – 300	100 – 200	< 100
Rock mass friction angle	> 45°	35° – 45°	25° – 35°	15° – 25°	< 15°

II.6.2 Rock Tunnel Quality Q-System

The Q-system was developed as a rock tunnelling quality index by the Norwegian Geotechnical Institute (NGI) (Barton et al 1974) [34]. The system was based on evaluation of a large number of case histories of underground excavation stability, and is an index for the determination of the tunnelling quality of a rock mass. The numerical value of this index Q is defined by:

$$Q = \frac{RQD}{J_n} \frac{J_r}{J_a} \frac{J_w}{SRF} \qquad (II.42)$$

RQD is the Rock Quality Designation measuring the fracturing degree.

Jn is the joint set number accounting for the number of joint sets.

Jr is the joint roughness number accounting for the joint surface roughness.

Ja is the joint alteration number indicating the degree of weathering, alteration and filling.

Jw is the joint water reduction factor accounting for the problem from groundwater pressure, and SRF is the stress reduction factor indicating the influence of in situ stress.

Table II.8 Rock mass classification Q system [22]

1.	**Rock Quality Designation**		**RQD**
A	Very Poor		$0 - 25$
B	Poor		$25 - 50$
C	Fair		$50 - 75$
D	Good		$75 - 90$
E	Excellent		$90 - 100$
Note:	(i) Where RQD is reported or measured as ≤ 10 (including 0), a nominal value of 10 is used to evaluate Q. (ii) RQD interval of 5, i.e., 100, 95, 90, etc., are sufficiently accurate.		

2.	**Joint Set Number**		J_n
A	Massive, no or few joints		$0.5 - 1$
B	One joint set		2
C	One joint set plus random joints		3
D	Two joint set		4
E	Two joint set plus random joints		6
F	Three joint set		9
G	Three joint set plus random joints		12
H	Four or more joint sets, heavily jointed		15
J	Crushed rock, earthlike		20
Note:	(i) For intersections, use $(3.0 \times J_n)$. (ii) For portals, use $(2.0 \times J_n)$.		

3.	**Joint Roughness Number**		J_r
(a)	*Rock-wall contact, and (b) Rock wall contact before 10 cm shear*		
A	Discontinuous joints		4
B	Rough or irregular, undulating		3
C	Smooth, undulating		2
D	Slickensided, undulating		1.5
E	Rough or irregular, planar		1.5
F	Smooth, planar		1.0
G	Slickensided, planar		0.5
Note:	(i) Descriptions refer to small and intermediate scale features, in that order.		
(c)	*No rock-wall contact when sheared*		
H	Zone containing clay minerals thick enough to prevent rock-wall contact		1.0
J	Sandy, gravelly or crushed zone thick enough to prevent rock-wall contact		1.0
Note:	(ii) Add 1.0 if the mean spacing of the relevant joint set ≥ 3 m. (iii) $J_r = 0.5$ can be used for planar slickensided joints having lineations, provided the lineations are oriented for minimum strength.		

4.	**Joint Alteration Number**	ϕ_r approx.	J_a
(a)	*Rock-wall contact (no mineral fillings, only coatings)*		
A	Tight healed, hard, non-softening, impermeable filling, i.e., quartz or epidote	–	0.75
B	Unaltered joint walls, surface staining only	$25 - 35°$	1.0
C	Slightly altered joint walls. Non-softening mineral coating, sandy particles, clay-free disintegrated rock, etc.	$25 - 30°$	2.0
D	Silty- or sandy-clay coatings, small clay fraction (non-softening)	$20 - 25°$	3.0
E	Softening or low friction mineral coatings, i.e., kaolinite or mica. Also chlorite, talc, gypsum, graphite, etc., and small	$8 - 16°$	4.0

(b)	**Rock wall contact before 10 cm shear (thin mineral fillings)**		
F	Sandy particles, clay-free disintegrated rock, etc.	25 – 30°	4.0
G	Strongly over-consolidated non-softening clay mineral fillings (continuous, but < 5 mm thickness)	16 – 24°	6.0
H	Medium or low over-consolidated softening clay mineral fillings (continuous, but < 5 mm thickness)	12 – 16°	8.0
J	Swelling-clay fillings, i.e., montmorillonite (continuous, but < 5 mm thickness). Value of J_a depends on percent of swelling clay size particles, and access to water, etc.	6 – 12°	8 – 12
(c)	**No rock-wall contact when sheared (thick mineral fillings)**		
K, L, M	Zones or bands of disintegrated or crushed rock and clay (see G, H, J for description of clay condition)	6 – 24°	6, 8, or 8 – 12
N	Zones or bands of silty- or sandy-clay, small clay fraction (non-softening)	-	5
O, P, R	Thick, continuous zones or bands of clay (see G, H, J for clay condition description)	6 – 24°	10, 13, or 13 – 20

5.	**Joint Water Reduction Factor**	Water pressure	J_w
A	Dry excavation or minor inflow, i.e., < 5 l/min locally	< 1 (kg/cm²)	1.0
B	Medium inflow or pressure, occasional outwash of joint fillings	1 – 2.5	0.66
C	Large inflow or high pressure in competent rock with unfilled joints	2.5 – 10	0.5
D	Large inflow or high pressure, considerable outwash of joint fillings	2.5 – 10	0.33
E	Exceptionally high inflow or water pressure at blasting, decaying with time	> 10	0.2 – 0.1
F	Exceptionally high inflow or water pressure continuing without noticeable decay	> 10 (kg/cm²)	0.1 – 0.05
Note:	(i) Factors C to F are crude estimates. Increase J_w if drainage measures are installed. (ii) Special problems caused by ice formation are not considered.		

6.	**Stress Reduction Factor**	SRF
(a)	**Weakness zones intersecting excavation, which may cause loosening of rock mass when tunnel is excavated**	
A	Multiple occurrences of weakness zones containing clay or chemically disintegrated rock, very loose surrounding rock (any depth)	10
B	Single weakness zone containing clay or chemically disintegrated rock (depth of excavation ≤ 50 m)	5
C	Single weakness zone containing clay or chemically disintegrated rock (depth of excavation > 50 m)	2.5
D	Multiple shear zones in competent rock (clay-free) (depth of excavation ≤ 50 m)	7.5
E	Single shear zone in competent rock (clay-free) (depth of excavation ≤ 50 m)	5
F	Single shear zone in competent rock (clay-free) (depth of excavation > 50 m)	2.5
G	Loose, open joint, heavily jointed (any depth)	5
Note:	(i) Reduce SRF value by 25-50% if the relevant shear zones only influence but not intersect the excavation.	

(b)	Competent rock, rock stress problems	σ_c / σ_1	σ_θ / σ_c	SRF
H	Low stress, near surface, open joints	> 200	< 0.01	2.5
J	Medium stress, favourable stress condition	200 – 10	0.01 – 0.03	1
K	High stress, very tight structure. Usually favourable to stability, may be unfavourable to wall stability	10 – 5	0.3 – 0.4	0.5 – 2
L	Moderate slabbing after > 1 hour in massive rock	5 – 3	0.5 - 0.65	5 – 50
M	Slabbing and rock burst after a few minutes in massive rock	3 – 2	0.65 – 1	50 – 200
N	Heavy rock burst (strain-burst) and immediate dynamic deformation in massive rock	< 2	> 1	200 – 400
Note:	(ii) For strongly anisotropic virgin stress field (if measured): when $5 \le \sigma_1 / \sigma_3 \le 10$, reduce σ_c to 0.75 σ_c; when $\sigma_1 / \sigma_3 > 10$, reduce σc to 0.5 σ_c; where σ_c is unconfined compressive strength, σ_1 and σ_3 are major and minor principal stresses, and σ_θ is maximum tangential stress (estimated from elastic theory). (iii) Few cases records available where depth of crown below surface is less than span width. Suggest SRF increase from 2.5 to 5 for such cases (see H).			
(c)	Squeezing rock: plastic flow in incompetent rock under the influence of high rock pressure		σ_θ / σ_c	SRF
O	Mild squeezing rock pressure		1 – 5	5 – 10
P	Heavy squeezing rock pressure		5	10 – 20
Note:	(vi) Cases of squeezing rock may occur for depth $H > 350\ Q^{1/3}$. Rock mass compressive strength can be estimated from $Q = 7\ \gamma\ Q^{1/3}$ (MPa), where γ = rock density in g/cm^3.			
(d)	Swelling rock: chemical swelling activity depending on presence of water			SRF
R	Mile swelling rock pressure			5 – 10
S	Heavy swell rock pressure			10 – 15
Note:	Jr and Ja classification is applied to the joint set or discontinuity that is least favourable for stability both from the point of view of orientation and shear resistance.			

Table II.9 Rock mass quality rating according to Q values [22]

| Q-value	Class	Rock mass quality
400 ~ 1000	A	Exceptionally Good
100 ~ 400	A	Extremely Good
40 ~ 100	A	Very Good
10 ~ 40	B	Good
4 ~ 10	C	Fair
1 ~ 4	D	Poor
0.1 ~ 1	E	Very Poor
0.01 ~ 0.1	F	Extremely Poor
0.001 ~ 0.01	G	Exceptionally Poor

In relating the value of the index Q to the stability and support requirements of underground excavations, Barton et al. (1974) defined an additional parameter which they called the Equivalent Dimension, De, of the excavation. This dimension is obtained by dividing the span, diameter or wall height of the excavation by a quantity called the Excavation Support Ratio, ESR. Hence:

De = Excavation span, diameter or height (m) / Excavation Support Ratio ESR

The value of ESR is related to the intended use of the excavation and to the degree of security which is demanded of the support system installed to maintain the stability of the excavation. Barton et al.

Table II.10 Excavation Support Ratio (ESR) for various tunnel categories [10]

	Excavation Category	ESR
A	Temporary mine openings	3-5
B	Permanent mine openings, water tunnels for hydro power (excluding high pressure penstocks), pilot tunnels, drifts and headings for large excavations	1.6
C	Storage rooms, water treatment plants, minor road and railway tunnels, surge chambers, access tunnels.	1.3
D	Power stations, major road and railway tunnels, civil defence chambers, portal intersections.	1.0
E	Underground nuclear power stations, railway stations, sports and public facilities, factories	0.8
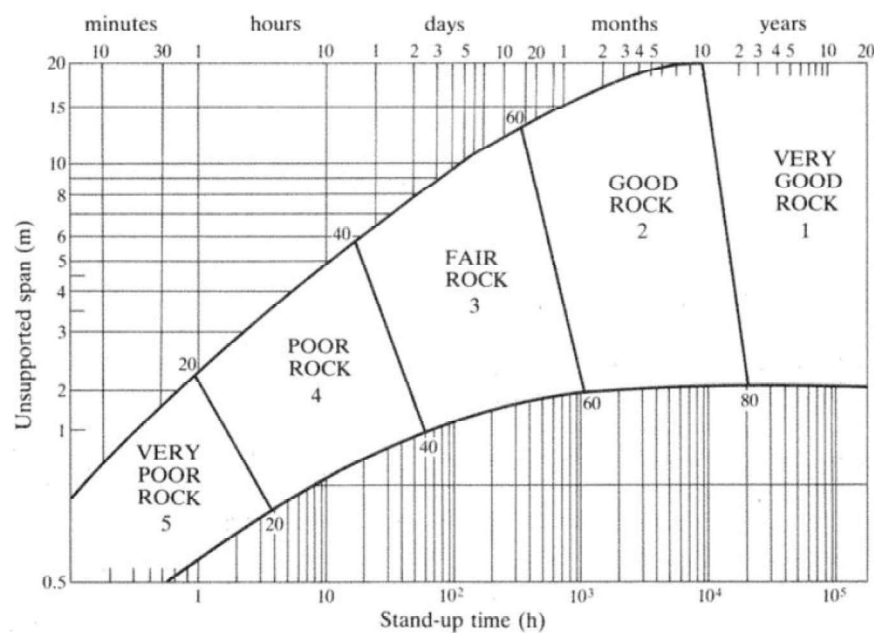
Figure II.35 Support design based on Q value [10]

II.6.3 Geological Strength Index GSI System

The Geological Strength Index (GSI) was introduced by Hoek in 1994. It was aimed to estimate the reduction in rock mass strength for different geological conditions. This system is presented in Tables II.11 The system gives a GSI value estimated from rock mass structure and rock discontinuity surface condition. The direct application of GSI value is to estimate the parameters in the Hoek-Brown strength criterion for rock masses. [24]
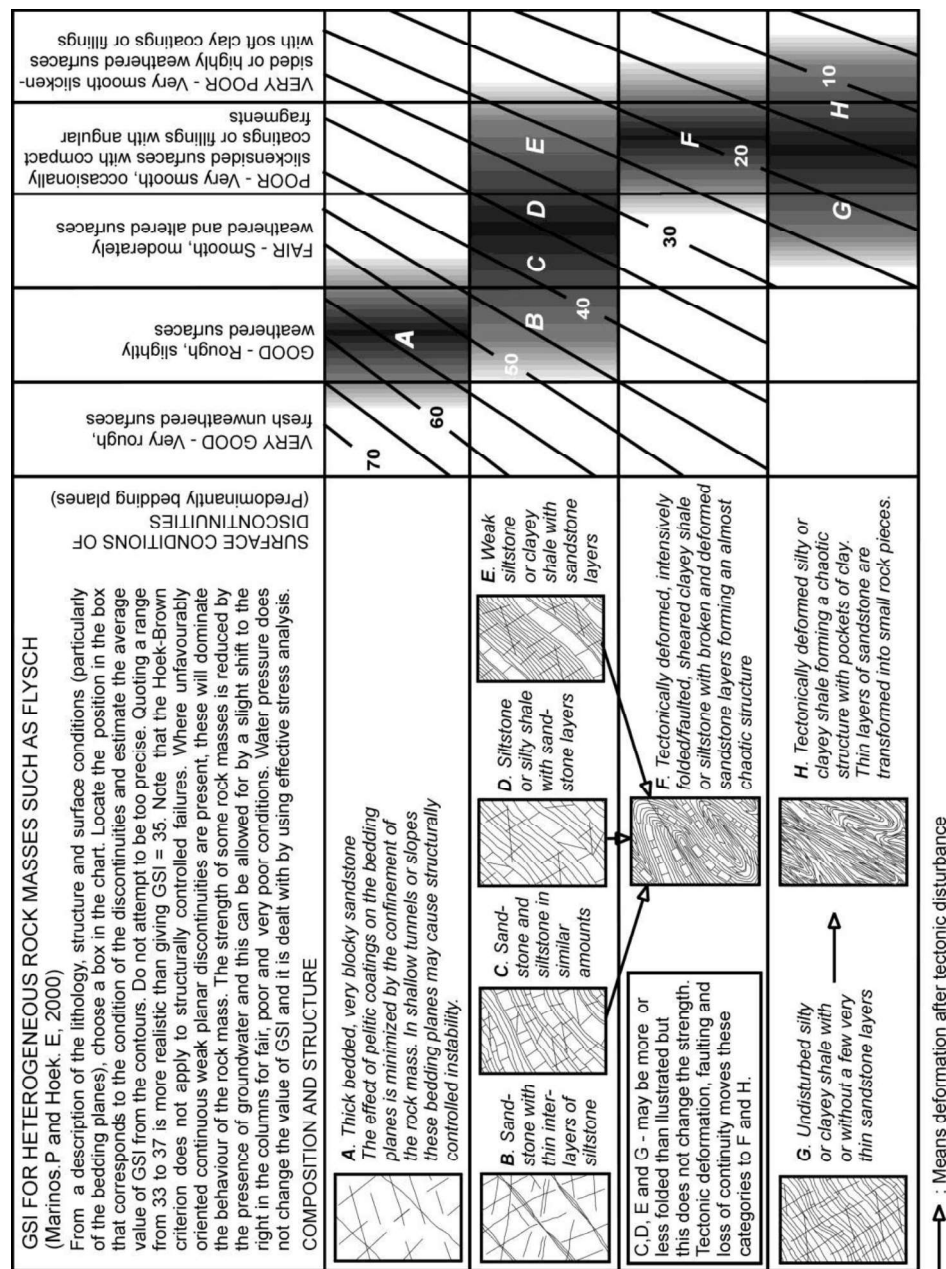
Figure II.36 *Estimate of Geological Strength Index GSI for heterogeneous rock masses, [11]*

Table II.12 *Rock mass classes determined from GSI* [10]

GSI Value	76 − 95	56 − 75	36 − 55	21 − 35	< 20
Rock Mass Quality	Very good	Good	Fair	Poor	Very poor

One of the practical problems that arises when assessing the value of GSI in the field is related to blast damage. As illustrated in Figure II.37, there is a considerable difference in the appearance of a rock face which has been excavated by controlled blasting and a face which has been damaged by bulk blasting. Wherever possible, the undamaged face should be used to estimate the value of GSI since the overall aim is to determine the properties of the undisturbed rock mass
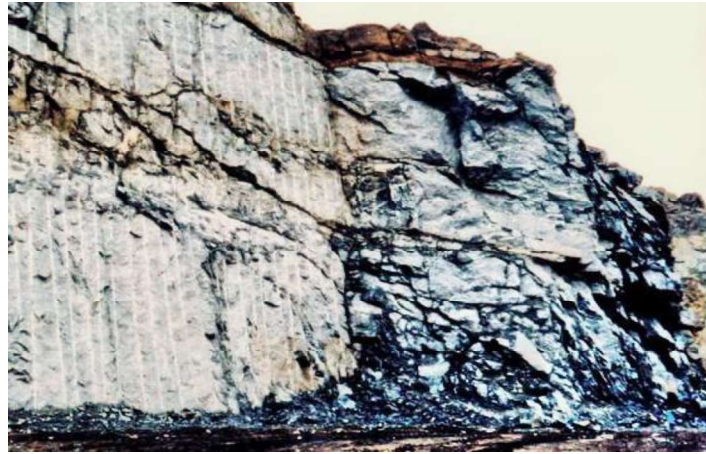
Figure II.37 *Comparison between the results achieved using controlled blasting (on the left) and normal bulk blasting for a surface excavation in gneiss.11]*

The influence of blast damage on the near surface rock mass properties has been considered in thef the Hoek-Brown criterion

$$m_b = m_i \, exp\left(\frac{GSI-100}{28-14D}\right)$$

(II.44)

$$s = exp\left(\frac{GSI - 100}{9 - 3D}\right)$$

(II.45)

$$a = \frac{1}{2} + \frac{1}{6}\left(e^{-GSI/15} - e^{-20/3}\right)$$

(II.46)

D is a factor which depends upon the degree of disturbance due to blast damage and stress relaxation. It varies from 0 for undisturbed in situ rock masses to 1 for very disturbed rock masses. Guidelines for the selection of D are presented in Figure II.38.

Note that the factor D applies only to the blast damaged zone. It should not be applied to the entire rock mass. For example, in tunnels the blast damage is generally limited to a 1 to 2 m thick zone around the tunnel, and this should be incorporated into numerical models as a different and weaker material than the surrounding rock mass.

Appearance of rock	Description of rock mass	Suggested D value
	Excellent quality-controlled blasting or excavation by Tunnel Boring Machine results in minimal disturbance to the confined rock mass surrounding a tunnel.	D = 0
	Mechanical or hand excavation in poor quality rock masses (no blasting) results in minimal disturbance to the surrounding rock mass. Where squeezing problems result in significant floor heave, disturbance can be severe unless a temporary invert, as shown in the photograph, is placed.	Mechanical excavation D = 0 No invert D = 0.5
	Very poor-quality blasting in a hard rock tunnel results in severe local damage, extending 2 or 3 m, in the surrounding rock mass.	D = 0.8
	Small scale blasting in civil engineering slopes results in modest rock mass damage, particularly if controlled blasting is used as shown on the left-hand side of the photograph. However, stress relief results in some disturbance.	D = 0.7 Good blasting D = 1.0 Poor blasting
	Very large open pit mine slopes suffer significant disturbance due to heavy production blasting and also due to stress relief from overburden removal. In some softer rocks excavation can be carried out by ripping and dozing and the degree of damage to the slopes is less.	D = 1.0 Production blasting D = 0.7

Figure II.38 *Guidelines for estimating the disturbance factor D.[11]*

CHAPTER III

ROCK SLOPE STABILITY

Chapitre III

Rock Slope Stability

III.1 Introduction

Slope stability has significant importance in open-pit excavation for the purpose of profitability. To achieve optimum slope design, visual observation of the condition of benches followed by engineering judgments, rock testing, geomechanic classification, and numerical analysis need to carry out.

The various design parameters of rock mass classification, such as, rock mass rating (RMR), slope mass rating (SMR) are used for pit slope design and support design. *[21]*

The several modes of possible failures, such as, planar, wedge and circular failure have to be analysed. Computer software programme 'Galena' is predominantly used for analysis of different modes of failures parameters, such as, slope angles and slope height are used to evolve safe and cost-effective stripping ratio and optimum exploitation mechanisms.

The factor of safety less than unity signifies a potential unstable zone. The stereo net analysis provides good presentation of structural data generated during the field mapping. The data on the joint orientation and the angle of internal friction is used as input for performing analysis.

In the majority of the cases, slope failure in rock mass are governed by joints that develop across surface form by one or several sets of joints. To determine the safe optimum slope angle and introduction of intensive of slope movements, slope stability investigation need to be carried for stability analysis.

Potential failures like toppling, planar, wedge is applicable to the jointed rock masses. In highly fractured or decompressed rock, circular failure may occur. Occurrences of any one fracture mode or combination thereof is controlled by the relative orientation of quarry face/dominant joint face, dominant joint sets, shear strength characteristics of joints, and their continuity/frequency. Ground water that influences the stability of quarry is responsible for major slope failures. Piezometer can be installed to measure the ground water pressure. The different types of failures are shown in Figure III.1.
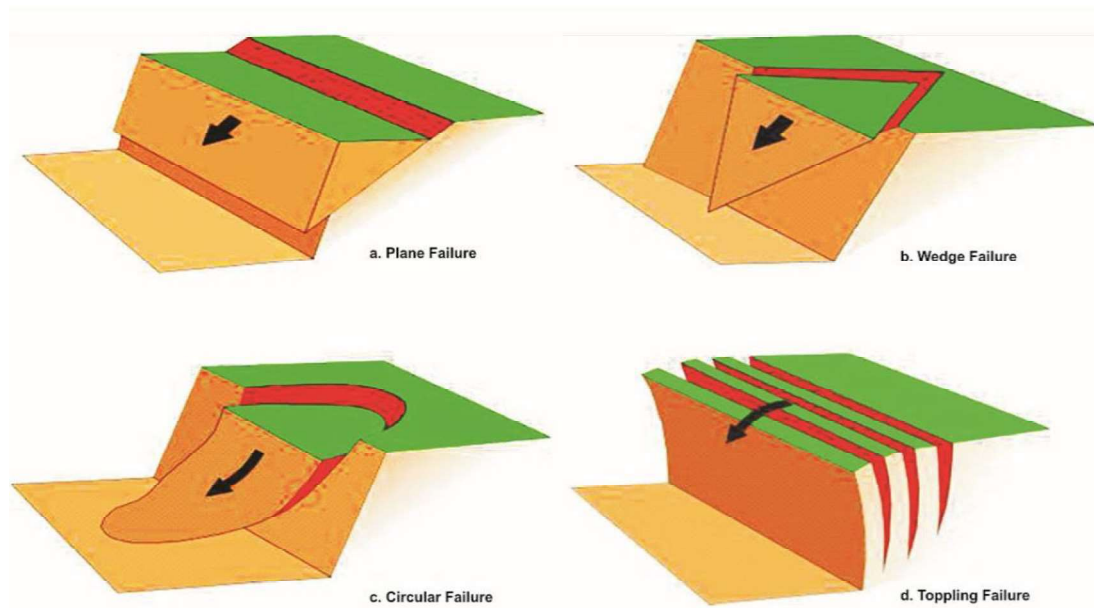
Figure III.1 *simplified illustration of most slope failure modes [15]*

III.2 Types of slope stability

III.2.1 Plane Failure

Simple plane failure is the easiest form of rock slope failure to analyse. It occurs when a discontinuity striking approximately parallel to the slope face and dipping at a lower angle intersects the slope face, enabling the material above the discontinuity to slide. *[13]*

Plane failure occurred along the prevalent or continuous joints dipping towards the slope with strike near to parallel to the slope face. It occurs when a geological discontinuity such as bedding plane strikes parallel to the slope face and dip into the excavation at an angle greater than the angle of friction. It has been shown in Figure III.2. *[15]*

there are two unstable conditions that occur when critical joint dip is less than the slope and when the mobilised shear strength in the joint is not enough to ensure stability. Plane failure depends on joint continuity and also when the difference between dip direction of the slope and failed joints is less than 90^0.
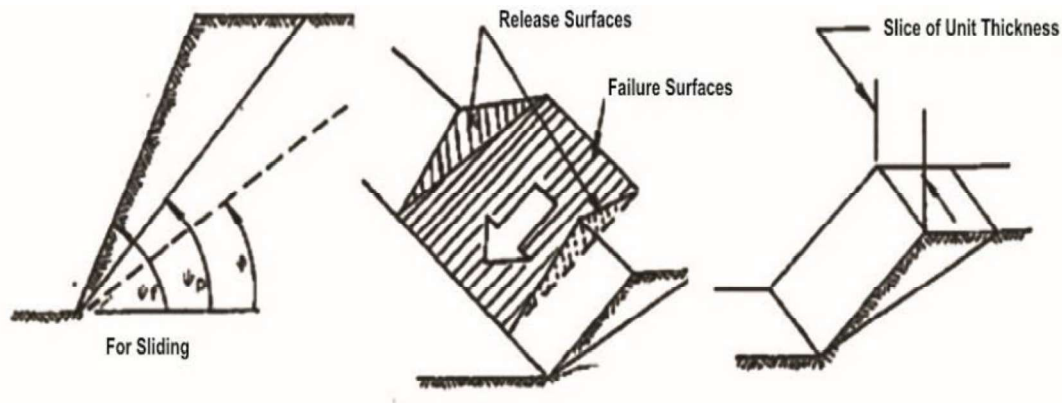
Figure III.2 *Plane failure [15]*

III.2.2 Wedge Failure

Wedge failure occurs along two joints from different sets with intersecting dip towards slope. When two discontinuities strike obliquely across the slope face and their line of interaction daylights in the slope face, the wedge of rock resting on these discontinuities will slide down the line of interaction, provided that the inclination of this line is significantly greater than the angle of friction. It is depicted   in Figure III.3. A wedge failure depends on the geometry, multiple the joint mobilize shear strength.

The size of the failure depends on the joint frequency and is usually minor as compared to plane failure.
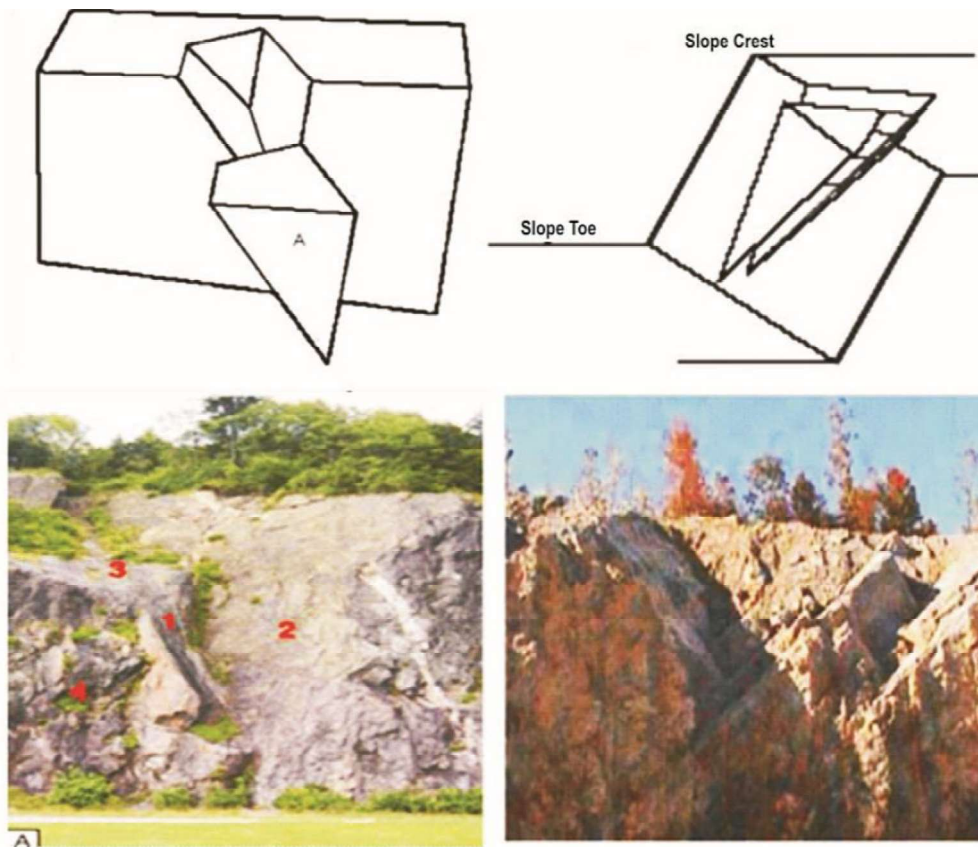
Figure III.3 *Wedge failure [15]*

III.2.3 Step-Path Failure

Step path failure is similar to plane shear failure, but the sliding is due to the combined mechanism of multiple discontinuities or the tensile failure of the intact rock connecting members of the master joint set.

III.2.4 Raveling

Weathering of material and expansion and contraction associated with freeze-thaw cycles are principle causes of raveling. This type of failure generally produces small rockfalls, not massive failures. *[21]*

III.2.5 Toppling Failure

Toppling failure occurs along a prevalent and is continuous set of joint, which dip against the slope, with strike near parallel to slope face. Joint slips between them and is frequently weathered. In practice, two types of instability can exist, such as, minor toppling occur near the surface of the slope and dip toppling which can produce both determinations. In both the cases failure develops slowly. Surface toppling can cause rock falls but dip toppling seldom fail suddenly. The difference between the dip direction value of the slope and joints is more than 90^0. The details of failure modes are illustrated in Figure III.4. *[15]*
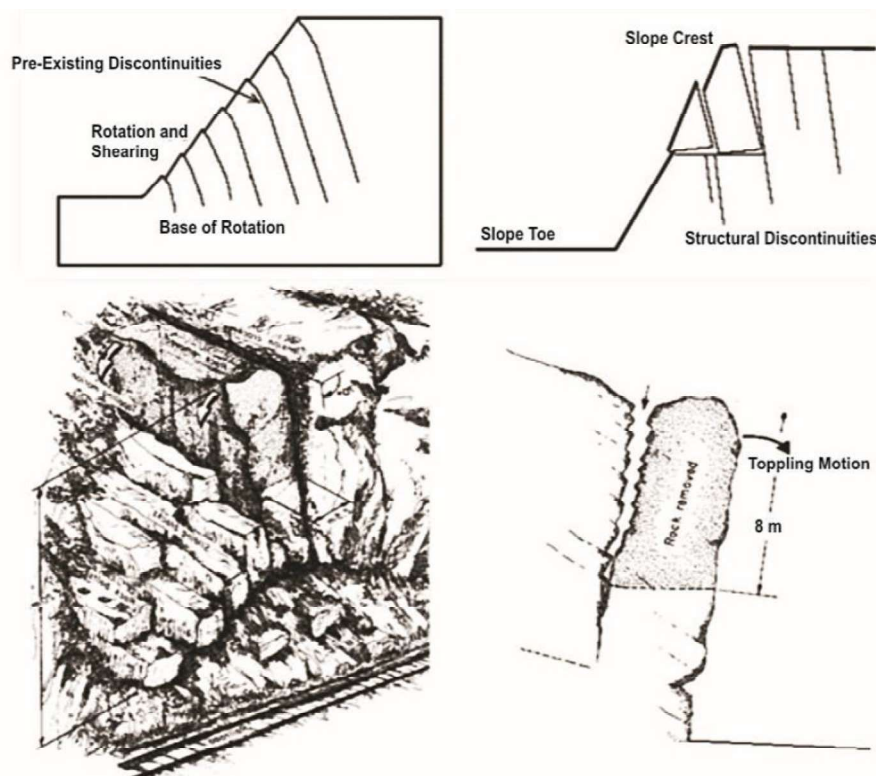
Figure III.4 *Toppling failure [15]*

III.2.6 Circular Failure

Circular failures generally occur in weak rock or soil slopes. Failures of this type do not necessarily occur along a purely circular arc, some form of curved failure surface is normally apparent. Circular shear failures are influenced by the size and mechanical properties of the particles in the soil or rock mass.

When the material is very weak as in tailing dump, in soil slope or when the rock slope or when the rock mass is very heavily jointed or broken, as in the waste rock dump, the failure is defined by a single discontinuity surface but will tend to follow the circular failure (see Figure III.5).

Face   Toe   Deep-Seated
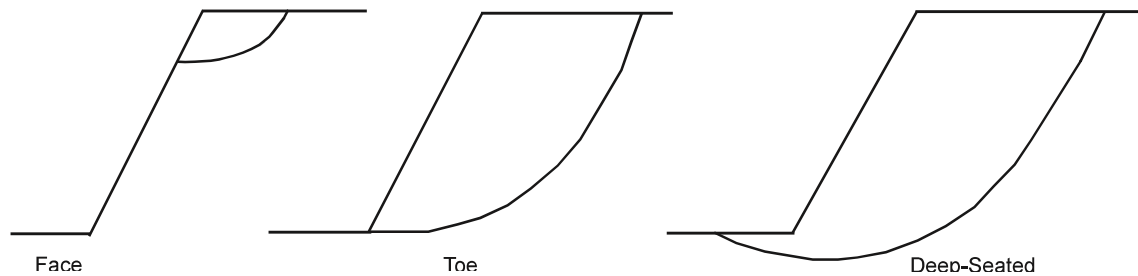
Figure III.5 *Circular Failure [11]*

Circular failure is classified into three types depending on the area that is affected by the failure surface. They are:

- **Slope Failure**

In this type of failure, the arc of the rupture surface meets the slope above the toe of the slope. This happens when the slope angle is very high and the soil close to the toe possess high strength.

- **Toe Failure**

In this type of failure, the arc of the rupture surface meets the slope at the toe.

- **Base Failure**

In this type of failure, the arc of the failure passes below the toe and in to base of the slope. This happens when the slope angle is low and the soil below the base is softer and more plastic than the soil above the base.

III.3 Groundwater flow

The incidence of slope failure in working mines during or shortly after periods of intense rainfall indicates the degree to which rainfall and subsequent movement of groundwater affect slope stability. A knowledge of groundwater conditions is needed for the analysis and design of slopes. The groundwater regime is often the only natural parameter that can be economically changed to increase the stability of slopes. Water affects the stability of slopes in the following ways:

    a)   By generating pore pressure, both positive and negative, which alter stress conditions;

b)   By changing the bulk density of the slope formimg material;

c)   By both internal and external erosion; and

d)   By changing the material constituents of the slope forming material.

III.3.1 Factors Affecting Slope Stability

III.3.1.1 Cohesion

It is the characteristic property of a rock or soil that measures how well it resists being deformed or broken by forces, such as, gravity. In soils/rocks true cohesion is caused by electrostatic forces in stiff over consolidated clays, cemented by Fe_2O_3, $CaCO_3$, NaCl, etc. and root cohesion.

However the apparent cohesion is caused by negative capillary pressure and pore pressure response during undrained loading. Slopes having rocks/soils with less cohesion tend to be less stable. *[21]*

III.3.1.2 Angle of Internal Friction

Angle of internal friction is the angle (φ), measured between the normal force (N) and resultant force (R), that is attained when failure just occurs in response to a shearing stress (S).

Its tangent (S/N) is the coefficient of sliding friction. It is a measure of the ability of a unit of rock or soil to withstand a shear stress. This is affected by particle roundness and particle size. Lower roundness or larger median particle size results in larger friction angle. It is also affected by quartz content.

III.3.1.3 Lithology

•   The rock materials forming a pit slope determines the rock mass strength modified by discontinuities, faulting, folding, old workings and weathering.

•   Low rock mass strength is characterised by circular raveling and rock fall instability like the formation of slope in massive sandstone restrict stability.

•   Pit slopes having alluvium or weathered rocks at the surface have low shearing strength and the strength gets further reduced if water seepage takes place through them. These types of slopes must be flatter.

III.3.1.4 Ground Water

It causes the following:

•   alters the cohesion and frictional parameters;

•   reduce the normal effective stress;

•   causes increased up thrust and driving water forces and has adverse effect on the stability of the slopes. Physical and chemical effect of pure water pressure in joints filling material can thus alter the cohesion and friction of the discontinuity surface.

- physical and the chemical effect of the water pressure in the pores of the rock cause a decrease in the compressive strength particularly where confining stress has been reduced.

III.3.1.5 Mining Method and Equipment

Generally, there are four methods of advance in opencast mines. They are:
strike cut – advancing down the dip *[20]*

- strike cut – advancing up the dip
- dip cut – along the strike
- open-pit working

Application of Rock Mechanics in Surface and Underground Mining :

* The use of dip cuts with advance on the strike reduces the length and time that a face is exposed during excavation. Dip cuts with advance oblique to strike may often be used to reduce the strata

* Dip cut generally offers the most stable method of working but suffer from restricted production potential.

* Open-pit method are used in steeply dipping seams, due to the increased slope height are more prone to large slab/buckling modes of failure.

* Mining equipment which piles on the benches of the open-pit mine gives rise to the increase in surcharge which in turn increases the force which tends to pull the slope face downward and thus causing instability. Cases of circular failure in spoil dumps are more pronounced.

III.3.1.6 Slope Geometry

The factors effecting the slope geometry are given in Figure III.6.

- The basic geometrical slope design parameters are height, overall slope angle and area of failure surface.
- With increase in height the slope stability decreases.
- The overall angle increases the possible extent of development of any failure to the rear of the crests and it should be considered so that the ground deformation at the mine peripheral area can be avoided.
- Generally overall slope angle of 45° is considered to be safe by Directorate General of Mines Safety .
- Steeper and higher the height of slope less is the stability.
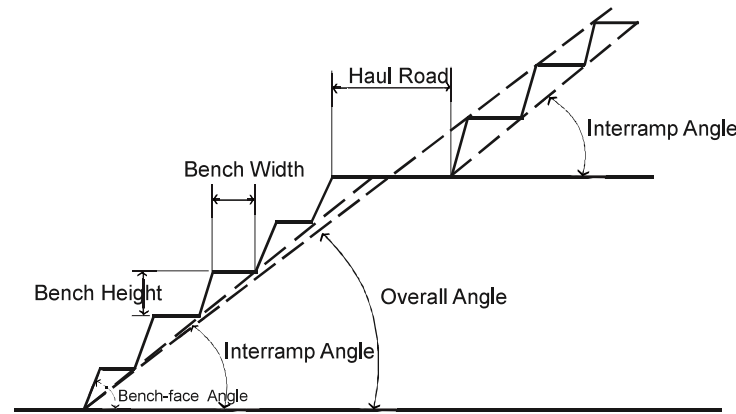
Figure III.6 Typical Pit Slope Geometry [21]

III.3.2 Water Balance and the Hydrological Cycle

Water, whether in the solid, liquid or gaseous (vapour) form, is continuously in a state of circulation and transforms from one state to other by its movement between land, sea and air. This continuous movement is called the hydrological cycle.

In terms of the stability of slopes, the land-based portion of the hydrological cycle is most intense. Inflow to the system arrives as rainfall which can be extremely intense. Water flow from the system can be as run-off, evapotranspiration and subsurface underflow. Changes of storage within the system is that part of the rainfall which becomes incorporated into the groundwater system as recharge. The above elements form the basis of the water balance equation.

Rainfall = Evaporation + Run-off + Subsurface underflow + Change in soil moisture + Change in groundwater storage.

Changes in groundwater are critical to slope stability as it is these elements in the water balance equation that effectively alter the degree of saturation of the ground above the water table and the elevation of the water table itself.

Run-off is that proportion of rainfall that flows from a catchment into streams, lakes or the sea. It consists of surface run-off and groundwater run-off, where groundwater run-off is derived from rainfall that infiltrates into soil down to the water table and then percolates into stream channels. The amount of run-off in any given catchment depends on variety of factors, such as, the condition and nature of the soil and bedrock, the intensity and duration of rainfall, the slope angle, the surface of cover and the antecedent conditions within the catchment. The amount or depth of run-off maybe calculated by gauging the flow in streams which drain the catchment. The run-off coefficient or run-off percentage is defined as the proportion of rainfall that flows from a catchment as a percentage of the total depth of rainfall over the catchment area. Infiltration is defined as the movement of water from the ground surface into the soil or rock with the pores or interstices of the ground mass (i.e., the absorption of water by the soil).

Infiltration can be further divided into that part which contributes to the water content of the unsaturated zone, and the part which recharges the saturated groundwater system. Some recharge to the saturated

groundwater system may be lost as groundwater run-off, whilst recharge to the unsaturated zone may be lost by transpiration or evaporation .When an unsaturated zone exists in a soil it is said to have a soil moisture deficit.

Recharge to this zone reduces the deficit until the soil becomes fully saturated, at which time the soil moisture deficit is equal to zero.

III.3.3 Types of Groundwater Flow

Water flows through soil or rock in various ways depending on the nature of the ground. Watertransmitting soil or rock units are called aquifers. Different types of aquifer demonstrate different modes of groundwater flow, such as, intergranular, fissure and conduit flow.

Intergranular flow is groundwater flow between the individual component grains that make up a soil or rock. This type of flow must closely follow the Darcy Concept of flow through an homogeneous isotropic medium of uniform grain size. In practice,however, most water-bearing strata exhibit intergranular or homogenous flow and path-preferential flow through fissures or conduits within the stratum. Joints within a soil/rock mass can have a significant effect on groundwater levels and hence contribute towards slope in stability.

An aquifer, therefore, can be simply defined as a permeable water-bearing stratum that transmits water under normal head or hydraulic gradient. An aquiclude is a stratum that may contain pore water but is not permeable enough to transmit water even under considerable hydraulic head. The term aquitard is used to indicate a stratum that shows limited water-transmitting capabilities.

III.4 Rock Slope Stability Analyses

The slope stability analyses are performed to assess the safety of economic design of a human-made or natural slopes (embankments, road cuts, open-pit mining, excavations, landfills etc.) and t heequilibrium conditions. The term slope stability may be defined as the resistance of inclined surface to failure by sliding or collapsing. The main objectives of slope stability analysis are finding endangered areas, investigation of potential failure mechanisms, determination of the slope sensitivity to different triggering mechanisms, designing of optimal slopes with regard to safety, reliability and economics, designing possible remedial measures, e.g. barriers and stabilisation mechanisms.

Before the computer age, stability analysis was performed graphically by using hand-held calculator. Today, engineers have a lot of possibilities to use analysis software that ranges from simple limit equilibrium techniques through computational limit analysis approaches (e.g. Finite element limi analysis, Discontinuity layout optimisation) to complex and sophisticated numerical solutions (finite- distinct-element codes). It is must for an engineer to fully understand the limitations of each technique. For example, limit equilibrium is most commonly used and is a simple solution method, but it can become inadequate if the slope fails by complex mechanisms (e.g. internal deformation and brittle fracture, progressive creep, liquefaction of weaker soil layers, etc.)

III.4.1 Limit Equilibrium Method

The conventional limit equilibrium methods investigate the equilibrium of the soil mass tending to slide down under the influence of gravity. Transitional or rotational movement is considered on assumed or known potential slip surface below the soil or rock mass. In rock slope engineering, methods are highly significant for detection of simple block failure along distinct discontinuities. All methods are based on comparison of forces (moments or stresses) resisting instability of the mass and those that cause instability (disturbing forces). Two-dimensional sections are analysed assuming plain strain conditions. These methods assume that the shear strengths of the materials along the potential failure surface are governed by linear (Mohr-Coulomb) or non-linear relationships between shear strength and the normal stress on the failure surface analysis provides a factor of safety, defined as a ratio of available shear resistance (capacity) to that required for equilibrium. If the value of factor of safety is less than 1.0, slope is unstable. The most common limit equilibrium techniques are methods of slices where soil mass is discretised into vertical slices

III.4.1.1 Planar Failure Analysis

Planar failure of rock slope occurs when the mass of rock in a slope slides down along a weak plane. There are number of conditions that must exist in a rock slope for planar failure to occur. First, the failure plane must be sub-parallel to the slope face (strike within 20 degrees to the slope face). Secondly, the failure planes must daylight into the slope face (dip than the slope angle of face) and intersect the face above the toe of the slope. Stability analysis for planar failure requires the resolution of forces perpendicular to and

parallel to the potential failure surface. This includes the shear strength along the failure surface, the effects of porewater pressures, and the influence of external forces such as reinforcing elements or seismic accelerations.

III.4.1.2 Sliding analysis of a block

Figure III.6 shows a solid block resting on a sliding plane. The block will try to move due to gravity along the slope plane inclined at an angle θ from horizontal. However, resistance between base of the block and surface of the slope will prevent slippage of the solid block. Weight of the block W is acting vertically downward (figure III.7), which can be resolved in normal as *Wcosθ* and in shear as *Wsinθ*. The stability of block against slippage is defined as ratio of shear strength to shear stress. The block is considered to undergoes slippage along the plane for the value of ratio < 1, else it is stable. *[19]*
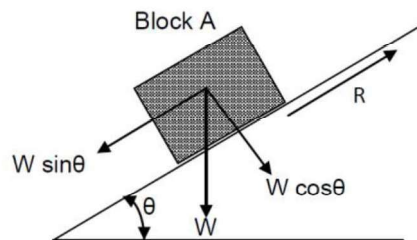
Figure III.7 Sliding block .

III.4.1.3 Plane failure analysis along a discontinuity

This type of failure can occur if a single discontinuity is present or a series of discontinuities form a single plane to initiate failure in a slope (Figure III. 2). This failure can be considered as an unstable block of weight (W) resting on a plane surface which is inclined at an angle θ to the horizontal. The height of slope is H and α is the slope angle. The block will try to move along the joint plane AC due to gravity. The factor of safety (FOS) is defined under limit equilibrium method as ratio of shear strength to shear stress.
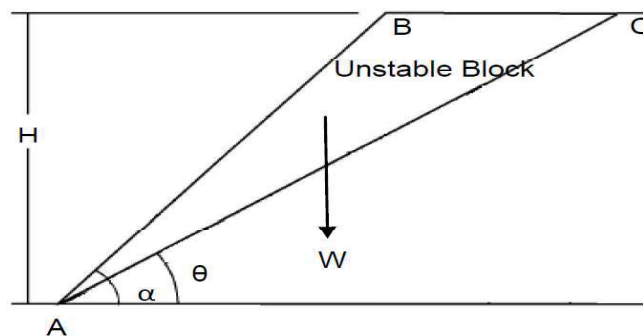
Figure III.8 Geometry of a slope for plane failure

Thus,

Factor of safety = *Shear Strength / Shear Stress*

Factor of safety =$(c + \sigma \tan\varphi)/ \tau s$

Length of discontinuities; *AC* =H/ *Sin*θ

Area of failure surface; AC x 1 m^2 (unit thickness of slope is assumed)

Weight of the unstable block; $W = \gamma\, H^2 (\cot\theta - \cot\alpha)/2$

Normal Stress;   σ =$W \cos\theta / A$

Shear Stress; τ =$W \sin\theta / A$

τ= Shear Stress, MPa

c = Cohesive strength of failure surface, MPa

φ = Friction angle of failure surface, Degree

γ = Density of rock, kN/m^3

γ$_w$ = Density of water, kN/m^3

Therefore,

$$\text{Factor of safety} = \frac{c + \dfrac{W \cos\theta}{A}\tan\phi}{\dfrac{W \sin\theta}{A}} = \frac{cA + W \cos\theta \tan\phi}{W \sin\theta}$$

(III.2)

III.4.1.4 Water is filled in discontinuities

When water is filled in the discontinuity, it exerts a water pressure that will reduce the normal stress on the discontinuity. Due to this, the shear strength of joint reduces which increases the chance of slope failure. The effect of water pressure can be estimated by determining the effective normal stress. The effective normal stress due to present of water in the joint, is given as

$$\sigma ' = \sigma - U \qquad\qquad\qquad (III.2)$$

Where,

$$U = 1/2 \rho g h^2 \qquad\qquad\qquad (III.3)$$

It is assumed that water is discharge from point A, therefore the water pressure is equal to atmospheric pressure at point A and C. Where,

U = water pressure, MPa

σ' = effective normal stress, MPa

σ = normal stress, MPa

ρ = density of water, kg/m^3

h= height of water column, m
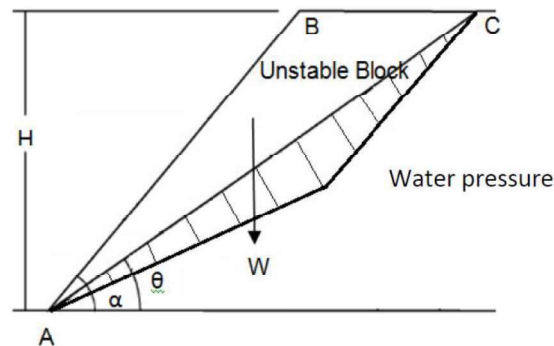
Figure III.9 *Geometry of a slope for plane failure with filled water*

III.4.1.5 Tension crack present in the upper slope surface

A tension crack is a void that runs parallel to a slope face (figure III.10). It effect on slope stability is considered based on specified location and depth determined by stability charts, or empirical judgements. Analytical methods are also available for locating the tension cracks along assumed slip surfaces If the position of a tension crack is known on the upper surface of a slope, its stability analysis should be based on this existing information. However, when the position of the critical tension crack position is unknown, it becomes necessary to use an optimization approach to locate the position and depth of the tension crack.
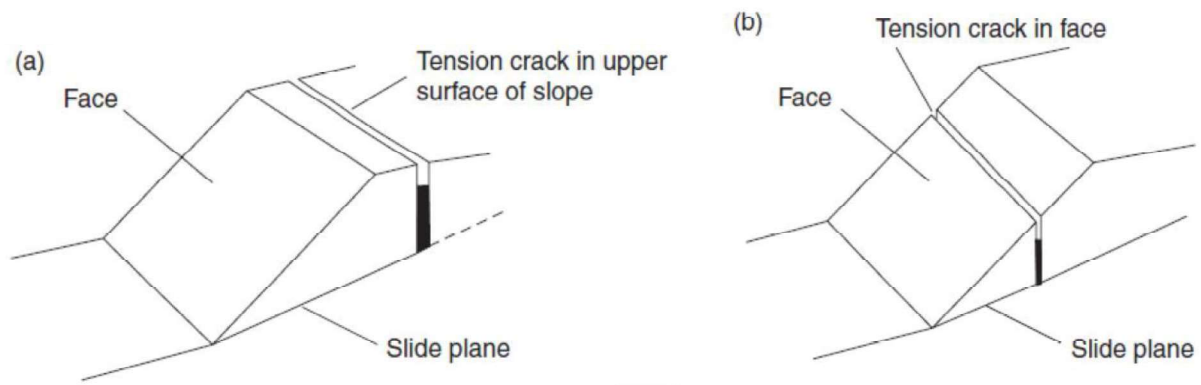
Figure III.10 *Tension crack in upper surface of slope and in the face [23]*

The location of the tension crack (figure III.11) is expressed by the dimension *b* When the upper surface is horizontal, the transition from one condition to another occurs when the tension crack coincides with the slope crest. The depth of critical tension crack, z_c and its location, b_c behind the crest can be calculated by the following equations:

$$\frac{z_c}{H} = (1 - cot\alpha \, tan\theta)$$

(III.4)

$$\frac{b_c}{H} = \sqrt{(\cot\alpha \cot\theta)} - \cot\alpha$$

(III.5)

If the location of tension crack is known then depth of tension crack can be determined by the following equation.

$$z = H - (b + H \, cot\alpha)tan\theta$$

Where, H is the slope height, α is the slope face angle and θ is the dip of the sliding plane. The factor of safety is calculated as follows:

Length of discontinuities; $AD = (H - CD)/ \, Sin\theta$

The weight of the block;

$$W = \frac{\gamma_r H^2}{2}\left(\left(1 - \left(\frac{z}{H}\right)^2\right)cot\theta - cot\alpha\right)$$

(III.6)

Factor of safety = $(cA + wcos\theta tan\varphi)/ \, wsin\theta$
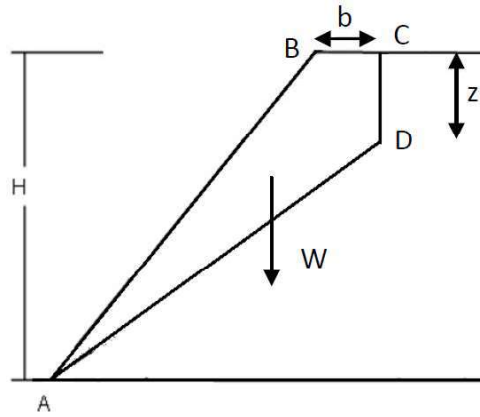
Figure III.11 *Plane failure with tension crack*

III.4.1.6 Tension crack present in the slope surface

In this case, the depth of tension crack can be determined by the following equation:

$$z = (H \, cot\alpha - b)(tan\alpha - tan\theta)$$

$$z = H - (Hcot\alpha - b)an\theta - btan\alpha$$
(III.7)

Length of discontinuities; $AD = (H - CD)/ \, Sin\theta$

The weight of the block =
$$W = \frac{\gamma_r H^2}{2}\left(\left(1 - \frac{z}{H}\right)^2 cot\theta \, (cot\theta \, tan\alpha - 1)\right)$$
(III.8)

Factor of safety = $(cA + w\cos\theta \tan\varphi)/ w\sin\theta$
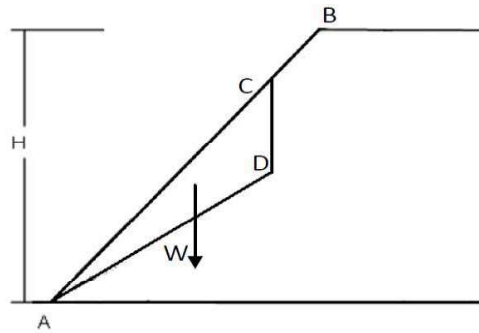
Figure III.12 *plane failure with tension crack*

III.4.1.7 The tension crack is filled with water with upper slope angle

Compound slopes have appreciable angle with the horizontal (α_c) (figure III.13). High slope formation has in generally a positive upper slope angle while the shorter slope has a negative slope angle. These types of slope are very common in complicated hilly terrains controlled by tectonics and geomorphic agents.
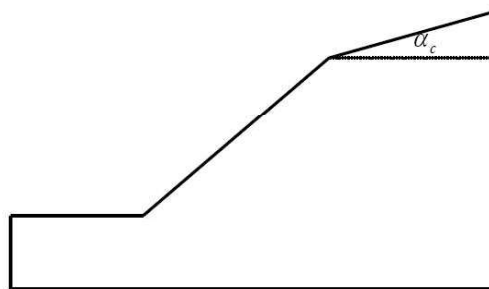
Figure III.13 *Compound slope with a positive upper slope angle*

 A simplified model consisting of a measured depth of water in the tension crack is shown in figure III.13. It is assumed that the tension crack is vertical and is filled with water to a depth z_w. Under this condition, the water pressure decrease linearly toward and exit at the toe of the slope. This pressure distribution results in a force V due to water filling in the subvertical discontinuity and an uplift force U due to water flowing at the surface between the block and its base.

It is considered that water enters the sliding surface along the base of the tension crack and seeps along the sliding surface, escaping at atmospheric pressure where the sliding surface daylights in the slope face. For slope stability analysis, a unit thickness of the slice is considered at right angle to the slope face.
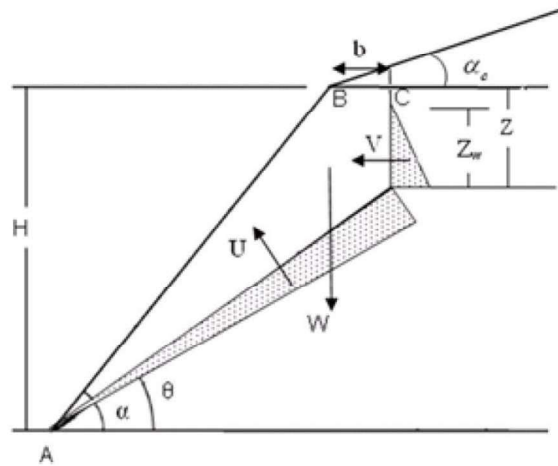
Figure III.14 *Geometry of slope with tension crack in upper slope angle*

Depth of tension crack,

$$Z = H + b\tan\alpha_c - (b + H\cot\alpha)\tan\theta$$

Weight of unstable block, $W = 1/2\,(H^2\cot\alpha X + bHX + bZ))$

$$X = (1 - \tan\theta\cot\alpha)$$

or
$$W = \frac{\gamma}{\gamma \cdot H_S}\left(\left(1 - \left(\frac{H}{Z}\right)_S\right)\cot\theta - \cot\alpha\right) + \frac{\gamma}{\gamma}\,(b \times \text{btan}\alpha^c)$$
(III.9)

Area of failure surface, $A = (H\cot\alpha + b)\sec\theta$

Driving water force, $V = 1/2\,\gamma_w Z_w^2$

Uplift water force, $U = \frac{1}{2}\gamma_w Z_w A$

$$\text{Factor of safety} = \frac{cA + (w\cos\theta - U - V\sin\theta)\tan\phi}{W\sin\theta + V\cos\theta}$$
(III.10)

III.4.1.8 Effect of rock bolts

when a rock bolt is installed at angle β from the normal to the failure plane, it increases the increase normal stress by Tcosβ and reduces the driving forces by Tsinβ (figure III.15), where T is the tension in the rock bolt.

$$\text{Factor of safety} = \frac{cA + (w\cos\theta - U - V\sin\theta)\tan\phi}{W\sin\theta + V\cos\theta}$$
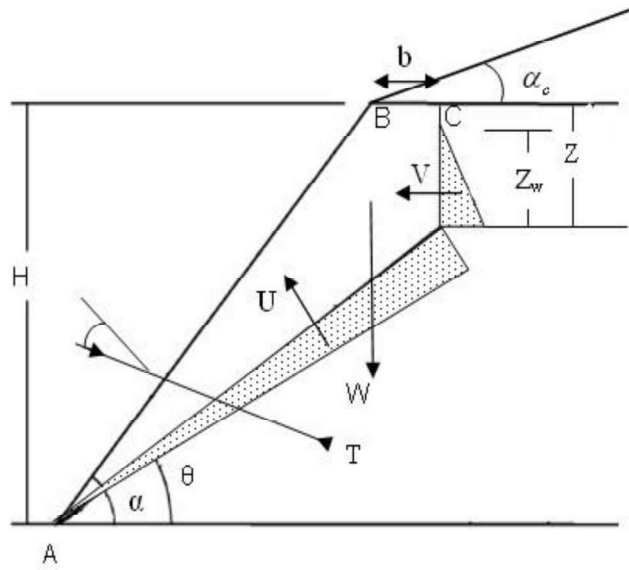
Figure III.15 *Geometry of slope with tension crack in upper slope and its interaction with rock bolt*

Therefore, the expression for factor of safety of the slope becomes

$$\text{FOS} = \frac{cA + (w\cos\theta - U - V\sin\theta + T\cos\beta)\tan\phi}{W\sin\theta + V\cos\theta - T\sin\beta} \qquad \text{(III.11)}$$

III.5 Wedge Failure Analysis

Failure of a slope in the form of wedge can occur when rock masses slide along two intersecting discontinuities, both of which dip out of the cut slope at an oblique angle to the cut face thus forming a wedge-shaped block. These rock wedges are exposed by excavations that daylight the line of intersection forming the axis of sliding. The size of a wedge failure can range from a few cubic meters to very large slides. Rock masses with well-defined orthogonal joint sets or cleavages in addition to inclined bedding or foliation are generally favorable condition for wedge failure. The geometry of the wedge for analyzing the basic mechanics of sliding is explained in figure III.16.
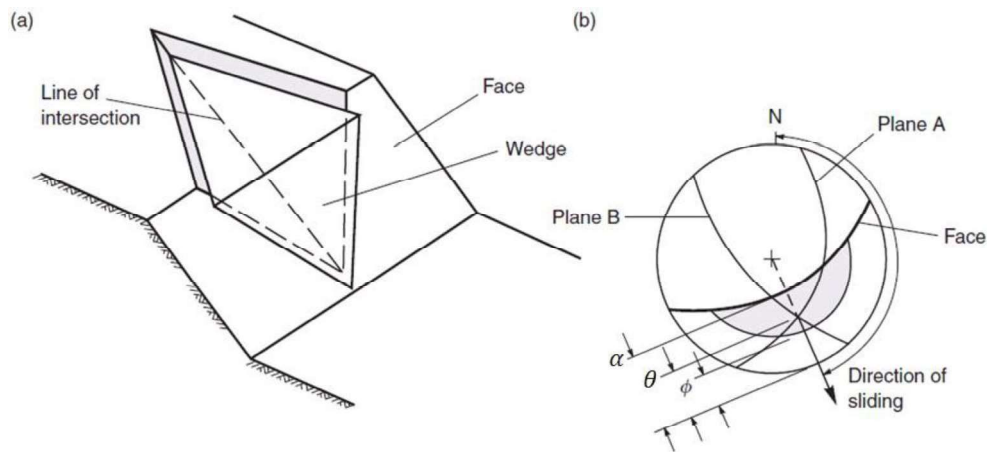
Figure III.16 *Geometric conditions of wedge failure: (a) pictorial view of wedge failure; (b) stereoplot showing the orientation of the line of intersection [23]*

III.5.1 Analysis of wedge failure considering only frictional resistance

The factor of safety of the wedge defined in figure III.17, is analysed assuming that sliding is resisted only by friction and there is no contribution of cohesion. The friction angle for the both the sliding plane is φ. Under this condition the factor of safety is given by:

$$FOS = \frac{(R_A + R_b)\tan\emptyset}{W\sin\theta}$$

where R_A and R_B are the normal reactions provided by planes A and B as illustrated in figure III.17, and the component of the weight acting down the line of intersection is *Wsin θ*. The forces R_A and R_B are found by resolving them into components normal and parallel to the direction along the line of intersection:

$R_A \sin \beta - 1/2\xi = R_B \sin (\beta + 1/2\xi)$ (III.12)

$R_A \cos \beta - 1/2\xi + R_B \cos \beta + 1/2\xi = W\cos\theta$ (III.13)
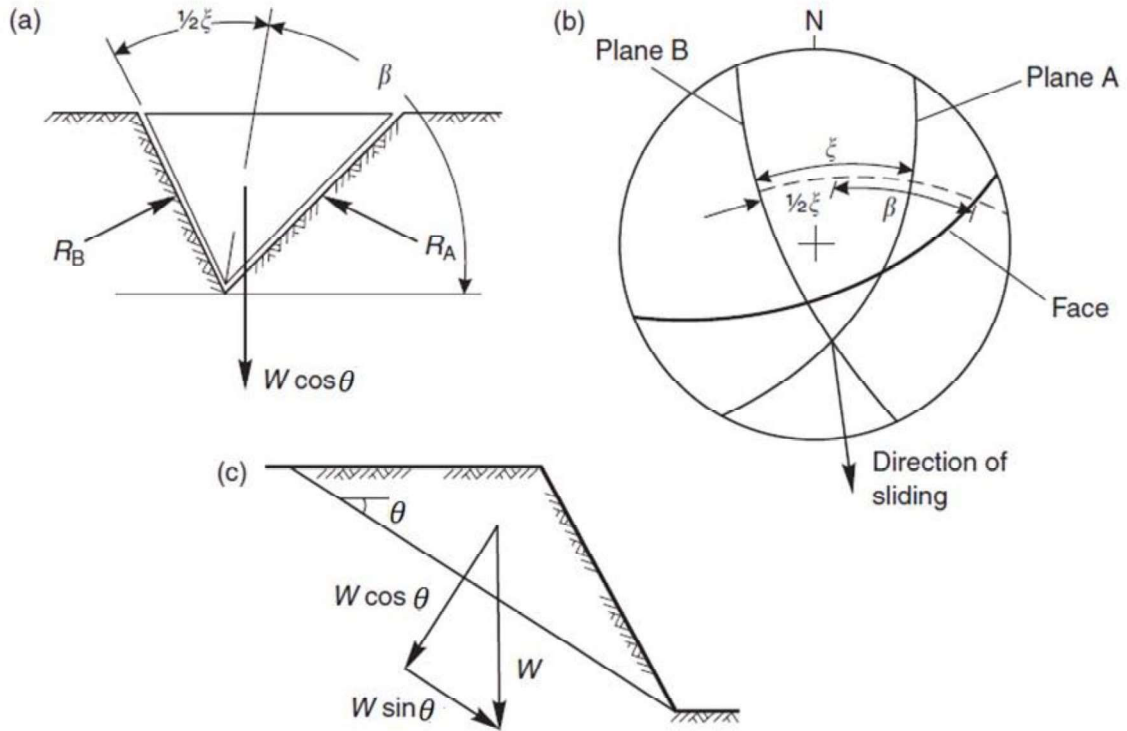
Figure III.17 *resolution of forces to calculate factor of safety of wedge: (a) view of wedge looking at face showing definition of angles β and α, and reactions on sliding Plane R_A and R_B, (b) stereonet showing measurement of angles β and α, (c) cross-section of wedge showing resolution of wedge weight W.*

Angles ξ and β are measured on the great circle containing the pole to the line of intersection and the poles of the two slide planes. In order to meet the conditions for equilibrium, the normal components of the reactions should be equal. Therefore, the sum of the parallel components should equal the component of the weight acting down the line of intersection. The values of R_A and R_B can be found by solving the equations as follows:

$$(R_A + R_b) = \frac{W\cos\theta\,\sin\beta}{\sin(\xi/2)} \qquad\qquad \text{(III.14)}$$

$$FOS = \frac{\cos\theta\,\sin\beta}{\sin(\xi/2)}\frac{\tan\emptyset}{\sin\theta} \qquad\qquad \text{(III.15)}$$

$$FOS = \frac{\sin\beta}{\sin(\xi/2)}\frac{\tan\emptyset}{\tan\theta} \qquad\qquad \text{(III.16)}$$

$$FOS_w = FOS_P \qquad\qquad \text{(III.18)}$$

where FOS$_W$ is the factor of safety of the wedge supported by friction only, and FOS$_P$ is the factor of safety of a plane failure in which the sliding plane with friction angle $_\varphi$, dips at the same angle as the line of intersection angle θ. Wedge factor (*K*) depends upon the included angle of the wedge ξ and the angle of tilt β of the wedge.

III.5.2 Analysis of wedge failure with cohesion and friction angle

The most commonly employed analytical technique for this purpose is a rigid-block analysis, in which failure is assumed as linear sliding along one of the discontinuities or along the line of intersection formed by the discontinuities. This analysis takes into account the dimensions and shape of the wedge, different cohesion and friction angles on each slide plane, water pressure and a number of external forces. The stability of the wedge can be evaluated by resolving the forces acting along normal to the discontinuities and in the direction parallel to the line of intersection. These forces include the weight of the wedge, external forces such as foundation loads, seismic accelerations, tensioned reinforcing elements, water pressure acting on the surfaces, and the shear strength developed along the sliding plane or planes. A complete explanation related to different features of the slope involved in this analysis is explained by Hoek (et.al). Geometry of the wedge is defined by the location and the orientation of as many as five bounding surfaces (figure III .18). This includes two intersecting discontinuities, the slope face, the upper slope surface, and the plane of representing a tension crack, if present. Because the calculation is extended, this general analysis is best adapted to computer solution. However, in most cases, assumptions can be made that significantly simplifies the controlling stability equations so that a simplified solution could be obtained. Figure III.10 defines the calculation of wedge stability under various assumptions. The formulas contain dimensionless factors (X, Y, A, and B), which depend on the geometry of the wedge. The calculation of these factors requires correct numbering of intersections of the planes[19] as given below:

1 – Intersection of plane a with the slope face

2 - Intersection of plane b with the slope face

3 - Intersection of plane a with the upper slope surface

4 - Intersection of plane b with the upper slope surface

5 - Intersection of planes a and b It is assumed that sliding of the wedge always takes place along the line of intersection numbered 5.
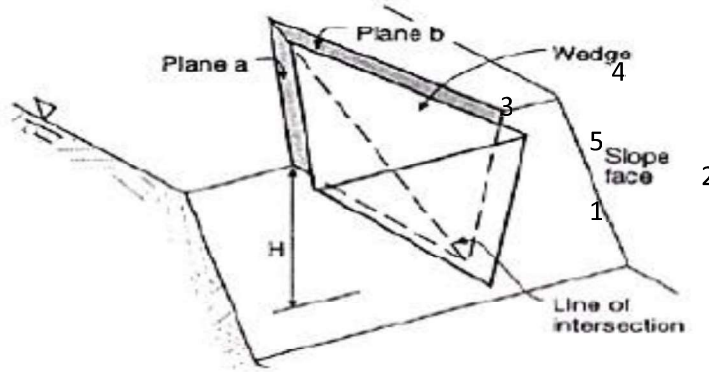
Figure III.18 *Pictorial View of wedge showing the numbering of intersection lines and planes*

$$FS = \frac{3}{\gamma_r H}(C_a X + C_b Y) + (A - \frac{\gamma_w}{2\gamma_r} X)\tan\phi_a + (B - \frac{\gamma_w}{2\gamma_r} Y)\tan\phi_b$$

(III.19)

$$X = \frac{\sin\theta_{24}}{\sin\theta_{45}\cos\theta_{na2}}$$

(III.20)

$$A = \frac{\cos\psi_a \cos\psi_b \cos\theta_{na.nb}}{\sin\psi_i \sin^2\theta_{na.nb}}$$

(III.21)

$$Y = \frac{\sin\theta_{13}}{\sin\theta_{35}\cos\theta_{na1}}$$

(III.22)

$$B = \frac{\cos\psi_b \cos\psi_a \cos\theta_{na.nb}}{\sin\psi_i \sin^2\theta_{na.nb}}$$

(III.24)

Where, C_a and C_b are the cohesive strength of plane a and b, ϕ_a and ϕ_b are the angle of friction along plane a and b, γ_r is the unit weight of the rock, and H is the total height of the wedge. X, Y, A and B are dimensionless factors, which depend upon the geometry of the wedge, Ψ_a and Ψ_b are the dips of planes a and b, whereas, Ψ_i is the plunge of the line of their intersection.

Under fully drained slope condition, the water pressure is zero. Therefore, factor of safety of the wedge against failure is given by:

$$FS = \frac{3}{\gamma_r H}(C_a X + C_b Y) + A\tan\phi_a + B\tan\phi_b$$

(III.25)

In case of frictional strength only, the cohesion is zero. Therefore, the factor of safety becomes

FS=Atanφ_a +Btanφ_b

III.6 Toppling Failure Analysis

Toppling failure of rock blocks along the slope occurs when there are formed by closely spaced and steeply inclined discontinuity system dipping into the excavation. For analysis of slope stability against toppling failure, a kinematic analysis of the structural geology is first carried out to identify potential toppling conditions. If failure condition exists, a stability analysis specific to toppling failure is conducted.

III.6.1 Kinematics of block toppling failure

The potential for toppling failure can be assessed from three kinematic tests. These tests examine shape of the block potential to failure, relationship between dip of the plane forming the slabs and face angle and alignment of the block with respect to the slope face.

a) Test for delineation of Block shape

The basic mechanics of stability of a block against toppling on an inclined plane are illustrated in Figure 11. The governing conditions for toppling failure are height (h) and width (t) and dip angle (θ). There are four cases to occur in similar conditions

Case 1: $\theta < \emptyset$ *and*   t/h $> tan\theta$; *the block is* **stable** and will neither slide nor topple h

Case 2: $\theta > \emptyset$ *and* t/h $>$ $tan\theta$; *the block will* **slide** but will not topple h

Case 3: $\theta < \emptyset$ *and* $tan\theta$; *the block will* **topple** *but will not slide*

Case 4: $\theta > \emptyset$ *and*   t/h $< tan\theta$; *the block can* **slide and topple** simultaneously
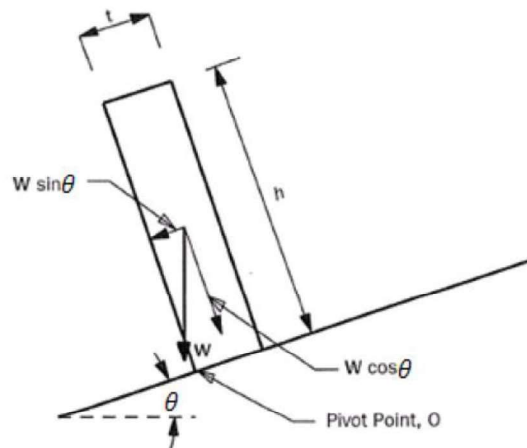
Figure III.19 Basic model for toppling failure [23]
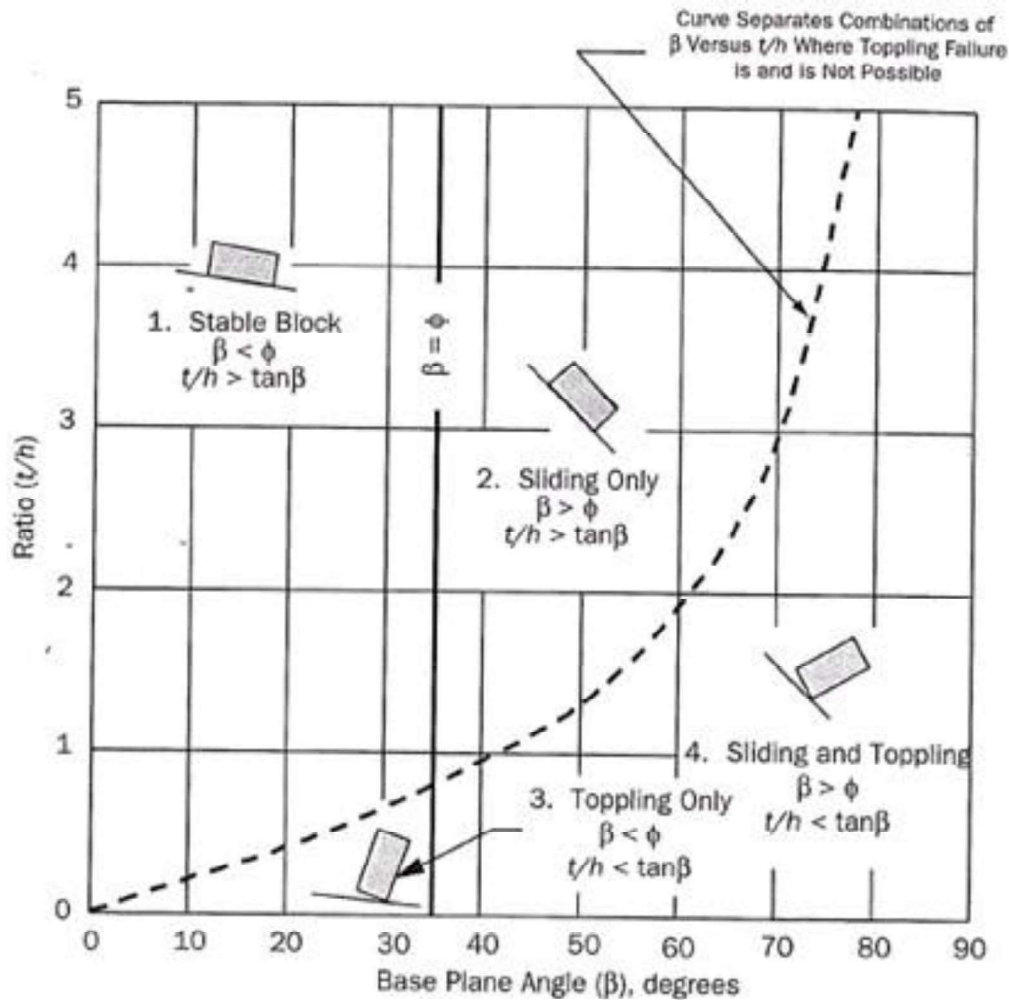
Figure III.20 Conditions for sliding and toppling of a block on an inclined plane [23]

Therefore, if the block thickness-to height ratio of the block is less than $\tan\beta$, then the resultant force due to its weight will exist out side the toe of the block. Thus an overturning moment will develop about the pivot point .

b) Inter-layer slip test

One of the essential prerequisites for toppling failure is shear displacement along the face to face contacts on the top and bottom faces of the blocks (figure III.21). The state of stress close to the slope face is uniaxial with the direction of the normal stress (σ) aligned parallel to the slope face. When the layers slip past each other, σ must be inclined at an angle φ with the normal to the layers, where φ is the friction angle of the sides of the blocks. If is the dip of slope face and $_\alpha$ is the dip of the planes forming the sides of the blocks, then the condition for interlayer slip is given by:

$$(180 - \theta - \alpha) \geq (90 - \varphi)$$

$$\text{or} \quad \alpha \geq (90 - \theta) + \varphi$$
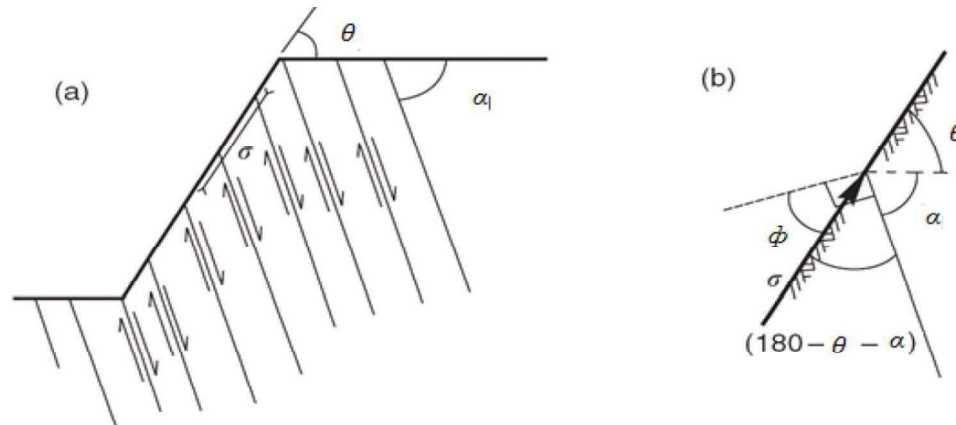
Figure III.21 *Block alignment test in toppling failure*

c) Block alignment test

The planes forming the blocks should strike approximately parallel to the slope face so that each layer is free to topple. Field observations shows that instability is possible where the dip direction of the planes forming sides of the blocks, α_d is within about 10^0 of the dip direction of the slope face α_f, i.e. $|(\alpha_f - \alpha_d)|$ <10∘
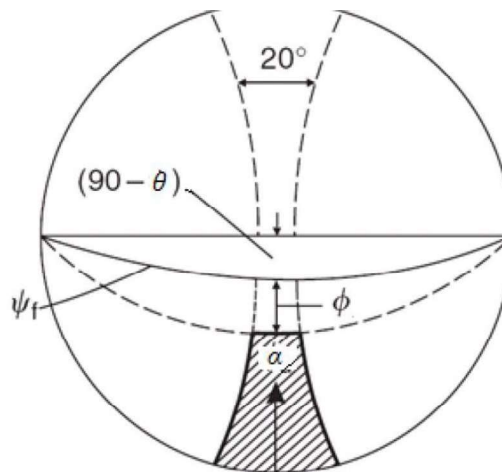
Figure III.22 *Stereographic projection for block alignment test [23]*

III.6.2 Limit equilibrium analysis for toppling failure

Toppling failure of an individual block or column can exist only in the following conditions
 - There is an inclined surface upon which the block rests,
 - There is a joint set approximately perpendicular to the inclined surface,
 - $\theta < \emptyset$ *nd* t/h $'< tan\beta$

Stability analysis involves an iterative process in which the dimensions of all the blocks and the forces acting on them are calculated, and stability of each block is examined, starting with

- A set of stable blocks in the upper part of the slope, where the friction angle of the base of the blocks is greater than the dip of this plane and the height is limited so the centre of gravity lies inside the base.

- An intermediate set of toppling blocks where the centre of gravity lies outside the base.

- A set of blocks in the toe region, which are pushed by the toppling blocks above.

The factor of safety can be calculated as the ratio of resisting moments to driving moments

$$FOS = \frac{\sum(resisting\ moments)}{\sum(driving\ moments)} = \frac{wcos\theta.(t/2)}{wsin\theta.(h/2)} = \frac{(t/h)}{tan\theta}$$ (III.27)

Figure III.23 shows a typical block (n) with the normal force (R_n) and shear forces (S_n) developed on the base. The forces developed at the interfaces with adjacent blocks are P_n, Q_n, P_{n-1}, Q_{n-1}. When the block is one of the toppling set, the points of application of all forces are known, as shown in figure III.24. The points of application of the normal forces P_n are M_n and L_n on the upper and lower faces respectively of the block, and are given by the following. The value of blocks, y_n, L_n and M_n can be determined graphically.

When sliding and toppling occurs, frictional forces are generated on the bases and sides of the blocks. If friction angles are different on the two surfaces, then the friction angle of the sides of the blocks (ϕd) will be lower than friction angle on the bases (ϕp). For limiting friction on the sides of the block:

$$Q_n = P_n\ tan\ \phi_d\ Q_{n-1} = P_{n-1}\ tan\ \phi d$$ (III.28)

 By resolving perpendicular and parallel to the base of a block with weight W_n, the normal and the shear forces acting on the base of block *n* are given by:

$R_n = W_n\ cos\theta\ + (P_n - P_{n-1})\ tan\ \phi_d$

$S_n = W_n sin\theta + (P_n - P_{n-1})$

$\sum F_Y = 0, \sum F_X = 0$

$S_n = R_n\ tan\ \phi_p$

$R_n = W_n\ cos\theta$

 Where, S_n is the shear force along the column-base contact and R_n is the normal force across the column base contact. Thus

$P_n - P_{n-1} - W_n sin\theta + W_n cos\theta tan\phi_p + (P_n - P_{n-1})tan\phi_p tan\phi_d = 0$

$(P_n - P_{n-1})(1 - tan\phi_p tan\phi_d) - W_n sin\theta + W_n cos\theta tan\phi_p = 0$

$(P_n - P_{n-1})(1 - tan\phi_p tan\phi_d) = W_n(W_n cos\theta tan\phi_p - sin\theta)$

$P_{n-1,s} = P_n - \dfrac{W_n(cos\theta tan\phi_p - sin\theta)}{(1 - tan\phi_p\ tan\phi_d)}$

$P_n - P_{n-1} - W_n sin\theta + W_n cos\theta tan\phi_p + (P_n - P_{n-1})an\phi_p tan\phi_d = 0$

$(P_n - P_{n-1})(1 - tan\phi_p tan\phi_d) - W_n sin\theta + W_n cos\theta tan\phi_p = 0$

$(P_n - P_{n-1})(1 - tan\phi_p tan\phi) = W_n(W_n cos\theta tan\phi_p - sin\theta)$

$$P_{n-1,s} = P_n - \frac{W_n(cos\theta tan\phi_p - sin\theta)}{(1 - tan\phi_p \, tan\phi_d)}$$

(III.29)

Considering rotational equilibrium, it is found that the force P_{n-1} that is just sufficient to prevent toppling has the value

$P_{n-1},t = [P_n(M_n - \Delta x \, tan\phi_d) + (W_n/2) (y_n \, sin\theta - \Delta x \, cos\theta)]/Ln)$

When the block under consideration is one of the sliding set

$S_n = R_n \, tan \, \phi_p$

$$P_{n-1,s} = P_n - \frac{W_n(cos\theta tan\phi_p - sin\theta)}{(1 - tan\phi_p \, tan\phi_d)}$$

(III.30)

To detemined the magnitude of P_n we set the momnets about the pivot point, O,

$$\sum M_0 = 0$$

$$= \left(\frac{h_n}{2}\right) W_n Sin\theta - \left(\frac{t}{2}\right) W_n cos\theta + m_i P_n - t(P_n tan\phi_d) - l_n P_{n-1}$$

$$= \left(\frac{W_n}{2}\right)(h_n Sin\theta - tcos\theta) + P_n(m_i - t.tan\phi_d) - l_n P_{n-1}$$

$$l_{n-1} P_{n-1} = \left(\frac{W_n}{2}\right)(h_n Sin\theta - tcos\theta) + P_n(m_i - t.tan\phi_d)$$

$$P_{n-1,t} = \frac{\left(\frac{W_n}{2}\right)(h_n Sin\theta - tcos\theta) + P_n(m_i - t.tan\phi_d)}{l_{n-1}}$$

If friction angle is same for both the surfaces,

$$P_{n-1,s} = P_n - \frac{W_n(cos\theta tan\phi_p - sin\theta)}{(1 - tan^2\phi)}$$
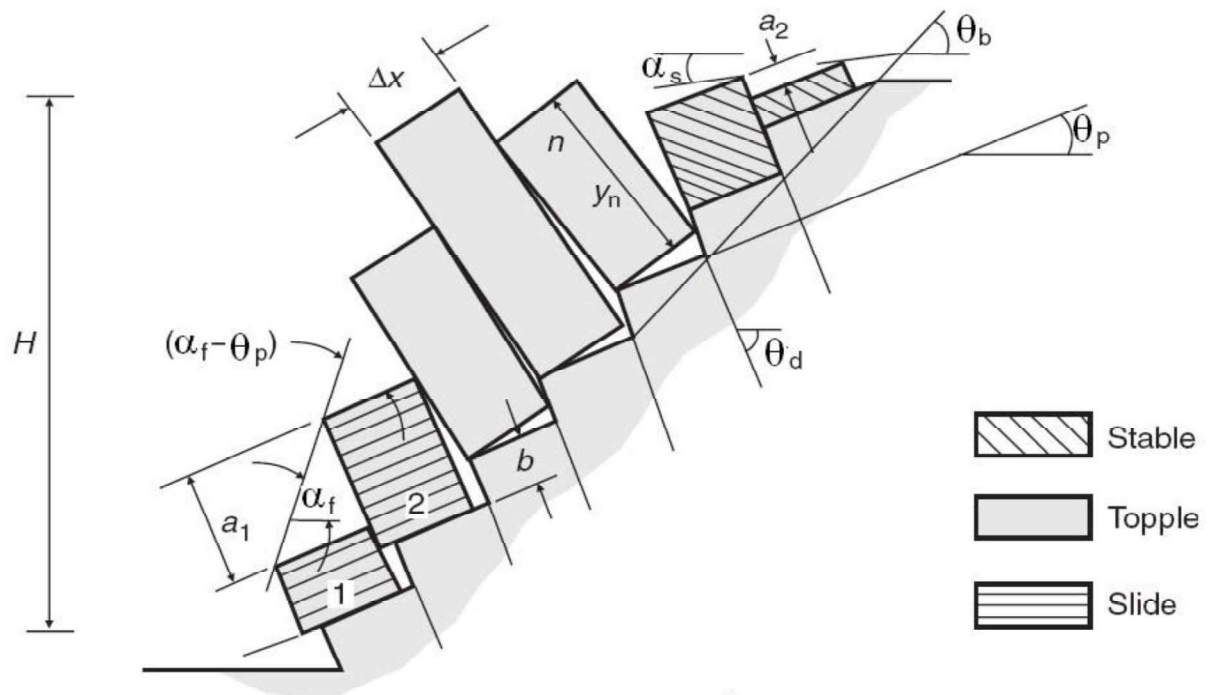
Figure III.23 *Model for limiting equilibrium analysis of toppling on a stepped base [23]*
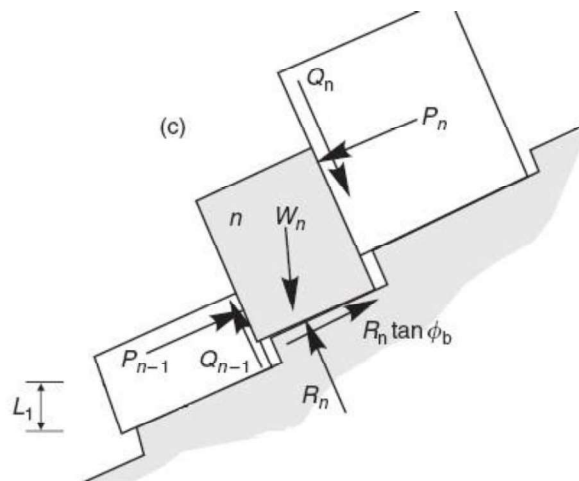
Figure III.24 *Forces acting on the nth column sitting on a stepped base*
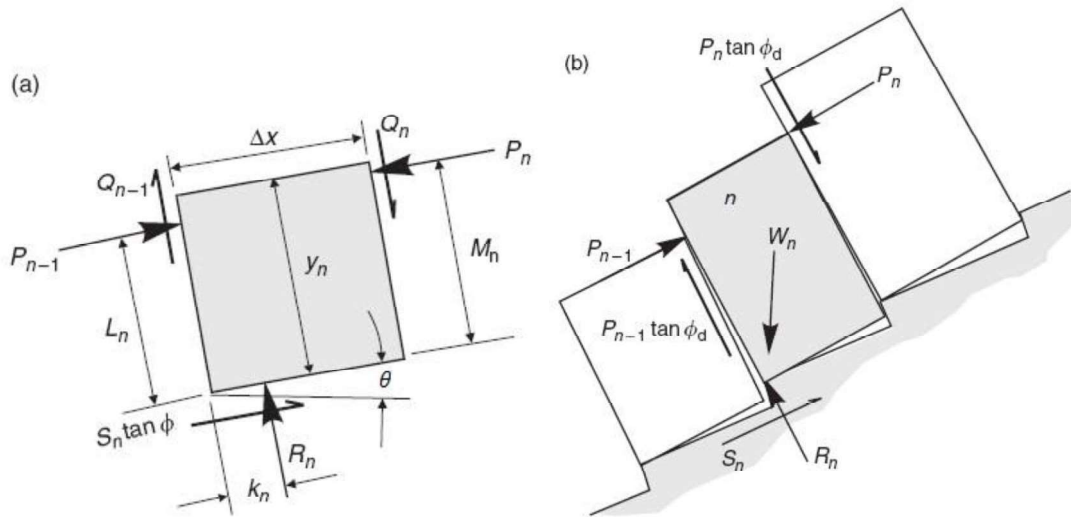
Figure III.25 *Limiting equilibrium conditions for toppling and sliding of nth block: (a) forces acting on nth block; (b) toppling of nth block*

III.6.3 Calculation procedure for toppling stability of a system of blocks

The calculation procedure for examining toppling stability of a slope comprising a system of blocks dipping steeply into the faces is as follows:

(i)   The dimensions of each block and the number of blocks are defined using equations.

(ii) Values for the friction angles on the sides and base of the blocks (ϕd and ϕp) are assigned based on laboratory testing, or inspection. The friction angle on the base should be greater than the dip of the base to prevent sliding (i.e. ϕp > θp).

(iii) Starting with the top block, equation is used to identify if toppling will occur, that is, when $y/x > \cot \phi_p$. For the upper toppling block, equations are used to calculate the lateral forces required to prevent toppling and sliding, respectively.

(iv) Letn_1 be the uppermost block of the toppling set.

(v) Starting with block n_1, determine the lateral forces $P_{n-1,t}$required to prevent toppling, and $P_{n-1,s}$to prevent sliding. If $P_{n-1,t} > P_{n-1,s}$, the block is on the point of toppling and P_{n-1} is set equal to $P_{n-1,t}$, or if $P_{n-1,s} > P_{n-1,t}$, the block is on the point of sliding and P_{n-1} is set equal to $P_{n-1,s}$. In addition, a check is made that there is a normal force R on the base of the block, and that sliding does not occur on the base, that is $R_n > 0$ and ($|S_n| > R_n \tan\phi_p$)

(vi) The next lower block *(n_1 − 1)* and all the lower blocks are treated in succession using the same procedure.. If the condition $P_{n-1,t} > P_{n-1,s}$is met for all blocks, then toppling extends down to block 1 and sliding does not occur.

(vii)   Eventually a block may be reached for which $P_{n-1,s} > P_{n-1,t}$. This establishes block n_2, and for this and all lower blocks, the critical state is one of sliding. The stability of the sliding blocks is checked using equation (9.24), with the block being unstable if $(S_n = R_n \tan\phi_b)$. If block 1 is stable against both sliding and toppling (i.e. $P_0 < 0$), then the overall slope is considered to be stable. If block 1 either topples or slides (i.e. $P_0 > 0$), then the overall slope is considered to be unstable.

In the toppling simulation where, the slope is composed of rock columns (blocks) on a flat base, an unstable rock column (n+1) will exert a force of P magnitude P_n on the down slope adjacent column (n). Therefore, the nth column is no longer be under gravitational forces only. The forces acting on the nth column for limiting equilibrium conditions are shown in figure III.24. When the base plane of the columns is flat, overturning of the columns is not kinematically possible without displacement of the pivot points (O) of the columns due to required dilation of the columnar structure. Such dilation is possible if the magnitude of the overturning forces exveeds the shear resistance of the rotation points of the columns.

When the slope is composed of rock columns on a steeped base, rotation of the nth block about its pivot will cause shear (S_n) and normal forces (N_n) to develop on the block. While overturning about the pivot point, O, the nth block will maintain contact with block n and n-1 as shown in Figure III.24 because the locations of the shear and normal forces are known, the stability of the column against rotation and sliding is determinate.

III.7 Rock slope stabilization techniques

In many cases, engineered slopes require stabilization to ensure their long-term viability and reduce localized slope failure (which includes erosion and rockfall). Generally speaking, the most effective strategy is to prevent the failure at the source through stabilization, not to install structures to protect against them in the future.

There are many methods that can be used to stabilize a rock slope. These include altering the slope geometry, installing drainage, adding reinforcement, or a using combinations of these methods. Table 8 provides an overview of common stabilization procedures. A more detailed discussion of each is included in this section.[47]

III.7.1 Scaling

Scaling is the process of removing loose or potentially unstable material (or a small section of slope) that might dislodge or affect the trajectory of falling rock by creating a launching point for materials falling from above. It is accomplished by hand or mechanical scaling, or by small blasting operations called trim blasting. Scaling is effective on natural and newly excavated slopes, and is done as periodic maintenance for any slopes that pose a potential rockfall hazard to roadways. .[33]

Scaling is used to reshape slopes and to stabilize existing slopes and mitigate rockfall. For new construction, scaling should be completed immediately after the initial slope construction and periodically thereafter to remove any loosened rocks. Hand scaling on existing slopes may be required on a more regular basis, depending on the construction and condition of the rock face.

Scaling is typically effective for a period of two to ten years, depending on site conditions, so it is not considered a permanent mitigation measure. However, it is relatively inexpensive and serves as an effective short-term strategy. Because it enhances site safety, it is routinely included with other mitigation efforts such as new rock excavation, rock reinforcement, or draped mesh.

Table III.1 *Overview of stabilization procedures and their limitations.* .[33]

Mitigation Measure	Description/purpose	Limitations
Slope Geometry Modification		
Hand/Mechanical Scaling	Used to remove loose rock from slope via hand tools and/or mechanical equipment. Commonly used in conjunction with other stabilization methods.	A temporary measure that usually needs to be repeated every 2 to 10 years, as the slope face continues to degrade.
Trim Blasting	Used to remove overhanging faces and protruding knobs and to modify the slope angle to improve rockfall trajectory and slope stability.	Possible right-of-way issues, debris containment, difficulty with drilling, and undermining or loss of support by key block removal (blocks which exert major control the stability of other blocks).
Reinforcement		
Internal Stabilization		
Rock Bolts	Tensioned steel bars used to increase the normal- force friction and shear resistance along discontinuities and potential failure surfaces. Applied in a pattern or in a specific block.	Less suitable on slopes comprising small blocks. Requires good access to slope. Visible bolt ends and hex nuts may need to be covered with shotcrete to improve aesthetics.
Rock Dowels	Untensioned steel bars installed to increase shear resistance and reinforce a block. Increase normal- force friction once block	Passive support system requires block movement to develop bolt tension. Requires good access to

	movement occurs. Less visible than rock bolts.	slope. Visible bolt ends may need to be covered.
Shear Pins	Provide shear support at the leading edge of a dipping rock block or slab using grouted steel bars. Can easily be blended with surrounding rock by colored concrete.	Cast-in-place concrete needed around bars to contact leading edge of block. Requires good access to slope.
Injectable Resin/Epoxy	Resin/epoxy injected into the rock mass through a borehole; travels along joints to add cohesion to discontinuities. Decreases the number of rock bolts or dowels needed in a rock slope. Great for aesthetics as it cannot be seen.	Joint apertures must be greater than 2 mm (1/16 in) for migration of product. In slopes with excessive moisture, product will expand and provide little increase in cohesion. Should not be used as the only mitigative measure on a rock slope.
External Stabilization		
Shotcrete	Pneumatically applied concrete requiring high velocity and proper application to consolidate. Primarily used to halt the ongoing loss of support caused by erosion and raveling. Adds small amount of structural support for small blocks. Sculpted and/or colored shotcrete can be used for improved aesthetics and to cover rock bolts and dowels. Drainage must be installed.	Reduces slope drainage. Can be unsightly unless sculpted or colored. Wire mesh or fiber reinforcement required to prevent cracking. Must be applied in a minimum thickness of 50 mm (2 in) to resist freeze/thaw. Quality and durability are very dependent on nozzleman skills.
Drainage		
Weep Drains	Reduce water pressures within a slope using horizontal drains or adits. Commonly used in conjunction with other design elements. Good for aesthetics because drains are rarely visible.	Difficult to quantify the need and verify the improvements achieved. Will need periodic cleaning to maintain water drainage.

III.7.1.1 Hand Scaling

Hand scaling is the most common and inexpensive form of scaling. Workers rappel from the top of the slope or work out of a crane or man lift basket and use steel pry bars or air bags (also known as pneumatic pillows) to remove any loosened rocks. In most cases, several workers are scaling a slope at one time. Hand scaling is effective on small areas that are accessible by workers and that have rocks that are not too big to be removed manually.

Scaling companies typically provide their own equipment, including rappelling ropes, harnesses, pry bars, air bags, air compressors, and safety equipment. If access from the roadway is not feasible, a helicopter may be used to transport the scalers to an area above the slope. Figure III.26 shows a typical hand-scaling operation.

Figure III.26 *Hand scalers removing loose material from a cut slope South Fork Smith River Road, California.* .[33]

III.7.1.2 Mechanical Scaling

Mechanical scaling is used on larger slope areas or to augment hand-scaling efforts. This process uses hydraulic hammers, long-reach excavators as shown in Figure III.26, or cranes that drag a heavy object, such as a blasting mat or old "Caterpillar" track, across the slope (contractors have developed many ingenious scaling implements, including bundled cables, large steel rakes, and a used tread from a bulldozer, although not all methods have been equally successful). For removing very large rocks, power-assisted mechanical equipment such as pneumatic pillows or splitters can be inserted into open cracks, and then expanded to dislodge the rocks.

Mechanical scaling can also be performed by placing explosives into cracks and drilled holes (a process known as crack blasting) or using heavy construction equipment such as a trackhoe. It should be noted that without confinement, crack blasting can be relatively ineffective and can also produce loud explosions and flyrock.

Figure III.27 *Using a long-reach excavator for mechanical scaling.* .[33]

The most important aspect of designing a rock scaling operation is ensuring the selected method is capable of handling the rock (or sections of rock) that need to be removed. Once scaling has begun on a feature, it will become unstable, and it cannot be left and the area re-opened to traffic restored until it is removed. Most mechanical scaling operations use a crane or excavator, plus a front-end loader and dump truck to haul rock from the site.

III.7.2 Reinforcement Systems

Most reinforcement systems work to strengthen the rock mass internally by increasing its resistance to shear stress and sliding along fractures. Other systems work externally to protect the rock from weathering and erosion and to add a small amount of structural support. An example of this is shotcrete (concrete or mortar that's "shot" onto the rock).

III.7.2.1 Internal Stabilization

Internal stabilization is accomplished by tensioned and untensioned rock anchors, injectable resin, and drainage.

III.7.2.1.1 Rock Anchors

The most common type of internal reinforcement are anchors, which are threaded steel bars or cables that are inserted into the rock via drilled holes and bonded to the rock mass by cement grout or epoxy resins. (Friction bolts are considered temporary measures and typically are not used in the transportation industry.) Because the bond strength between the cement grout or resin and the rock is less than the maximum yielding stress of the steel, it has a large impact on the design load of the rock reinforcement.
Rock anchors can be used to secure a single loosened block or to stabilize an entire rock slope that is affected by a prevalent rock structure. Bolt and cable lengths are highly variable and are compatible with a

variety of rock types, structural characteristics, and strengths. Anchors can be combined with other stabilization techniques if they cannot mitigate the hazard alone. Disadvantages include relatively high cost, susceptibility to corrosion, and lengthy installation times, which can slow the construction of the rock slope. The anchors used for slope stabilization are typically 6 m in length, 20 mm to 50 mm in diameter and made of high-strength steel (bars can be coupled to increase the length up to 30 m, but the total length of a stabilization bar is generally limited to 12 m). Rock anchors can be tensioned or untensioned.

III.7.2.1.2 Tensioned Anchors (Rock Bolts)

Tensioned anchors (also known as rock bolts) are used on rock masses that already show signs of instability or on newly cut rock slopes to prevent movement along fractures and subsequent decrease of shearing resistance. A hex nut and bearing plate are used to distribute the tensile load from the bolt to the rock mass as illustrated in Figure III.27.

Rock bolts are considered a type of active reinforcement due to the post-tensioning they provide, and are used to add compressive stress to joints within a rock mass. This force increases the friction along the fracture planes and helps to reduce block movement.

Tensioned rock bolts can require more time to install than dowels because installation involves several steps: drilling, grouting the bond length and inserting the bar or cable, then tensioning the anchor and grouting the free length. Because the tension in the bolt can reduce over time due to creep and become "seized" by small shears in the rock mass, rock bolts may need periodic re- tensioning.
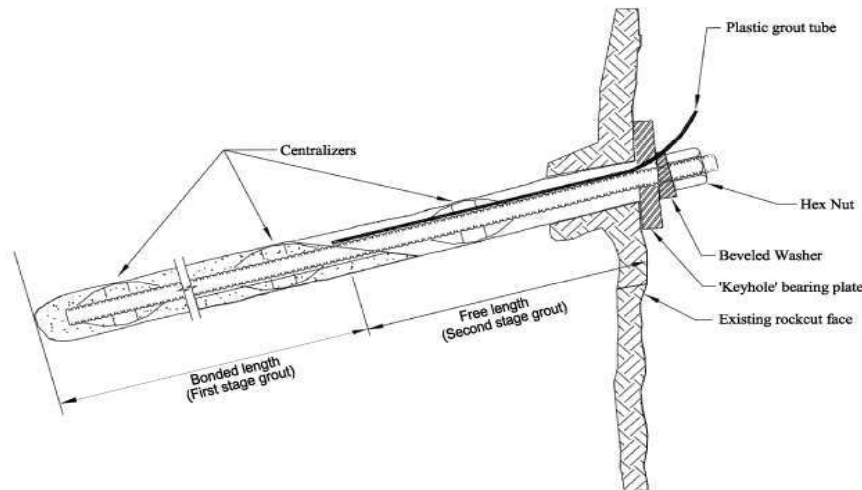
Figure III.28 *Illustration. Typical tensioned anchor (or rock bolt).*[33]

III.7.2.1.3 Untensioned Anchors

There are two types of untensioned anchors used in rock stabilization: rock dowels and shear pins. Both are untensioned, fully grouted steel bars used for passive reinforcement. Dowels are used on steep slopes in the same fashion as rock bolts, while shear pins are used on flatter slopes where bedding planes and discontinuities determine the slope angle and failure plane.

Rock dowels as illustrated in Figure III.28, are typically used on newly excavated slopes. They can be installed in a grid pattern to support an entire face or used to support one block. They provide initial reinforcement through the shear strength of the steel, which increases friction along the potential plane of weakness. Once block movement occurs, depending on dowel orientation, the tensile strength of the bar is engaged and the normal force between opposing discontinuities is increased. [33]

Dowels can be used in highly fractured and weak rocks that cannot hold a tensioned rock bolt. They also can create a more natural-looking slope face, as the plates can be removed in massive rock formations without close jointing that would inhibit the face support contribution of the dowel. The boreholes can be covered with grout that's been colored to match the surrounding rock. Because dowels are installed in one step, they are quicker to install than tensioned bolts.
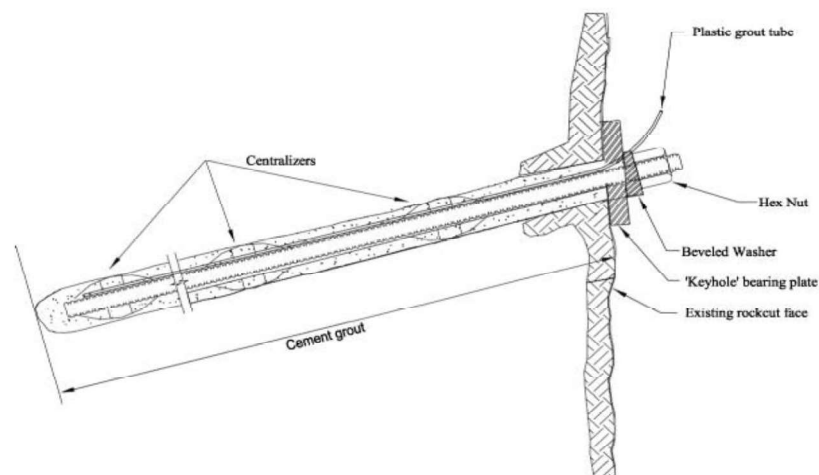
Figure III.29 Illustration. Typical untensioned rock dowel. [33]

III.7.2.1.4 Rock Anchor Installation

Rock anchors are usually installed in a grid pattern, where each anchor is the same length and set at a predetermined distance from the surrounding bolts. Following a set pattern can improve the structural stability of an entire rock face, especially for weathered or highly fractured rock. On competent rock masses with large block sizes, engineers typically identify "key blocks" (i.e., blocks of rock that control support for surrounding blocks), then design a bolting pattern around them that makes it more difficult for the surrounding blocks to move. Designing a key block pattern requires engineers to map the three-dimensional fracture orientations, but can decrease the number of rock bolts required to stabilize a slope. [33]

In both tensioned and untensioned anchors, the bearing plate and hex nut are used to distribute the load of the anchor to the rock face; a beveled washer is used to apply the load evenly when the bolt is angled in relation to the rock face. In rock masses with few discontinuities, the plate can be removed and the tendon

(bar or cable) cut to allow for the installation of a grout cover or plug. This method is highly contingent on the quality of rock and stability of the rock mass. [33]

In the tunnel shown in Figure III.29, dowels were used to support a tunnel crest; the visible ends were covered with a colored grout to help mask their presence. Only the grout at the end of the tunnel is visible because the surrounding rock is darker and provides more contrast with the lighter-colored grout than the rock in the center of the tunnel.

Figure III.30 Tunnel crest supported with dowels that have been covered with colored grout. [33]

Design analysis determines the depth of the boreholes required for rock bolts and dowels. The reinforcing element is grouted into place using either cement- or epoxy resin-based grout. Both bonding agents use either a one- or two-step application process, depending on the type of anchor being used. .[47]

Grouting for rock bolts is typically applied in two steps. In the first step, the grout or resin is injected into the base of the borehole-the section known as the "bond length" of the bolt-and allowed to set. After the bond length is dry, the bearing plate and hex nut are installed, the bolt is tightened, and the remaining length (the "free length") is filled with grout or resin. In some cases, contractors can accomplish the grouting in a single step, by using two types of grout or resin, each with a different set time. In this method, the bond length is filled with a quick-set product while the remainder of the hole is filled with a slow-set product; the quick-set resin is allowed to harden, then the bolt is tightened before the slow-set resin sets. Shear pins and dowels can be grouted in one stage, using cement grout or a single resin. [33]

The rock reinforcement is determined in the field during construction. It is imperative that the reinforcement is correctly located on a rock surface that is not prone to weathering, as erosion around the bearing plate can cause a loss of tension. Figure III.30 shows bolts that have failed because of erosion of the surrounding rock.

Figure III.31 *Rock bolts installed in an area where the surrounding rock has eroded away, reducing the effectiveness of the bolts.* .[33]

Installing bolts, dowels, and shear pins most often requires a hand-held or mounted rock drill (normally percussion style), reinforcing tendon (rod or tensionable cable), hex nuts, washers and bearing plates, either epoxy or cement grout for adhesion, and a hydraulic jack or torque wrench.

Figure III.31 illustrates the typical track drilling equipment used to install rock reinforcement. In areas where access is difficult, a man lift or crane may be needed as shown in Figure III.32.

Figure III.32 *Installation of rock bolts using a track drill*. [33]
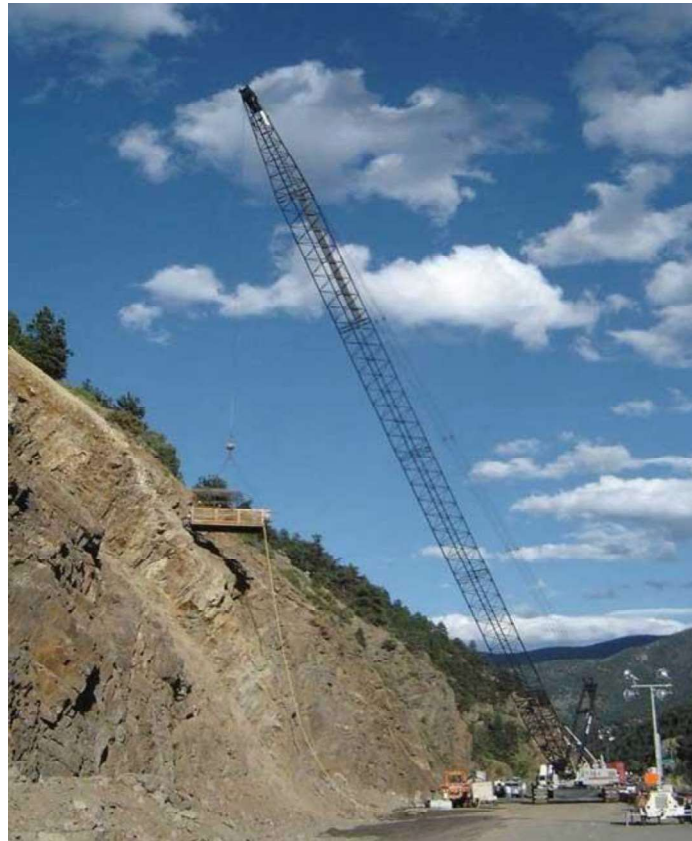
Figure III.33 *Installing rock reinforcement using a drill rig suspended from a crane*. .[33]

III.7.2.1.5 Rock Mass Bonding

In the mining industry, injectable resin and epoxy have been used since the 1960s to stabilize underground coalmines. Since then, they have also been used on numerous geotechnical and geological engineering projects. When injected into a rock mass via drilled boreholes as shown in Figure III.33, these materials follow any fractures and discontinuities around the holes, thus increasing the rock's stability. Rock masses that are excessively fractured and/or contain voids will require large amounts of filler, which can result in excessive cost overruns (for proper resin/grout movement and to keep pumping pressures at a minimum, the discontinuity aperture spacing should be at least 2 mm, or 1/16 in.). [33]

In suitable slopes, injecting resin or epoxy is very effective in providing additional slope stability without negatively effecting aesthetics. There is virtually no maintenance required after resin/epoxy injection. And while research on the application and effectiveness for the use of injectable resin/epoxy as the primary means of slope stabilization is ongoing, initial findings indicate that it can reduce the number of rock bolts needed for slope stabilization.
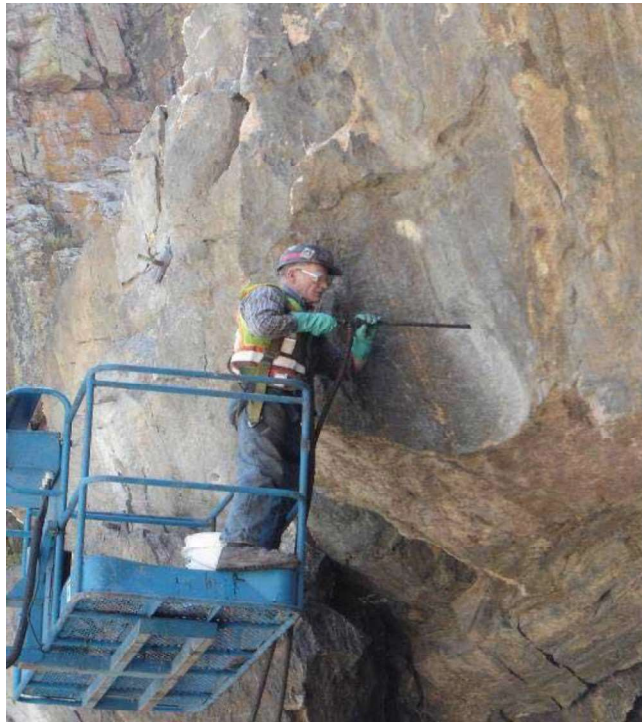
Figure III.34 *Installation of polyurethane resin from man lift, Poudre Canyon, Colorado.* [33]

III.7.2.2 External Stabilization

III.7.2.2.1 Shotcrete

Shotcrete is a wet- or dry-mix mortar with a fine aggregate (up to 23 mm) that is sprayed directly onto a slope using compressed air. Several applications may be needed to build the shotcrete up to the required thickness. Unreinforced shotcrete gives little structural support or protection against weathering, but can be used to prevent differential erosion between units, slope raveling, and loosening of blocks. Shotcrete can also be applied around the exposed ends of rock bolts to help prevent weathering around the bearing plates and limit slope degradation.

To increase tensile strength and structural support, the contractor can include fibers in the shotcrete mix or apply the shotcrete to welded wire mesh shown by Figure III.34.

***Figure III.35** Welded wire mesh can be attached to the rock face before shotcrete is applied.*

Shotcrete can vary in appearance from very rough-in its natural, "as-shot" (unfinished) condition-to moderately rough in the "rodded" condition, to as smooth as cast-in-place concrete (with appropriate finishing). Architectural shotcrete (known as façade or sculpted shotcrete) can produce a wide range of finished surfaces. [33]

In contrast to cast-in-place concrete, shotcrete can be shaped, contoured, and colored to match the surrounding rock as shown in Figure III.35.

***Figure III.36** Shotcrete can be used to protect a slope from erosion-and sculpted to mimic the natural rock face [33]*

In most instances, structural shotcrete is applied to rock slopes to protect a surface which, left untreated, would erode (such as a fault zone or clay seam), or to provide structural support for otherwise sound rock that is either undermined by erosion or is unstable due to unfavorable orientations or degree of fracturing.

This type of shotcrete application can be part of the original construction or part of the remediation of an existing unstable rock slope.

Structural shotcrete can also be used to form part of a retaining system supporting the rock slope as shown in Figure III.37. The system typically includes other components such as welded wire mesh, rock bolts, and/or dowels (the shotcrete also may be fiber-reinforced to improve its tensile capacity). In these applications, the shotcrete will be required to resist or transfer loads and may also have an essential surface protection function in conjunction with its structural function.

Unreinforced shotcrete can be used to cover a well-defined strip (or strips) of rock with a higher rate of erosion than the surrounding rock (faults or shale lenses in sandstone, for example) or an entire slope composed of highly erodible material. In the latter case, the designer should consider laying the slope back to avoid a structured solution, as differential erosion of the rock slope will create stability problems that become worse with time.

Figure III.37 Sculpted shotcrete used to stabilize a tunnel portal (the area directly below the dry-stack wall is the sculpted shotcrete). [33]

A façade of sculpted (or architectural) shotcrete can be used to improve the appearance of structural shotcrete as well as an engineered slope.

In any shotcrete application, drainage (in the form of weep holes or wick drains) will be required to draw water from behind the shotcrete to prevent elevated water pressure from causing cracking and instability in both the shotcrete and localized blocks. [33]

Applied shotcrete varies in thickness, from 50 mm to 0.6 m). For thicker applications, shotcrete should be applied in multiple layers of about 50 to 100 mm each and allowed to cure between applications. Installing shotcrete requires an air compressor, application nozzle, and cement mixer. The application nozzle is either hand held or attached to a man lift or crane. Reinforcing the shotcrete with welded wire mesh or fibers can greatly increase its tensile strength, stand-up time, and rock-bonding potential, as well as the overall stability of the rock mass.

Figure III.38. *Application of the first layer of structural shotcrete*. .[33]

Figure III.38 shows the installation near completion of the first layer of shotcrete on the slope, which took three days to achieve. It is necessary for each layer to dry and gain enough strength for the application of the subsequent layer.

Figure III.39 *Installation of the first layer of structural shotcrete* [33]

III.7.2.2.2 Drainage Systems

Slope stability can also be improved through the installation of drainage systems, which most often consist of horizontal weep drains.

Water in a rock slope often contributes to slope instability, as excessive pore pressure acts on the rock mass and lowers the shear strength along any discontinuities. Water also contributes to rock degradation and fracture expansion and during the process of freeze-thaw weathering.

Normally, drainage systems are used in weak, highly fractured, or layered rock where instabilities could occur along a potential sliding surface. Drainage is generally used to mitigate larger rockslides and failures. In most cases, the drains are installed as uncased holes in massive rock units, drilled with a track rig or portable drill. In weak or highly fractured rock, the drain may be cased with a slotted polyvinylchloride (PVC) pipe to maintain the drain opening. Drains are installed at the base of the slope, and require periodic maintenance to prevent clogging. Usually, they are used in conjunction with other stabilization measures. Horizontal drains can be installed in a rock slope to reduce pore pressure and improve stability, and are a cost-effective, aesthetically pleasing, and relatively low-maintenance option for most slopes with excessive flowing water. They are most effective for large-scale slope instability, where the potential sliding planes are deeply seated within the rock mass. [33]

The most important factor in designing horizontal drains is to orient the holes so they intersect the maximum number of water-carrying fractures, as very little water is contained within the intact rock. Drainage holes should be spaced about 3 to 10 m apart and drilled to a depth of at least one-third of the slope height. Once the water is drained from the slope, it must be diverted away from the slope base to prevent infiltration, which could create additional stability issues. In addition, the slope base must be protected from motorists and any obstructions that could damage the drains or inhibit water movement.

Piezometers installed in the slope can monitor the water pressure and the effectiveness of the installed drainage, allowing engineers to determine if the drainage is sufficient or if additional drains are needed.

Horizontal drains are constructed used conventional rock drilling equipment. The hole location, orientation, and angle are determined based on the fracture patterns in the rock. The installer may need to adjust the assumed orientation and angle based on water conditions encountered. Normally, drainage holes in rock can be drilled using a track rig or hand-held drill (hand-held drills are limited to relatively shallow drainage holes). In highly fractured or weak rock, the hole should be cased with a perforated PVC pipe to prevent collapse. Perforation size should limit the amount of fine particles that infiltrate into the pipe. Surface drainage produced from slope de- watering can be diverted or contained using a lined gutter, culvert, or collection system.

CHAPTER IV

STABILITY OF ROCK CAVITIES

Chapter IV

Stability of rock cavities

IV. 1 Introduction

The stability of rock cavities is a critical consideration in geology and engineering, particularly in relation to their potential for failure and the safety of structures above or around them. Several factors influence the stability of these cavities, including rock properties, cavity geometry, and external conditions.

The shape and size of the cavity play a crucial role in its stability. For instance, rectangular cavities are generally less stable than those with square ceilings, as indicated by the stability number, which is a dimensionless measure comparing actual stresses to critical values. The aspect ratio of the cavity (length to breadth) also affects stability

IV.2 Types of underground Cavities

IV.2.1 Natural Cavities

The majority of natural cavities are created by the dissolution of sedimentary rocks due to the circulation of water, forming cavities of very variable sizes. There are three types of natural cavities: dissolution cavities, suffosion cavities, and volcanic cavities.

IV.2.1.1 Karst Cavities

"Karst" is a landscape created when water dissolves rocks. In Wisconsin, dolomite and some limestone are typical soluble rocks. The rocks are dissolved mostly along fractures and create caves and other conduits that act as underground streams. Water moves readily through these openings, carrying sediment (and pollutants) directly into our groundwater.

Karst landscapes may have deep bedrock fractures, caves, disappearing streams, springs, or sinkholes. These features can be isolated or occur in clusters, and may be open, covered, buried, or partially filled with soil, field stones, vegetation, water or other miscellaneous debris. .[52]
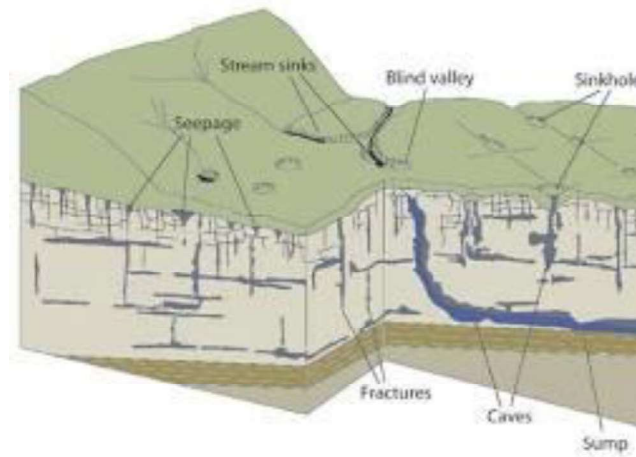
Figure IV.1 Karst Cavities .[52]

IV.2.1.2 Lava Tubes

A lava tube, or pyroduct, is a natural conduit formed by flowing lava from a volcanic vent that moves beneath the hardened surface of a lava flow. If lava in the tube empties, it will leave a cave.

A lava tube is a type of lava cave formed when a low-viscosity lava flow develops a continuous and hard crust, which thickens and forms a roof above the still-flowing lava stream. Tubes form in one of two ways: either by the crusting over of lava channels, or from pāhoehoe flows where the lava is moving under the surface.

Lava usually leaves the point of eruption in channels. These channels tend to stay very hot as their surroundings cool. This means they slowly develop walls around them as the surrounding lava cools and/or as the channel melts its way deeper. These channels can get deep enough to crust over, forming an insulating tube that keeps the lava molten and serves as a conduit for the flowing lava. These types of lava tubes tend to be closer to the lava eruption point. .[52]
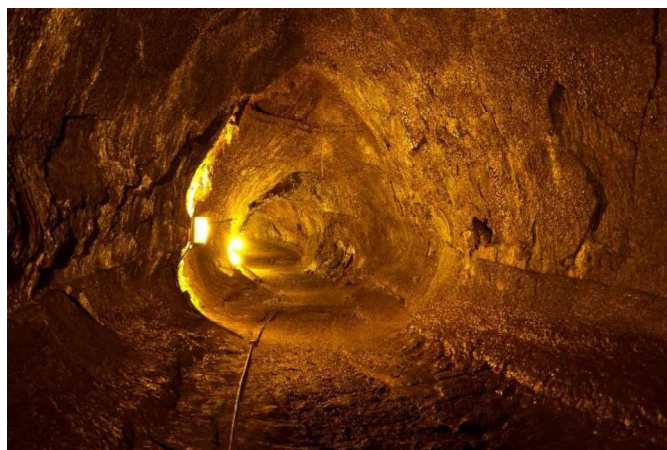
Figure IV. 2 Thurston Lava Tube in Hawaii Volcanoes National Park, .[52]

IV.2.1.3 Sea Caves

A sea cave, is also known as a littoral cave, a type of cave formed primarily by the wave action of the sea. The primary process involved is erosion. Sea caves are found throughout the world, actively forming along present coastlines and as relict sea caves on former coastlines. Some of the largest wave-cut caves in the world are found on the coast of Norway, but are now 100 feet or more above present sea level.[1] These would still be classified as littoral caves. By contrast, in places like Thailand's Phang Nga Bay, solutionally formed caves in limestone have been flooded by the rising sea and are now subject to littoral erosion, representing a new phase of their enlargement. *[34]*

Figure IV.3 Sea cave formation along a fault on Santa Cruz Island, CaliforniaSea Caves

IV.2.1.4 Suffosion cavities

Suffosion cavities are smaller cavities, which can reach several m3. Formed by erosion due to the circulation of water, suffosion cavities develop particularly in loose sedimentary formations.

IV.2.1.5 Volcanic cavities

Like karst cavities, volcanic cavities are made up of guts and chambers. On the other hand, they are of more modest dimensions and do not show any change in the volume of the void over time, once the volcanic activity has ended.

IV.2.2 Man-made Cavities

IV.2.2.1 Mines

Mines are **u**nderground excavations for the extraction of minerals like coal, gold, and diamonds. The entry from the surface to an underground mine may be through a horizontal or vertical tunnel, known as an adit, shaft or decline.

Developed for the exploitation of mineral raw materials (for construction, industry or agriculture), quarries are at the origin of underground cavities of sometimes a large surface area or centred around a shaft (for example in the case of marl pits). Generally located at a depth of between 5 and 50 metres (sometimes less than 5 metres in Gironde), underground cavities from quarries can locally reach 60 to 70 metres in some

chalk mines and gypsum and exceptionally more than a hundred metres for some hard rock mines located on the mountainside in the the Jura, the Pyrenees and the Alps.

Figure IV.4 *Mines*

IV.2.2.2 Tunnels

Tunnels are an iconic feature of the parkway. In fact, 36% of all road tunnels found in national parks across the United States are found here on the parkway.Excavated for transportation, water supply, or other purposes.

Figure IV. 5 *Tunnels*

IV.2.2.3 Underground Structures

refers to the construction of underground tunnels, shafts, chambers, and passageways,[1] it is also sometimes used to describe the portion of traditional construction that takes place below grade. Built for various purposes, such as bomb shelters, storage facilities, or even entire cities.

Figure IV.6 *The construction of the Sanford underground research Center. Source: sanfordlab.org*

IV.2.2.4 Troglodyte facilities and cellars

Excavated for storage, storage (wine cellars), industrial (excluding quarry) or agricultural activities, housing, or the development of facilities for collective use (churches, ovens, presses, etc.), troglodyte installations and cellars are generally close to the surface and generally limited to 1 or 2 rooms.

Fgure IV. 6 Underground wine caves

IV.2.2.5 Buried military works (saps, trenches and galleries)

Dug for military needs (sheltering troops, penetrating enemy lines), these structures (trenches, access galleries, underground rooms) are generally located in areas with relatively flat topography. While history and archives tell us which regions are potentially affected and where some of the structures can be located, their precise location is most often not known. Divided into real networks, they were linked together in a way that was difficult to locate.

Figure IV.7 Buried military works

IV.3 Origins and consequences of associated phenomena

The presence of a cavity causes a change in the balance of elements in the soil. For all types of cavities, degradation is to be expected due to the progressive decrease in the mechanical strength of the surrounding material. Underground cavities and the disorders they are likely to cause constitute a major risk for developments and sometimes for human life.

IV.3.1 Subsidence

A subsidence is a flexible, unbreakable and progressive deformation of the ground surface resulting in a basin-shaped depression, generally with a flat bottom, and on rather elastic ground that will withstand the deformation without breaking.

This type of disorder sometimes develops over several hectares in the right of vast quarries or mines. This is often a symptomatic phenomenon of underground quarries that are either poorly backfilled or, when they are deep, covered by "soft" formations.

Generally, it is not so much the subsidence itself (vertical displacements) that affect buildings and surface infrastructure, but rather the deformations of the ground (horizontal displacements, bending, etc.) While significant disorders can affect the buildings and infrastructures (in particular underground networks) present in the cavities, surface subsidence only very exceptionally and often indirectly presents a danger to people due to the progressiveness of the phenomenon.
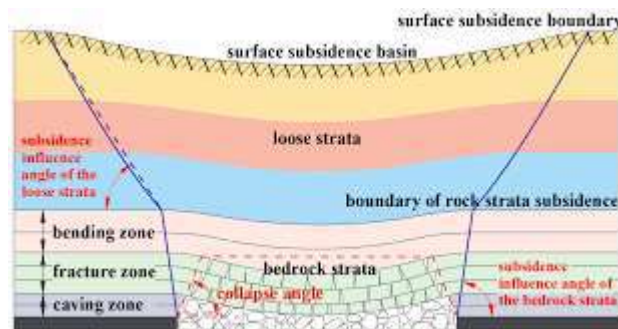
Figure IV.8 *Subsidence [38]*

IV.3.2 Localized collapses

A localized collapse is classically manifested by the sudden appearance of a collapse crater whose extension varies from less than one meter in diameter to a few tens of meters at most. Several phenomena can be at the origin of this type of disorder on the surface: the raising of the fontis bell, the breaking-in, and the suffosion.
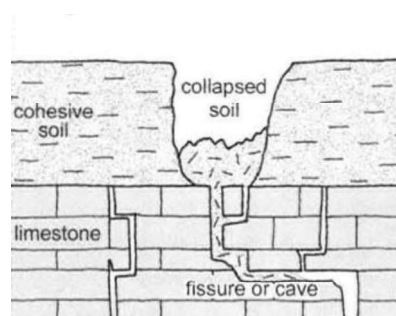
Figure IV.9 *Localized collapses [38]*

IV.3.3 The raising of the fontis bell

A sudden and localized collapse in the form of a funnel or a crater, the fontis is most often caused by the rise, more or less slowly, of a vacuum bell to the surface following the rupture of the roof of a cavity. This phenomenon can cause significant damage to structures and casualties due to the speed and size of the phenomenon.

Figure IV. 10 Collapse sinkhole in Chinchón, Spain.[36]

IV.3.4 Breaking-in

Most often caused by massive water circulation, bud removal corresponds to the gravitational entrainment of the filling material of a cavity:

- pocket of clay in a chimney or karst fissure;
- backfilled plug of a marl pit or quarry well.

This phenomenon can lead to the appearance, suddenly or gradually, of a void on the surface, generally of fairly small size (a few m2). It particularly affects the natural groundwater circulation networks developed in limestone massifs (karst networks). Indeed, during heavy rainfall, the circulation of water in the cracks and karst chimneys encourages the budding of the filling materials in these cavities.

IV.3.5 Widespread collapses

Widespread collapses, also known as mass collapses, result in a violent and spontaneous lowering of the surface to a depth of sometimes several hectares and several meters, with all the land above the cavity collapsing at once. Generally associated with quarries with a significant lateral extension, generalized collapses are most often initiated by a chain failure of the pillars of the operation, the roof (ceiling) then descending en masse.

They assume the existence of a mining area with high defruiting rates (ratio of the void area to the total area), large void volumes and fragile mining configurations (undersized pillars, large slenderness, etc.). These phenomena, which are fortunately exceptional, are likely to generate very damaging consequences for the people and property located in their area because the repercussions of the disorder on the surface are generally sudden and brutal.

IV.4 Cavities in an elastic continuous medium

In this section, we will study the redistribution of stresses and deformations in a massif that behaves in an elastic manner (the failure criterion is not met).

IV.4.1 Cavities and boreholes with isotropic initial stress state

We will first deal with the case of axisymmetric cavities excavated in a continuous, homogeneous and isotropic medium, where an initially lithostatic (or isotropic) stress state prevails, the objective being to determine the variations of stresses and the displacements following the excavation. Given the cylindrical geometry of the cavities, we will adopt the hypothesis of plane deformations perpendicular to the axis of the cylinder. If the cavity is not supported, the digging results in a cancellation of the normal stress on the wall. It must therefore be simulated by applying a tensile to the wall, of the same absolute value as the initial stress.[25]

If this loading is axisymmetric, the problem becomes one-dimensional and we can easily calculate the stresses and displacements from the equilibrium equations of the continuous medium, the stress-strain and strain-displacement relationships. In addition, the principal directions are then given by the axes of the cylindrical coordinates r, 0 and z (axis of the cavity). This assumption of axisymmetry is accurate in the case of vertical **drilling** or a well, since the entire section is at the same depth. Moreover, the medium can be considered infinite in a horizontal plane, with a horizontal constraint σ^0 initially constant in this plane. We then obtain the following variations in stress and displacements:

$$\Delta\sigma_r = -\sigma^0 \frac{R^2}{r^2} \; ; \Delta\sigma_\theta = +\sigma^0 \frac{R^2}{r^2} \; ; \Delta\sigma_z = 0 \tag{IV.1}$$

$$u = -\sigma^\circ \frac{R^2}{2Gr} \; ; v = 0 \; ; w = 0 \tag{IV.2}$$

where R is the radius of the cavity and G is the shear modulus of the medium.

The displacement (called convergence) is greatest at the wall and decreases as it moves away from it.

The total stresses after digging are therefore:

$$\sigma_r = \sigma^0 - \sigma^0 \frac{R^2}{r^2} \; ; \sigma_\theta = \sigma^0 + \sigma^0 \frac{R^2}{r^2} \; ; \sigma_z = \sigma^0 \tag{IV.3}$$

It can be seen that the radial stress decreases as the cavity approaches, that the orthoradial stress increases to a value of $2\sigma^0$, and that the longitudinal stress does not vary during digging. The evolution of the first two as a function of distance from the wall is shown in Figure IV.7, as well as the Mohr circle at the wall. Note that expressions (5) and (6) remain valid if the initial stress state is isotropic only in the horizontal plane. In this case, the total stresses σ_r and σ^0 are still given by equation (7), but σ_z is equal to the initial vertical stress, different from the horizontal stress σ^0.
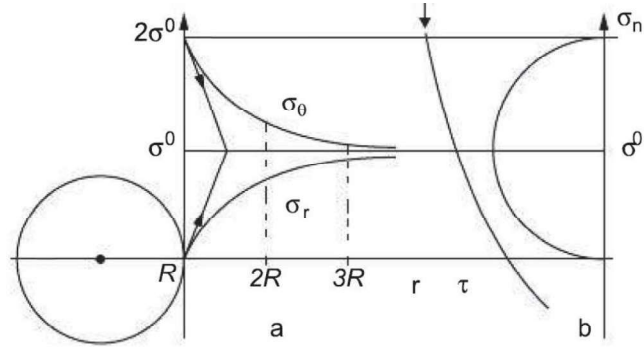
Figure IV.11 (a) Evolution of radial and orthoradial stresses around a borehole (b) and Mohr circle representing the state of stresses at the wall .[19]

It should be noted that these stresses could have been obtained directly by applying a load (σ^0 to infinity and zero stress to the wall), but the displacements due to the application of 0 would have been obtained σ^0 on a block that had already been dug, which does not correspond to any reality (gravity was exerted before the excavation). In the same way, if we want to model convergence numerically, we must first model the natural stresses exerted in the middle, then simulate the digging by applying a tension to the wall.

In the case of a **horizontal roadway,** the assumption of axisymmetric loading can be adopted, if the relative variation of the initial stress between the top and the bottom of the section is sufficiently small. The lithostatic stress being proportional to the depth *H,* sa valeur autour de la section est comprise entre : $(\overline{\gamma}H - \overline{\gamma}R)$ et $(\overline{\gamma}H + \overline{\gamma}R)$

The relative variation around the mean value is therefore equal to *R/H.* In practice, this loading model can be adopted from a depth equal to 10 times the radius. But unlike in the case of drilling, the medium is no longer infinite in the plane of deformation, because it is limited upwards by the surface of the ground. We can try to « frame » reality between two models, that of the hole in an infinite medium and a model of a hollow cylinder of thickness equal to the depth of the gallery (the stresses and displacements in a hollow cylinder subjected to internal and external loading. It can be seen that the orthoradial stress and the displacement at the wall differ by only about 2 % between the infinite model and a cylinder with an outer radius equal to 10 times its inner radius. The results of the infinite model (equations IV.5 and IV.6) can therefore be applied to a horizontal gallery located at a depth equal to 10 times its radius. The total stresses are obtained by adding the stress variations (equation 5) to the initial stresses, which are proportional to the depth h of the point considered (h tends to 0 as it approaches the surface) :

$$\sigma_r = \sigma^0(h) - \sigma^0 \frac{R^2}{r^2} \;\; ; \;\; \sigma_\theta = \sigma^0(h) + \sigma^0 \frac{R^2}{r^2} \;\; ; \;\; \sigma_z = \sigma^0(h)$$

(IV.4)

On ne peut considérer σ^0 (h) égal à γH avec une erreur relative inférieure à 10 %, que dans une zone située à une profondeur comprise entre 0,9H et 1,1 H (cela revient alors à négliger le poids de cette zone). Si ce n'est pas le cas, l'évolution des contraintes représentée sur la figure IV.7 n'est valable que sur les axes radiaux horizontaux (sur lesquels σ^0 est constant). Pour des axes verticaux, l'asymptote n'est plus horizontale, mais a une pente égale au gradient de la contrainte naturelle. Cependant, l'erreur reste acceptable, même à une profondeur de 10 fois le rayon, si l'on s'intéresse seulement à la paroi *(r - R)*. On obtient alors :

$$\sigma_r = 0 \ ; \ \sigma_\theta = 2\sigma^0 \ ; \ \sigma_z = \sigma^0$$

(IV.5)

Note that expressions (5), (6), (8) and (9) remain valid if the initial stress state is isotropic only in the vertical plane perpendicular to the gallery.

Since the major principal stress is zero at the gallery wall (equations 9), there is **a failure** at the wall if the major principal stress σ_θ (or $oz°$) is greater than the uniaxial compressive strength σ_c of the medium, i.e. if max $(2\sigma^0, \sigma_z^0) > \sigma_c$. In this case, failure can be avoided by applying a support pressure p. The stresses and radial displacement then become:

$$\Delta\sigma_r = -(\sigma^0 - p)\frac{R^2}{r^2} \ ; \ \Delta\sigma_\theta = +(\sigma^0 - p)\frac{R^2}{r^2} \ ; \ \Delta\sigma_z = 0$$

(IV.6)

$$u = -(\sigma° - p)\frac{R^2}{2Gr} \ ; v = 0 \ ; w = 0$$

(IV.7)

With a Mohr-Coulomb failure criterion, the pressure required to avoid failure (if $\sigma_z^0 < \sigma_c$) must be equal to:

$$p_e = \sigma^0(1 - sin\phi) - c\cos\phi$$

(IV.8)

where (φ and *c* are respectively the angle of friction and the cohesion of the medium.

Figure IV.8 shows σr and σ_θ in this case, as well as the Mohr circle at the wall.

At the wall, the absolute value of the displacement (which we will call convergence) is written:

$$|u| = u_R = (\sigma° - p)\frac{R}{2G}$$

The curve giving *p* as a function of |*u*| is called the characteristic curve of the massif. It gives the necessary pressure to stabilize the convergence at the u-value .
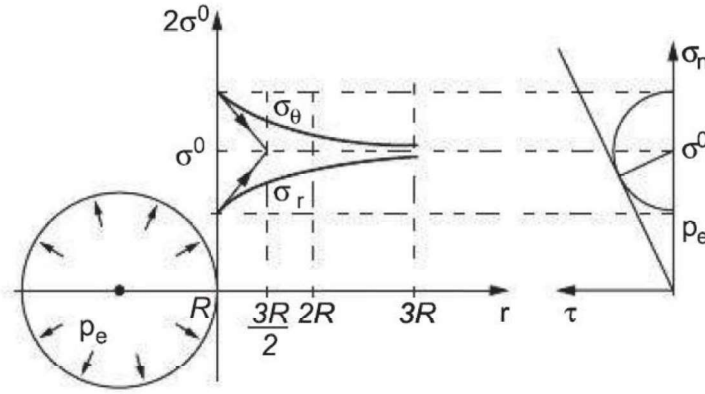
Figure IV.12 *Evolution of radial and orthoradial stresses around a borehole with just enough support pressure to prevent failure.[19]*

IV.4.2 Drifts and boreholes with anisotropic initial stress state

Lorsque les contraintes initiales ne sont pas isotropes, nous allons considérer le cas où l'axe de la cavité est parallèle à une des contraintes principales initiales (σ_z^0), qui est généralement horizontale ou verticale. Soient (σ_1^0)^ et (σ_2^0) les contraintes principales initiales orthogonales à l'axe, telles que ($\sigma_2^0 = K_0\ \sigma_1^0$, avec *K0<1*.

Comme précédemment, pour modéliser les déplacements consécutifs au creusement, il faut appliquer à la paroi une contrainte opposée à celle qui règne initialement. Mais ce chargement n'est plus axisymétrique, donc les directions principales ne sont plus r, θ et *z* et le déplacement comporte une composante radiale u et une composante orthoradiale v (sauf sur les deux axes de symétrie) :

$$-u = \frac{\sigma_1^0}{4G}\left\{(1 + K_0)\frac{R^2}{r} + (1 - K_0)\left[\frac{R^4}{r^3} - 4(1 - \nu)\frac{R^2}{r}\right]\cos 2\theta\right\}$$

$$-v = \frac{\sigma_1^0}{4G}(1 - K_0)\left[\frac{R^4}{r^3} - 2(1 - 2\nu)\frac{R^2}{r}\right]\sin 2\theta \qquad\qquad \text{(IV. 9)}$$

θ=0 correspond à la direction orthogonale à $\boldsymbol{\sigma_1^0}$

A la paroi de la cavité (r = *R),* les déplacements radiaux sont en général négatifs (convergence), mais il peut y avoir divergence dans la direction orthogonale à $\boldsymbol{\sigma_1^0}$

(θ = 0), si *K₀ < (l-2υ)/2(l-υ).* Pour υ = 0,25, cette valeur critique vaut 1/3. Il faut donc une forte anisotropie des contraintes pour observer une divergence.

Les contraintes totales sont les suivantes :

$$\sigma_r = \frac{\sigma_1^0}{2}\left[(1 + K_0)\left(1 - \frac{R^2}{r^2}\right) - (1 - K_0)\left(1 - 4\frac{R^2}{r^2} + 3\frac{R^4}{r^4}\right)\cos 2\theta\right] \qquad \text{(IV.10)}$$

$$\sigma_\theta = \frac{\sigma_1^0}{2}\left[(1+K_0)\left(1+\frac{R^2}{r^2}\right)+(1-K_0)\left(1+3\frac{R^4}{r^4}\right)\cos 2\theta\right] \tag{IV.11}$$

$$\tau_{r\theta} = \frac{\sigma_1^0}{2}\left[(1-K_0)\left(1+2\frac{R^2}{r^2}-3\frac{R^4}{r^4}\right)\sin 2\theta\right] \tag{IV.12}$$

$$\sigma_z = \sigma_z^0 + 2\nu\sigma_1^0(1-K_0)\frac{R^2}{r^2}\cos 2\theta \tag{IV.13}$$

At the cavity wall, the orthoradial stress varies between a maximum value $\sigma_\theta = (3K0-1)$ at the points $\theta = 0°$ and $\theta = 180°$ and a minimum value $\sigma_\theta = (3K_0-1)$ at the points $\theta = 90°$ and $\theta = 270°$. The latter is negative (traction) if $K0$ is less than 1/3. In this case, we have a tensile fracture if the failure criterion is met, rather than in compression, because the compressive strength of the rock material is generally at least 10 times greater than its tensile strength. The maximum compression at the wall is increased from σ_1^0

for $K_0 = 1$ (isotropic case dealt with in the previous paragraph) at $3\sigma_1^0$

for $K_0 = 0$, passing through $2.5\sigma_1^0$ for $K_0 = 0.5$. The stress state therefore becomes more and more critical with respect to the failure criterion, as the anisotropy of the initial stresses increases. It is at points of maximum compression that the phenomenon of spalling can occur (observable in drilling or in a roadway), if the orthoradial stress exceeds the uniaxial compressive strength of the medium. The extreme case where $K_0 = 0$ is illustrated in figure IV.9.
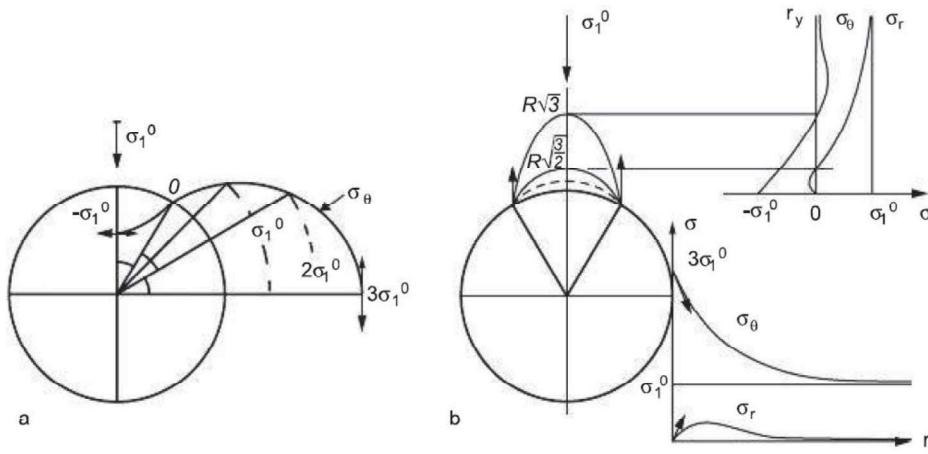
Figure IV.13 Case of an initial uniaxial stress state. A: Evolution of the orthoradial stress along the wall; B: Evolution of constraints in [19]

IV4.3 Cavités cylindriques non axisymétriques

The analytical calculation of stresses in the case of a cylindrical cavity of elliptical cross-section, parallel to an initial principal stress (σ_z^0).

When the other two initial principal stresses are equal ($\sigma_1^0 = \sigma_1^0 = \sigma^0$), the stress parallel to the wall σ_t is maximum at the points of intersection of the elliptical section with its major axis (Figure IV.20A). It has as

its value $\sigma_A = 2\sigma^0 a/b$, where a and b are the major and minor axes of the ellipse, respectively. The minimum of σ_t to the wall are at the points of intersection of the elliptical section with its minor axis. They have the value : $\sigma_B = 2\sigma^0 a/b$. It can be seen that the more flattened the ellipse, the greater the concentration of stress at its ends.

For a uniaxial initial stress state, compression is maximum at the ends of the ellipse, when the major axis is perpendicular to the stress. For a ratio of 2 between the axes of the ellipse, it is 5 times the initial stress (this case is shown in Figure iv.10B). On the contrary, compression is minimal when the major axis is parallel to the stress (Figure iv.10). We can therefore see the importance of the orientation of a cavity to avoid excessive compression. In all cases, and whatever the ratio of the axes of the ellipse, the stress tangent to the wall on the axis parallel to the initial stress σ_t is always equal to - σ^0_1
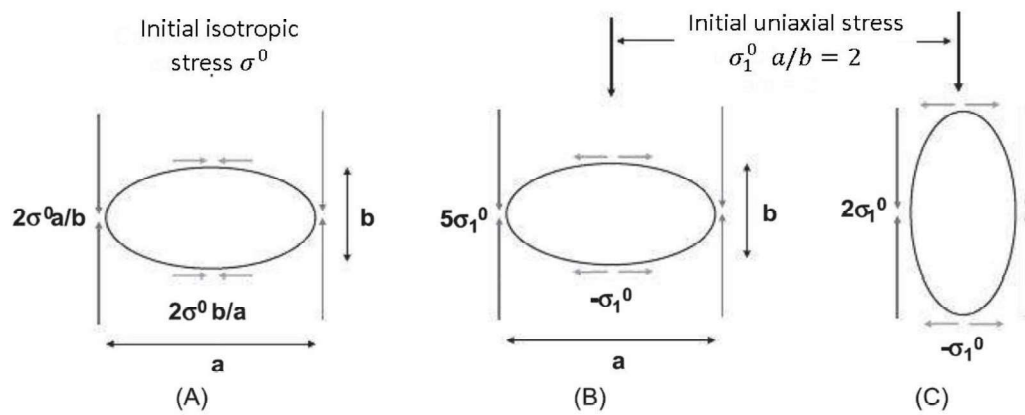
Figure IV.14 Elliptical cross-sectional gallery, with isotropic (general case) or uniaxial (for an axis ratio equal to 2) stress state.[15]

For any anisotropic initial stress state, the compression tangent to the wall is equal to ($\sigma^0_1 + \sigma^0_2$) over the entire cross-section, when the ratio of the axes of the ellipse (**a/b)** is the same as that of the main constraints (σ^0_1/σ^0_2)

For cylindrical cavities of any cross-section, numerical modeling is required to calculate stresses and displacements. Hoek and Brown (1980) presented the calculated stresses for different roadway sections. Some examples are given on figs IV.15 and IV.16. The right-hand side of the figures represents the iso-value curves of the major (solid line) and minor (dash) principal stresses, for the values of the initial stresses shown at the bottom right. The left side
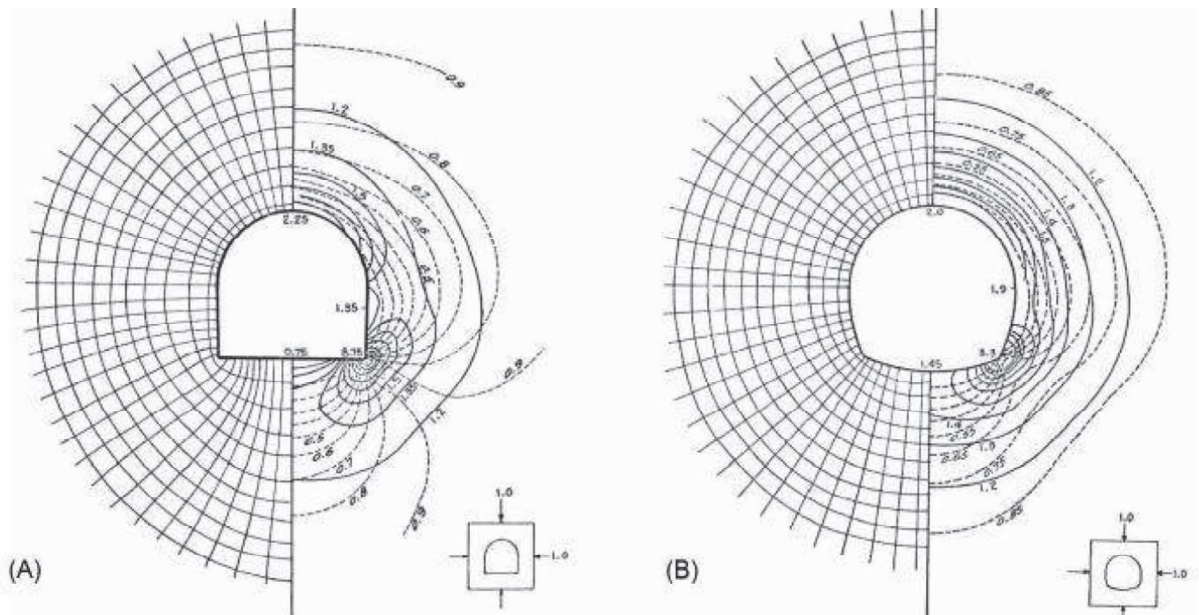
Figure IV.15 Main constraints around a vaulted gallery, numerically modelled by the method of boundary elements [12].
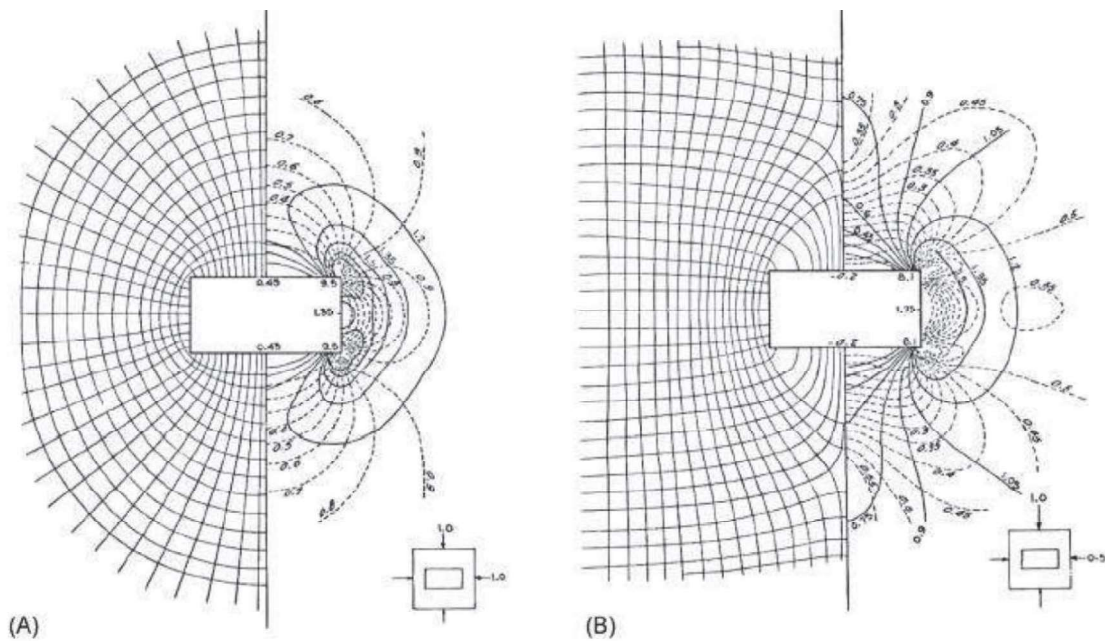
Figure IV.16 *Main stresses around a rectangular cross-sectional gallery, numerically modelled by the boundary element method [12]*

represents the trajectories of the principal constraints, which are curves parallel to the principal directions. Figure IV.15 shows two different cross-sections with isotropic initial stress state. For the horseshoe section in Figure IV.15a, it can be seen that in the upper part in the form of an arch, the stress tangent to the wall

is slightly higher than that obtained analytically for a circular section (σ^0 is multiplied by 2.25 instead of 2). In the lower part, there is a strong

Stress concentration at right angles at the base of the walls (amplification of 8.75), where local shear failures can occur, which can damage the support structures. It can be seen in Figure IV.15b that this concentration is reduced with an inverted vault-shaped raft, which softens the right angles (concentration reduced to 3.3). Figure IV.16 shows a rectangular cross-section with two different initial stress states. As before, we observe high concentrations of stresses at right angles, but also a tensile stress at the roof, for a stress parallel to the major axis σ^0_2 equal to half of the σ^0_1. This phenomenon can be accentuated if the gallery is dug in horizontal beds, which can bend under their own weight.

IV4.4 Stresses Around Elliptical Openings

The stresses around elliptical opening can be treated in analogous way to that just presented for circular opening. There is much greater utility associated with the solution for elliptical opening than circular opening, because these can provide a first approximation to a wide range of engineering geometries, especially opening with high with/height ratios (mine slopes, power house caverns, etc.)

Assuming isotropic rock conditions, an elliptical opening is completely characterized by two parameters: aspect ratio (major to minor axis) which is the eccentricity of ellipse; and orientation with Respect to the principle stresses. The position on the boundary, with reference o the x-axis, is given by the angle χ.

$$\sigma_\theta = \frac{p}{2q}\left\{(1+k)\left[(1+q^2)+(1-q^2)\cos 2\,(\chi-\beta)\right]\right.$$
$$\left. -(1-k)\left[(1+q)^2\cos 2\chi+(1-q^2)\cos 2\beta\right]\right\}$$

where $q = \dfrac{W}{H}$
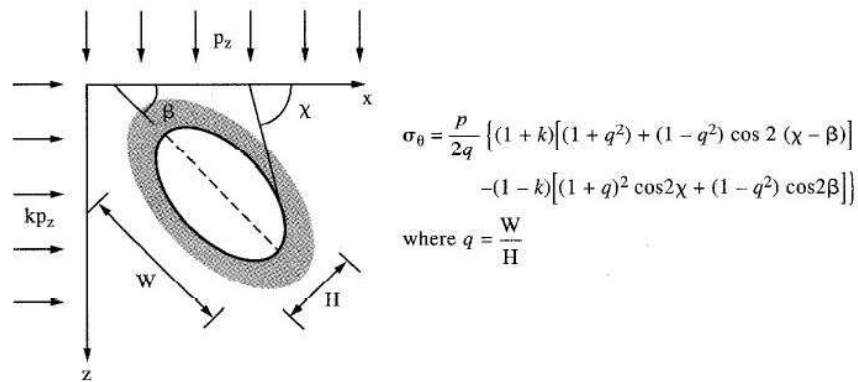
It is instructive to consider the maximum and minimum values of the stress concentrations around the ellipse for the geometry of an ellipse aligned with the principal stresses. It can be easily established that the extremes of stress concentration occur at the ends of the major and minor axes

$$\sigma_A = p(1-k+2q) = p\left(1-k+\sqrt{\frac{2W}{\rho_A}}\right),$$

$$\sigma_B = p\left(k-1+\frac{2k}{q}\right) = p\left(k-1+k\sqrt{\frac{2H}{\rho_B}}\right)$$

where, for an ellipse, the radii of curvature are

$$\rho_A = \frac{H^2}{2W} \text{ and } \rho_B = \frac{W^2}{2H}$$
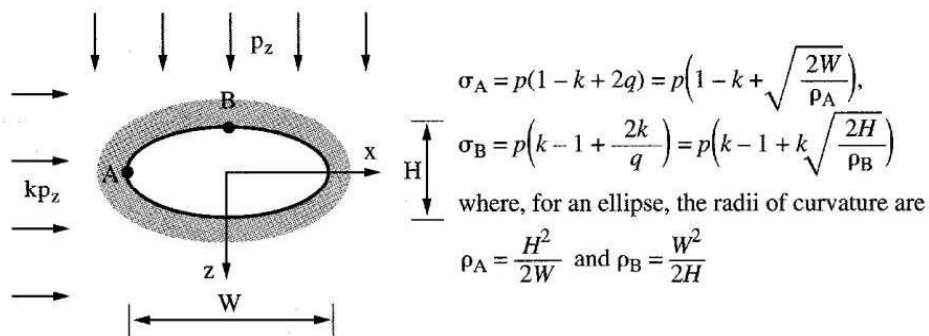
Zone of Influence

Elliptical   approximation   to   the   zone   of   influence   around   an   elliptical   excavation.

$$W_i = H\sqrt{A\alpha|q(q+2)-k(3+2q)|}$$
or
$$W_i = H\sqrt{\alpha\{A(k+q^2)+kq^2\}}$$
Whichever is greater

$$H_i = H\sqrt{A\alpha|k(1+2q)-q(3q+2)|}$$
or
$$H_i = H\sqrt{\alpha\{A(k+q^2)+1\}}$$
Whichever is greater

$$A = \frac{100}{2c} \qquad q = \frac{W}{H} \qquad \alpha = \begin{cases} 1 \text{ if } k < 1 \\ 1/k \text{ if } k > 1 \end{cases}$$

c% zone of influence
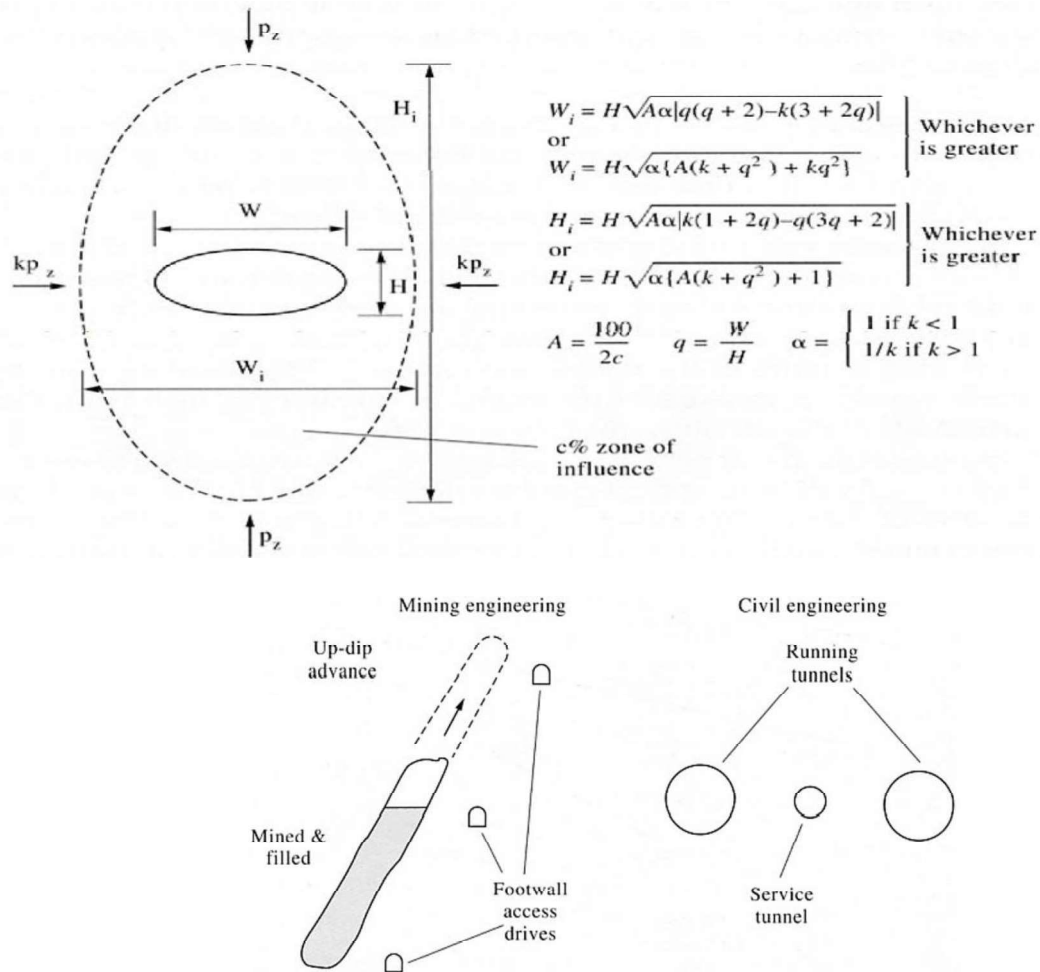
IV.5 Plasticity and Fracture in a Continuous Media

To explain the mechanism of plasticizing the ground during the digging of a cavity, we will first study the case of a circular cross-sectional gallery, with an isotropic initial stress state.

IV.5 .1 Galerie avec état de contraintes initial isotrope

When a roadway is drivaged, it can be seen that deformations and displacements begin to occur in front of the face and only stabilize at a certain distance behind it, as shown in the figure IV.13. Three-dimensional modelling in elastic behaviour shows that about 25% of the final convergence has already occurred at the face (Panet, 1995). This phenomenon is called deconfinement, because the ground around the gallery gradually changes from a confined state (before excavation) to a deconfined state (after excavation if there are no supports). To model in two dimensions the evolution of a section of the roadway during the passage of the face, it is assumed that the radial stress on the wall (σ_R) gradually decreases in value σ^0 until O, whereas in reality, it is abruptly cancelled out when the front passes (Figure IV.15). This fictitious radial stress (or fictitious pressure) is expressed as afunction of the parameter λ, called the deconfinement rate:

$$\sigma_R = (1 - \lambda_e)\, \sigma_0 \qquad\qquad\qquad (IV.14)$$

Using equation from the two-dimensional model, we can express the convergence to the wall uR:

$$u_0 = \frac{\sigma_0}{2G} R \qquad\qquad\qquad \textbf{(IV.15)}$$

The phenomenon is illustrated in Figure IV.17, where the changes in constraints and convergence during the deconfinement are represented, in the event that the criterion of rupture is not met. Figure IV.14 shows the case where the criterion of environmental failure is achieved with perfect elastoplastic behaviour. In the initial stress state, σ_r (R) and σ_θ(R) are equal to σ^0. As the front approaches, σ_r (R) decreases with the end of lockdown and σ_θ(R) increases, until it reaches the breakout criterion for the $\sigma_{\theta max}$(R) is then equal to p_e $\lambda = \lambda e$ and . From that moment on,, σ_r (R), minor main stress, continues to decrease, resulting in a decrease in the major major stress σ_θ(R) because the two constraints are linked by the criterion of rupture. In the absence of support, σ_r (R) decreases to the uniaxial compressive strength oc of the medium. It should be noted that the evolution of σ_r (R) and σ_θ(R) during the deconfinement is the same as that of σ_r (R) and σ_θ(R) as a function of *r* when the digging is completed. Indeed, the fracture is not limited to the wall, but propagates up to a distance *Rp* from the axis of the gallery, called the plastic radius. The area that is broken is called the plastic ring. The rupture in *r=R* can occur before or after the passage of the front. In the first case, a plastic area appears on the forehead.

When a roadway is drivage, it can be seen that deformations and displacements begin to occur in front of the face and only stabilize at a certain distance behind it, as shown in Figure IV.13
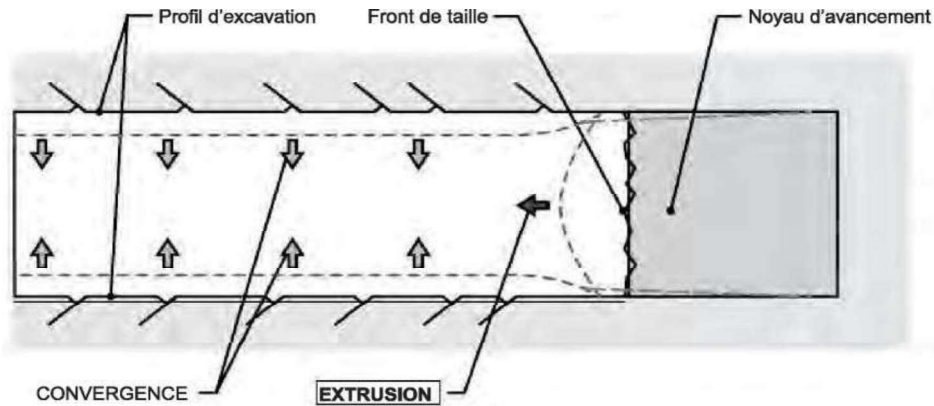
Figure. IV.17 Deformations and displacements in the vicinity of the face of a tunnel [19]

The phenomenon is illustrated in the figure. IV.24, where the changes in constraints and convergence during the deconfinement are represented, in the event that the criterion of rupture is not reached.

The rate of deconfinement λ characterizes the state of the massif at the location x considered. It varies from 0 (initial state, in front of the face for x<0) to 1 (completely deconfined state, far behind the front for x>0). For this problem, we will set the cylindrical coordinates : r, θ, x. These coordinates are the main guidelines. The displacements, deformations and stresses generated by the excavation of the tunnel in

relation to the initial state are calculated. If r tends to infinity then u tends to 0. We can consider the variations in stresses with respect to the initial stress assumed to be geostatic when we are at great depths $\sigma_r=\sigma_\theta=\sigma_0=\gamma h$. with h average tunnel depth
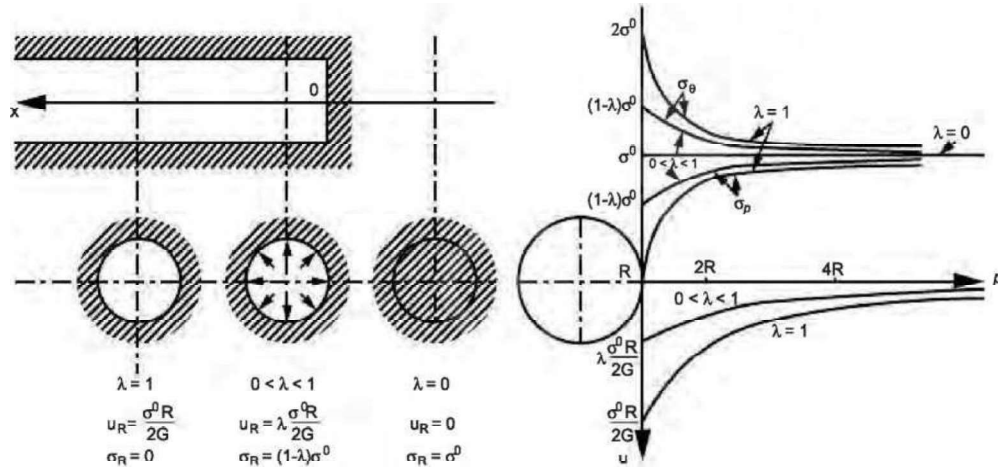
Figure IV.18 *Elastic deconfinement of a tunnel at the passage of the quarry face [20]*

For a complete deconfinement, at the wall of the tunnel, we have a state of simple compression of the ground since $\sigma_R=0$ andt $\sigma^\theta=2\ \sigma^0$.

The simple compressive strength of the ground Rc can be easily calculated according to the following equations:

$$R_c = \frac{2.c.\cos\varphi}{1-\sin\varphi} \tag{IV.16}$$

$$R_c = 2c\tan\left(\frac{\pi}{4}+\frac{\varphi}{2}\right) = 2c\sqrt{k_p}$$

k_p : Passive coefficient

$$k_p = \frac{1+\sin\varphi}{1-\sin\varphi} = \tan^2\left(\frac{\pi}{4}+\frac{\varphi}{2}\right) \tag{IV.17}$$
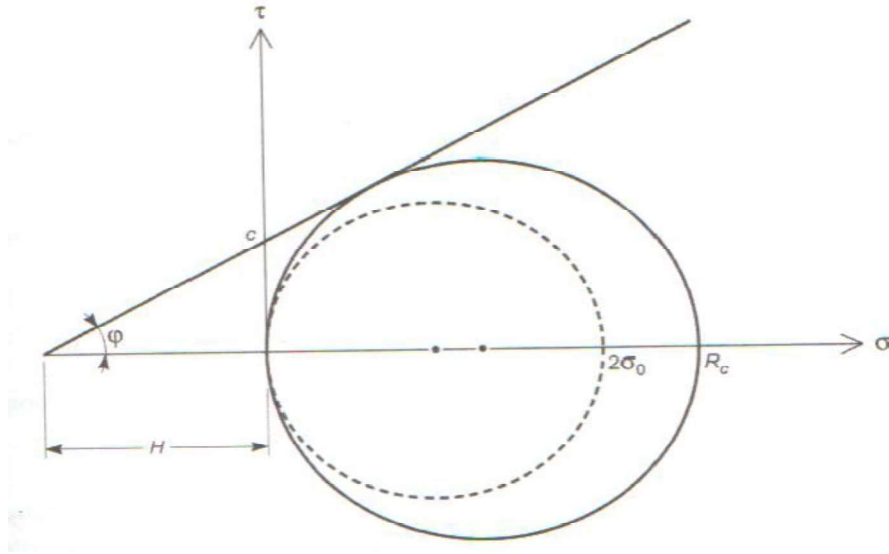
Figure IV.19 *Mohr circles of complete deconfinement and simple compressive strength [20]*

For **R$_c$** > 2σ$_0$

The soil remains entirely in the linear elastic domain regardless of the deconfinement (Fig. IV.19). We are therefore brought back to the previous problems, the land remaining in the linear elastic domain, even for a complete deconfinement.

For **R$_c$** < 2σ$_0$

For a complete disconfederation, it is impossible for 2σ$_0$ > ***R$_c$***, for then the circle of simple compression would intersect the Mohr-Coulomb line. This means that the soil is in the elastic domain near the face (the deconfmement being low) and gradually enters the plastic domain away from the face (the deconfmement increases).

From the appearance of the plastic zone (Fig. IV.20), the Mohr circle (**σ$_R$** = [1 - λ(x)] σ$_0$, [1 + λ(x)] σ$_0$) remains tangent to the right of Mohr-Coulomb .

In the field of plastics, the main constraints **σ$_R$** and σ$_\theta$ verify the Mohr-Coulomb criterion. When ***R$_c$*** < 2σ$_0$, the circle therefore comes into contact with the line before the extreme values of the stresses σ$_R$ = 0 et σ$_\theta$ = 2σ$_0$ are not achieved.
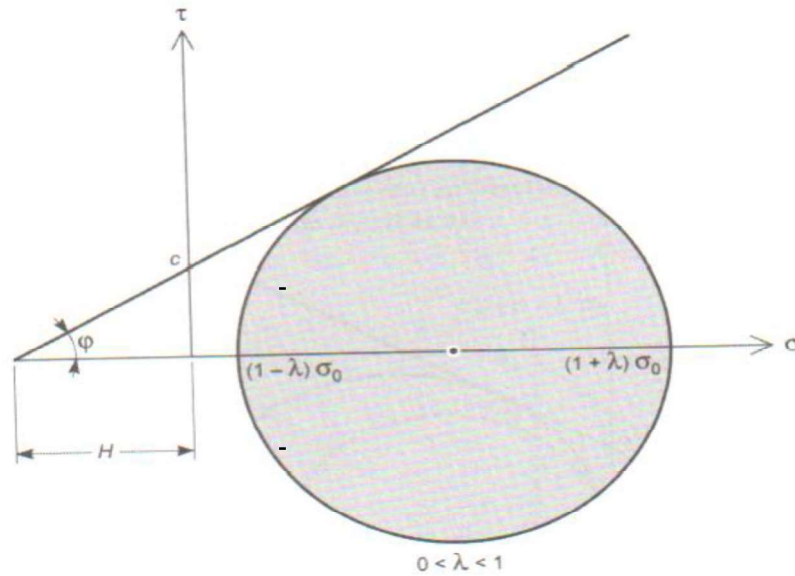
Figure IV.20 *Entry of the field into the plastic field before complete deconfinement [20]*

More precisely, along the axis of the tunnel and away from the front (x > 0):

1. near the front, the terrain is first in elasticity when the confinement is sufficient for the triaxial effect to allow the Mohr circle to remain below the Mohr-Coulomb line;

2. As it moves away from the front, the terrain becomes more flexible before the total deconfinement;

-   the Mohr circle then remains tangent to the right of the Mohr-Coulomb until the last simple compression circle for total deconfinement (Fig. IV.21).
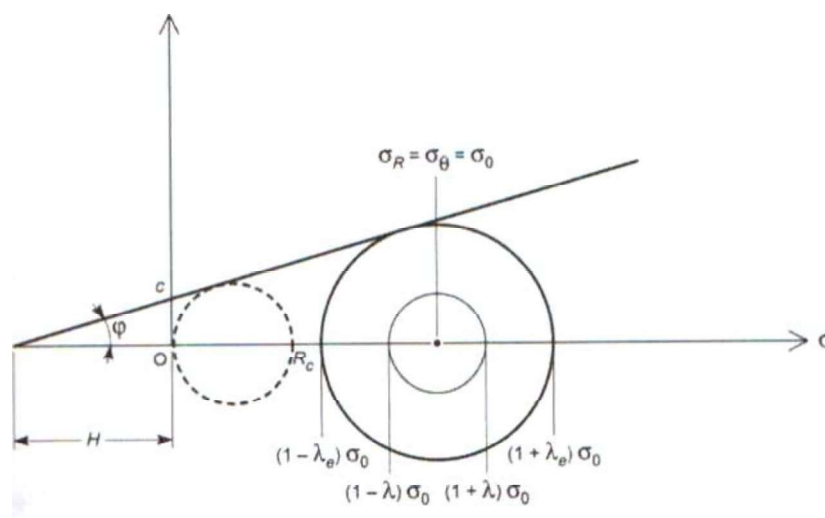
Figure IV.21 *Evolution of constraints as a function of the déconfinement [20]*

We will therefore determine at what distance *x* from the face [i.e. for what value of the rate of deconfinementt λ(x)] plasticity appears on the intrados of the tunnel. Then for a value of *x* greater than this distance, we study the plastic zone in the soil section orthogonal to *x*.
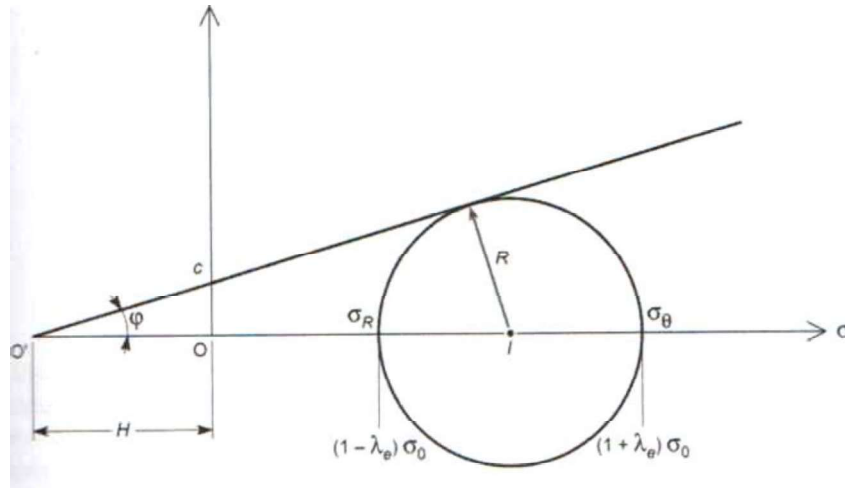
Figure IV.22 *Determination of plasticity pairing [20]*

We first determine the deconfinement λ_e necessary for the entry into perfect plasticity with the Mohr-Coulomb criterion of the field For values less than λ_e the ground remains in elasticity.

$$R = (OI + H)\sin\varphi \qquad\qquad\qquad (IV.18)$$

$$\sigma_\theta = \frac{1+\sin\varphi}{1-\sin\varphi}\,\sigma_R + \frac{2c\,\cos\varphi}{1-\sin\varphi} \qquad\qquad (IV.19)$$

$$\sigma_\theta = k_p\,\sigma_R + 2c\,\sqrt{k_p}$$

$$\sigma_\theta = k_p\,\sigma_R \qquad\qquad\qquad (IV.20)$$

$\sigma_R = (1 - \lambda)\,\sigma_0$ and $\sigma_\theta = (1 + \lambda)\,\sigma_0$ verify equality $\sigma_0 = k_p\,\sigma_r + R_c$ when the Mohr circle becomes tangent to the right of Mohr Coulomb (Fig. IV.22).

$$(1 + \lambda_e)\sigma_0 = k_p\,(1 - \lambda_e)\sigma_0 + R_c \qquad\qquad (IV.21)$$

With R = Tunnel Radius

$$\lambda_e = \frac{1}{k_p+1}\left(k_p - 1 + \frac{R_c}{\sigma_0}\right) \qquad\qquad (IV.22)$$

$$\lambda_e = \frac{c\,\cos\varphi}{\sigma_0} + \sin\varphi \qquad\qquad (IV.23)$$

λ_e: Rate of deconfinement at the end of the elastic phase

The constraints to the appearance of the zone in the limit state of plasticity are therefore :

$$\sigma_R = (1 - \lambda_e)\,\sigma_0 \qquad\qquad\qquad (IV.24)$$

$$\sigma_R = \frac{2\sigma_0 - R_c}{k_p+1} \qquad\qquad\qquad (IV.25)$$

$$\sigma_R = (1 + \lambda_e)\,\sigma_0 \qquad\qquad\qquad (IV.26)$$

$$\sigma_R = \frac{2k_p\sigma_0 + R_c}{k_p + 1} \qquad\qquad (IV.27)$$

The displacement of the wall at the appearance of plasticity is equal to :

$$u_e = \lambda_e\, u_0 \qquad\qquad (IV.28)$$

Study of the plastic area in a section x such as $\lambda > \lambda_e$, Study of the plastic area in a section x such that of the plastic department

The area of plasticized land is studied for $\lambda > \lambda_e$. In a given section *x* and in this area. we place ourselves at a distance *r* between *R* and r_p, plastic radius : *R < r < rp* (Fig. IV.23).
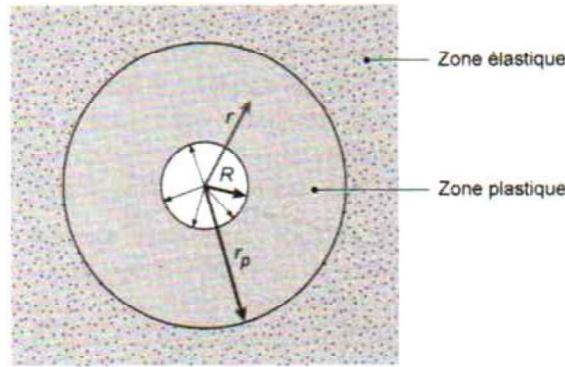
Figure IV.23 *Definition of plastic and elastic zones [20]*

σ_{Re}: Radial stress corresponding to the end of the elastic phase

$$\sigma_{Re} = (1 - \lambda_e).\sigma_0 \qquad\qquad (IV.29)$$

The calculation of the ground curve according to the deconfinement rate varying from 0 to 1 is done in 3 steps :

1. Calculation of the fictitious pressure at the forehead

$$\sigma_R = (1 - \lambda)\sigma_0 \qquad\qquad (IV.30)$$

2. Plastic radius calculation R_P for λ_i With

$$R_p\,(\lambda) = R\left[\frac{2}{(k_p+1)}.\frac{(k_p-1).\sigma_0 + R_c}{(1-\lambda)(k_p-1)\sigma_0 + R_c}\right]^{\frac{1}{(K_P-1)}}$$

or, depending on λ_e:

$$\frac{R_p}{R} = \left[\frac{2.\lambda_e}{(1-\lambda)(k_p-1)+\frac{R_c}{\sigma_0}}\right]^{\frac{1}{(K_p-1)}} \qquad\qquad (IV.31)$$

$$u_R\big/R\,(\lambda,\sigma_0) = \frac{1+\upsilon}{E}.\lambda_e.\sigma_0\,(\frac{R_p}{R})^{\alpha+1} = u_{\infty pl}\big/R.\lambda_e.(\frac{R_p}{R})^{\alpha+1}$$
$$(IV.32)$$

IV.5 .2 Support - Convergence-Containment Method

The convergence-confinement method (or characteristic curve method) is used to determine the final equilibrium between the ground and a support. In the axisymmetric case (paragraphe The method uses the characteristic curves of the ground and the supports. The first gives the pressure necessary to stabilize the conveigig of the ground (example: figure IV.21B). The second gives the pressure exerted in reaction by the support when it undergoes a displacement *at* the upper surface. In its elastic behavior domain, it can be expressed as follows:

$$P = KS\ Ug/R \qquad\qquad (IV.33)$$

Ks is the modulus of rigidity of the support. Equilibrium is reached when the two pressures are equal (intersection of the two curves).

A support is also characterized by its elastic limit and by its brittle or plastic behavior. For certain types of retaining (shotcrete or formwork, segments), only elastic deformations are generally considered. For other types (bolts or sliding hangers), which are intended for the case of strong convergences, the plastic phase of the deformation must also be considered. It is generally accepted that the plastic behaviour is ideal, i.e. that plastic deformations occur at a constant confinement pressure. The limit pressures supported by most supports range from 0.05 to 0.5 MPa Only the segments are capable of a higher containment (from 1 to 2 MPa).

once contact has been established between the two. From this moment on, the convergence of the terrain increases the pressure at the interface, until it is sufficient to stabilize the convergence of the terrain, i.e. until the intersection of the two characteristic curves. The coordinates of this intersection give the final convergence and support pressure
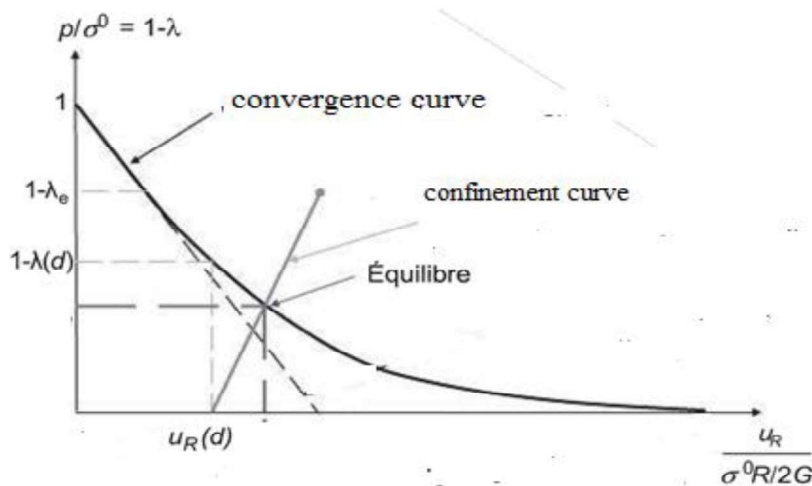
Figure IV.24 Convergence-confinement method.[20]

*IV.5.3 **Influence of depth***

We have seen that for an axisymmetric cavity in a continuous, homogeneous and isotropic medium, the maximum stress in the wall varies between 2 and 3 times the initial major main stress (depending on the anisotropy of the stress state). If this stress is less than one-third of the resistance of the medium, then there should be no failure.

According to [39], the experiment leads to an empirical value of 1/5. For a medium of resistance 100 MPa, the critical initial stress would therefore be 20 MPa, which corresponds to a depth of about 740 m if the major stress is vertical.

*IV.6 **Delayed Cavity Behaviour***

The laws of behaviour used so far assume that deformations and displacements occur immediately after loading. If tunnelling stops for any reason, travel should not continue. However, we have seen in many tunnels that convergence continues for a few days to a few weeks before stabilizing. It has also been observed on some old tunnels that there is pressure on the linings put in place long after the excavation. These phenomena may be due to a change in the hydraulic pressures in the massif or to a delayed mechanical behaviour of the rock massif. Several rheological models have been proposed to explain them. We will briefly present them in the following paragraphs. A more detailed description is given by [26].

VI.6.1 Delayed elastic behaviour (viscoelastic solid)

The deformation of this type of solid consists of an instantaneous elastic part, characterized by two instantaneous elastic parameters (G_0 and K_0 for example), and a deferred part that tends asymptotically towards a value corresponding to an elastic deformation characterized by two other parameters qualified as deferred *(G_1 and K_1)*. This delayed behavior is symbolically represented by a spring (elastic behavior) and a damper (viscous behavior) in parallel, the whole constituting the solid Kelvin model. The total deformation is characterized by two long-term parameters (G_∞ and K_∞). Thus the long-term convergence of an unsupported tunnel is equal to *$2\sigma 0R/2G_\infty$*, with $1/G_\infty = 1/G_0 + 1/G_1$. The greater or lesser rate at which the strain approaches its asymptotic value depends on the viscosity.

To take into account the delayed behavior in the convergence-confinement method, two characteristic curves of the massif are used, the first obtained with instantaneous elastic parameters, the second with long-term parameters[19]

IV.6.1.1 progressive Rupture

Experience shows that stress levels below the failure criterion, but applied for a very long time (several years or decades) can

cause the rupture of a specimen or a pillar, by propagation of micro-cracks that may exist in the rock matrix. This phenomenon is sometimes referred to as brittle creep. The limit stress state to ensure long-term stability is defined by the long-term failure criterion. Thus, the uniaxial compressive strength of a rock in the long term can be as low as half of its short-term strength. A law linking the time to failure to the applied stress was proposed by [8] and recently used by [50] to estimate the long-term strength of the Lac du Bonnet granite.

To take into account the progressive rupture in the convergence-confinement method, two characteristic curves of the massif are used, the first obtained with the instantaneous resistance criterion, the second with the long-term criterion.

IV.6.1.2 Visco-elastic and visco-elasto-plastic fluid behaviour

It can be seen that for some rocks, deformation under constant load continues without stabilizing. This is the case for ice and salt, for example. The deformation has an elastic part, characterized by two elastic parameters (G and *K)* and a viscous part, characterized by a viscosity η. This delayed behavior is symbolically represented by a spring (elastic behavior) and a damper (viscous behavior) in series, the whole constituting Maxwell's fluid model. [19]

For some rocks, viscous deformation only occurs if a criterion (called visco-plastic criterion) is met. This is called visco-elasto-plastic behaviour. This viscous behavior at the threshold is symbolically represented by a damper (viscous behavior) and a pad (plastic behavior) in parallel, the whole constituting the Bingham model.

IV.7 *Shallow Cavities*

IV.7.1 Mechanisms of Rupture

IV.7.1.1 Continuous medium

By shallow depth, we mean the depth below which axisymmetric analytical models can no longer be applied. In this case, the action of gravity on the immediate vicinity of the cavity (or its area of influence) becomes preponderant in relation to the stresses exerted by the surrounding mass. The problem can be approached by using a limit equilibrium method and considering two surfaces of ruptureure verticales, qui délimitent un compartiment potentiellement instable, suffisamment cohérent. If *B* is the width of the cavity, *H* is the depth of the roof, and γ the density, the weight of the compartment is *γHB*. The resisting forces on the two vertical surfaces are due to the cohesion c of the medium and the friction mobilized by the average horizontal stress $K_0 Y h^2 / 2$. The compartment collapses (formation of a fontis) if these resisting forces are less than the weight, i.e. if: [19]

$$B > K_0 H \tan\phi + 2c/\gamma \qquad\qquad (IV.32)$$

This simple model makes it easy to calculate the support pressure needed to ensure balance.

Equation (IV.32) shows that the stability increases with depth for the mechanism under consideration. But as the depth increases, the vertical stress on the side walls increases and other mechanisms must be considered, for which there are analytical solutions, given in soil mechanics works. Numerical methods in stress/strain, however, provide more precise results.

IV.7.1.2 Milieu stratifié ou fracturé

The models described above for stratified and fractured media apply regardless of depth. However, buckling of the benches, which requires high stress, is unlikely at shallow depths. On the contrary, bending under their own weight is favored when the stress decreases. [19]

IV.7.2 Deformations

Even if the stability of the cavity is ensured (with or without supports), the ground deforms (convergence). Axisy metric models show that the radial displacement is, to a first approximation, inversely proportional to the distance from the axis of the cavity. In terrain with a low modulus of deformation, the displacement can be noticeable on the surface, even at a depth greater than 10 times the radius. For a shallower depth, numerical modeling is necessary to correctly estimate the displacements. As a first approximation, it can be assumed that the volume of the subsidence trough in a vertical section perpendicular to the tunnel is equal to the volume lost in the tunnel by convergence.[19]

IV.8 Tunnel design using "empirical" methods

We have seen in Chapter I the so-called "classification" methods of rock masses : Q, RMR, GSI. The various authors who have developed these methods have done so not only for the purpose of classification, but above all to propose simple methods for choosing the necessary supports to be installed in tunnels. These methods make it possible to move towards a type of support and an initial dimension, which can then be modelled using the methods described above. In all cases, adaptations to progress will necessarily have to be expected, based on the measurements carried out (observational method). [19]

IV.8.1 AFTES Recommendations

We have already talked about AFTES, the French Association of Tunnels and Underground Space. This association is very active and brings together almost all the players in the underground world. Within the association, numerous working groups (WGs) prepare recommendations on various topics related to the underground. We have previously talked about WG1, which produced useful recommendations for the description of the rock mass, similarly, WG7 produced in particular the recommendation GT7R1F2: "choice of a type of gallery support" which gives indications on suitable or unsuitable supports, depending on the terrain. A titre d'exemple, The figure IV.20 reproduces Table IV.1 of the above-mentioned AFTES recommendation and indicates the recommended supports (•), feasible if other criteria are good ( ), not recommended even if feasible (x), and infeasible (X).

Discontinuités (cas où l'excavation est faite à l'explosif avec découpage)

1 - Matériaux rocheux (R1 à R4)

Nombre de familles	Orientation	Espacement	pas de soutènement	béton projeté	Boulons à ancrage ponctuel	Boulons à ancrage réparti	Boulons barres foncées	Cintres lourds	Cintres légers coulissants	Voussoirs plaques métal assemblées	Voussoirs béton	tubes perforés	bouclier ou pousse tube	injection	air comprimé	congélation
N1			•				X			X	X	X	X	X	X	X
N2	Or2 ou Or3	S1 à S3	•				X			X	X	X	X	X		X
N2 N3 ou N4	Quelconque	S1			•		X			X	X	X	X	X		X
		S2			•	•	X			X	X	X	X	X		X
		S3		•	• (Gr)	• (Gr)	X				X	X	X			X
		S4	X	•	• (Gr ou Bp)	• (Gr ou Bp)	X	• (Gr ou Bp)	• (Gr ou Bp)			X			X	X
		S5	X	•	X		X (Bp)	• (Bl ou Bp)	• (Bl ou Bp)				X		X	X
N5			X	•	X	X (Bp)	X	• (Bl ou Bp)	• (Bl ou Bp)	•			X	•	X	X

ANNEXE

EXERCISES

Chapter I

Exercise 01

A granitic rock is composed of a mixture of 30% quartz, 40% plagioclase,and 30% augite. Its porosity is 3.0% and its longitudinal wave velocity measured in the laboratory is 3200 m/s. Describe its state of fissuring.

solution:

$v_1^* = 6440 \, m/s$;   moderatlyto strongly fissured

Exercise 02

A sandstone with porosity of 15% is composed of a mixture of 70% quartz grains and 30% pyrite grains. Determine its dry density in meganewtons per cubic meter and he water content when the rock is saturated with water.

solution:

γ_{dry} = 0.028MN/m^3

w=5.25%

Exercise 03
A granitic rock is composed of a mixture of the following minerals: 30% quartz, 40% plagioclase and 30% clay.
The porosity of the rock is equal to 3% and the longitudinal wave propagation speed measured in the laboratory is equal to 3200m/s.Estimate the degree of fracturing
Answer
DF = 48.6 %

Chapter II

Exercise 01

Laboratory tests on specimens of a limestone have produced unconfined compressive and tensile strengths of 80 MPa and 10 MPa, respectively. Using the Hoek-Brown and plane Griffith criteria, estimate the maximum principal stress at failure for **two** biaxial tests in which σ_2 = 20 MPa and σ_2 = 40 MPa. Which of these **two** criteria would best predict peak strength under these conditions?
solution:

m=7.88,

Hoek-Brown criterion
If we substitute $\sigma_3 = \sigma$, and $\sigma_1 = 0$ into the Hoek-Brown criterion,
for $\sigma_2 = \sigma_3 = 20$ MPa we find that

$$\sigma_1 = 20 + \sqrt{7.88 \times 20 \times 80 + 1 \times 80^2} = 157.8 \text{ MPa}$$

and **for $\sigma_2 = \sigma_3 = 40$** MPa we find that

$$\sigma_1 = 40 + \sqrt{7.88 \times 40 \times 80 + 1 \times 80^2} = 217.8 \text{ MPa}$$

However, it is likely that these will both be over-estimates of the major principal stress at failure.

$$(\sigma_1 - \sigma_3)^2 = 8T_0(\sigma_1 + \sigma_3) \quad \text{when } \sigma_1 + 3\sigma_3 > 0$$

$$\sigma_3 = -T_0 \quad \text{when } \sigma_1 + 3\sigma_3 < 0$$

Rearranging the first of the Griffith criterion equations gives us

$$\sigma_1 = \sigma_3 + 4T_0 \pm 4\sqrt{T_0\sigma_3 + T_0^2}$$

from which, on substitution **of T_0 = 10** MPa and the appropriate value **of σ_3,** we can determine the major principal stress at failure.
Thus, for $\sigma_2 = \sigma_3 = 20$ MPa we find that

$$\sigma_1 = 20 + 4 \times 10 \pm 4\sqrt{10 \times 20 + 10^2} = 129.3 \text{ MPa}$$

and for $\sigma_2 = \sigma_3 = 40$ MPa we find that

$$\sigma_1 = 40 + 4 \times 10 \pm 4\sqrt{10 \times 40 + 10^2} = 169.4 \text{ MPa}.$$

Assessment
Determining which **of** these criteria is the best predictor of peak strength is difficult. Strictly, neither **of** the criteria are valid for biaxial conditions, but the Hoek-Brown criterion is for strength (i.e. a structure breakdowncriterion), whereas the Griffith criterion relates to the onset of fracturing.
As the onset of fracturing occurs before peak strength and usually well before complete failure, perhaps the **Hoek-Brown** criterion is the better of the two. However, it is more likely that the peak strength will lie somewhere between the two sets of results.

Exercise 02

Comment on the applicability of each of the Griffith, Mohr-Coulomb, and Hoek-Brown criteria for the following triaxial test results on quartzite:

| $(\sigma_1 + \sigma_3)/2$ | −6.65 | 100 | 135 | 160 | 200 | 298 | 435 MPa |
| $(\sigma_1 - \sigma_3)/2$ | 6.65 | 100 | 130 | 150 | 180 | 248 | 335 MPa |

solution:
The first step is to convert the given data into principal stress values:

$(\sigma_1 + \sigma_3)/2$	−6.65	100	135	160	200	298	435
$(\sigma_1 − \sigma_3)/2$	6.65	100	130	150	180	248	335
σ_1	0	200	265	310	380	546	770
σ_3	−13.3	0	5	10	20	50	100

From the final two rows **of** the table we can see that **ot** = **-13.3** MPa and σ, = 200 MPa. The values of **01** and σ_3 are plotted at the end of this answer.

Griffi'th criterion

The relevant expression for the Griffith criterion in compression is

$$(\sigma_1 − \sigma_3)^2 = 8T_0(\sigma_1 + \sigma_3)$$

where compression is positive and **To** is also positive. For given values of σ_3 we need to compute values of **σ1,** using a value **of To = 13.3 MPa.**

The result is

σ_3	−13.3	0	5	10	20	50	100
σ_1	39.9	106.4	120.6	133.6	157.4	219.3	308.5

The data are clearly curvilinear, whereas the Mohr-Coulomb criterion is linear. **As** a result, the Mohr-Coulomb criterion will not be a good fit to the data, at least not over their entire range. However, if we wish to fit a straight line to the data, the results are

σ_3	−13.3	0	5	10	20	50	100
σ_1	118.6	201.0	232.0	263.0	324.9	510.9	820.7

Hoek-Brown criterion

We can either simply take appropriate values for the parameters in the criterion from a table or attempt to statistically fit the criterion to the data. Using the former method, we have **s = 1** and **m = 15,** and with **σc** = 200 MPa we obtain:

σ_3	−13.3	0	5	10	20	50	100
σ_1	−3.3	200.0	239.5	274.6	336.2	485.9	683.1

while constraining the solution to pass through the origin. The result is a parameter value of m = 20.5, with corresponding stress values of

σ_3	−13.3	0	5	10	20	50	100
σ_1	−10.4	200.0	251.0	294.6	369.3	545.1	770.9
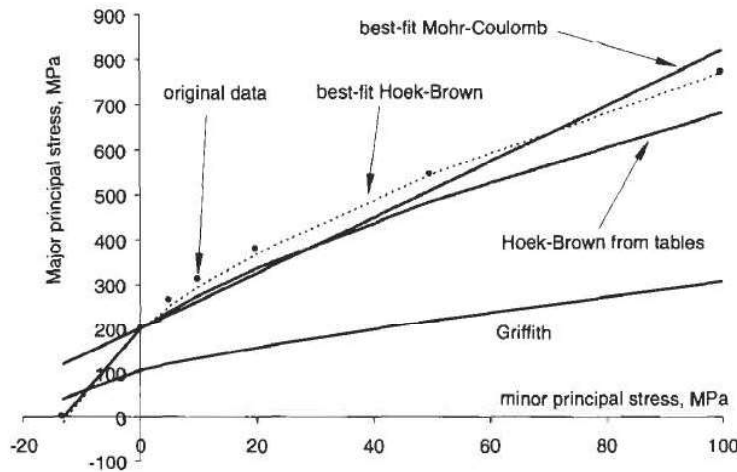
Assessment

As the plot above shows, the statistical fit of the **Hoek-Brown** criterion is the best of the three criteria. The curvilinear nature of the results means that the Mohr-Coulomb criterion will never be a good fit over the entire stress range, and the fundamental behaviour of rock over large stress ranges means that this is a general conclusion.

Exercise 3

A sandstone rock mass, fractured by 2 joint sets plus random fractures, average RQD is 70%, average joint spacing is 0.11 m, joint surfaces are slightly rough, highly weathered with stains and weathered surface but no clay found on surface, joints are generally in contact with apertures generally less than 1 mm, average rock material.

uniaxial compressive strength is 85 MPa, the tunnel is to be excavated at 80 m below ground level and the groundwater table is 10 m below the ground surface.

Here, groundwater parameter is not directly given, but given in terms of groundwater pressure of 70 m water head and overburden pressure of 80 m ground. Since there is no indication of in situ stress ratio, overburden stress is taken as the major in situ stress as an approximation.

solution:

Joint water pressure = groundwater pressure = 70 m$\times\gamma(w)$

In situ stress = 80 m$\times \gamma$

Joint water pressure / In situ stress = $(70 \times 1)/(80 \times 2.7) = 0.32$

Selection of RMR parameters and calculation of RMR are shown below:

Rock material strength	85 MPa	Rating	7
RQD (%)	70%	Rating	13
Joint spacing (m)	0.11 m	Rating	8
Condition of joints	slightly rough, highly weathered, separation < 1mm	Rating	20
Groundwater	water pressure/stress = 0.32	Rating	4
		RMR	52

The calculated basic RMR is 52. It falls in rock class C which indicates the rock mass is of fair quality.

Exercise 04

A highly fractured siltstone rock mass, found to have 2 joint sets and many random fractures, average RQD is 41%, joints appears continuous observed in tunnel, joint surfaces are slickensided and undulating, and are highly weathered, joint are separated by about 3-5 mm, filled with clay, average rock material uniaxial compressive strength is 65 MPa, inflow per 10 m tunnel length is observed at approximately 50 litre/minute, with considerable outwash of joint fillings. The tunnel is at 220 m below ground.

Estmate Q parameters and calculate of Q-value

solution:

RQD	41%	RQD	41
Joint set number	2 sets plus random	J_n	6
Joint roughness number	slickensided and undulating	J_r	1.5
Joint alteration number	highly weathered filled with 3-5 mm clay	J_a	4
Joint water factor	large inflow with considerable outwash	J_w	0.33
Stress reduction factor	$\sigma_c/\sigma_1 = 65/(220 \times 0.027) = 11$	SRF	1
Q	(41/6) (1.5/4) (0.33/1)		0.85

The calculated Q-value is 0.85, and the rock mass is classified as very poor quality.

Again, judgement is frequently needed to interpret the descriptions given in the geological and hydrogeological investigation reports and in the borehole logs to match the descriptive terms in the Q table. Closest match and approximation is to be used to determine each of the Q parameter rating.

Exercise 5

Granite rock mass containing 3 joint sets, average RQD is 88%, average joint spacing is 0.24 m, joint surfaces are generally stepped and rough, tightly closed and unweathered with occasional stains observed, the excavation surface is wet but not dripping, average rock material uniaxial compressive strength is 160 MPa, the tunnel is excavated to 150 m below the ground where no abnormal high in situ stress is expected. Estimate the GSI

solution:
Refer to the GSI chart, Rock Mass Structure for the above granite is blocky, and Joint Surface Condition is very good. Therefore GSI is 75 5. The rock mass is classified as good to very good quality.

Chapter III

Exercise 01

Derive an equation for the factor of safety of the dry planar wedge shown below
a) first ignoring cohesion, then b) incorporating cohesion. Include the influence of friction at the joint surface in both equations
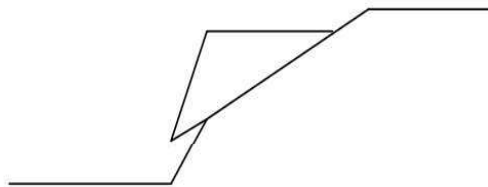
solution:
Define the positive direction as the direction of sliding
Factor of Safety =resisting forces/driving forces
a) No Cohesion:
W = weight of the planar wedge
N = normal force
θ = angle of incline
$\emptyset$ = angle of friction
driving force = W sin θ
resisting force = N tan ϕ
$\qquad\qquad$ = W cos θ tan ϕ

$$FS = W \cos \theta \tan \phi \: / \: W \sin \theta = \tan \phi / \tan \theta$$

For the simple case of no cohesion and no water pressure, the Factor of Safety against sliding is simply given by the ratio of tan ϕ /tan θ
b) Incorporating Cohesion:
driving force = W sin θ
shear stress = τ = c + δ_n tan ϕ
$\Rightarrow$ resisting force = T = cA + δ_n A tan ϕ
; where A is the contact area of the wedge with the failure plane
and c is the cohesive strength of the joint surface
Since $\delta_n = \dfrac{N}{A}$ and N = W cos θ
resisting force = cA+ W cos θ tan ϕ

$$FS \quad \frac{cA + w \cos \theta \tan \phi}{w \sin\theta}$$

Exercice 02

For the rock slope shown below, derive an equation for the factor of safety against sliding using the plane failure equilibrium technique. The slope face is vertical with a height H, the failure plane is oriented at an angle ψ

    a)   vertical load, L, is applied to the upper slope. The unit weight of the rock is γ. The equation derived must be a function of H, L, c,ϕ, ψ, γ

b) Using the equation derived in Question 2a, determine the factor of safety against failure of a slope with the following properties: H=15m, ψ =50 , γ =2.7 tonnes/m3 , c=5 tonnes/m2 , φ =35 , and L=20 *tonnes*

c) Calculate the value of L that will cause a failure in the slope described in Question 2b.
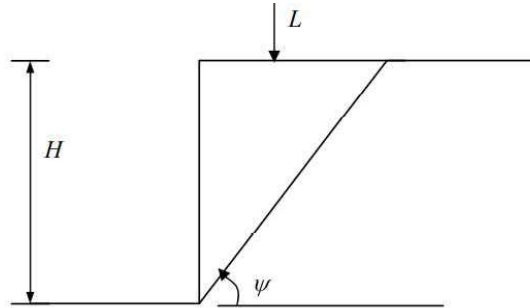
solution

Wedge Weight =W =V. γ   Assuming depth is 1 unit length:
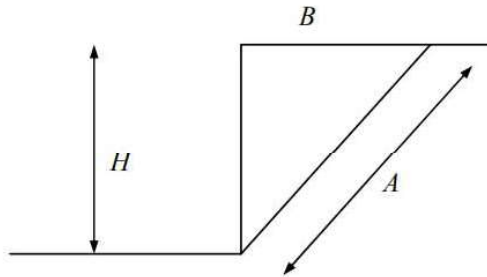
$$\Rightarrow V = \frac{1}{2}BH(1)$$

$$A = \frac{H}{\sin \Psi} \qquad B = \frac{H}{\tan \psi}$$

$$V = \left(\frac{1}{2}\right)\left(\frac{H}{\tan \psi}\right)(H) = \frac{H^2}{2\tan \psi}$$

$$W = V\gamma = \frac{H^2 \gamma}{2\tan \psi}$$

$$Factor\ of\ Safety = \frac{Factor\ of\ Safety}{driving\ Forces} = \frac{cA+(W+L)cos\theta \tan \phi}{(W+L)sin\theta}$$

$$FS = \frac{c\left(\frac{H}{\sin \psi}\right)+\left(\frac{H^2\gamma}{\tan \psi}+L\right)cos\psi tan\phi}{\left(\frac{H^2\gamma}{\tan \psi}+L\right)sin\psi}$$

b)

$$FS = \frac{c\left(\frac{H}{\sin \psi}\right)+\left(\frac{H^2\gamma}{2\tan \psi}+L\right)cos\psi tan\phi}{\left(\frac{H^2\gamma}{2\tan \psi}+L\right)sin\psi}$$

$$= \frac{5\left(\frac{15}{\sin(50)}\right)+\left(\frac{(15)^2(2,7)}{2\tan(50)}+20\right)cos(50)\tan(35)}{\left(\frac{(15)^2(2.7)}{2\tan(50)}+20\right)sin(50)}$$

$$= \frac{97.906 + 123.718}{210.568}$$

FS = 1.0525

The slope will fail when FS=1. Using the equations developed in Question a, setting FS to 1, substituting the values given in Question 2b and rearranging to isolate L:

$$1 = \frac{c\left(\frac{H}{\sin\psi}\right) + \left(\frac{H^2\gamma}{2\tan\psi} + L\right)\cos\psi\tan\phi}{\left(\frac{H^2\gamma}{2\tan\psi} + L\right)\sin\psi}$$

$$\text{L} = \frac{\frac{cH}{\sin\psi} + \left(\frac{H^2\gamma\cos\psi\tan\phi}{2\tan\psi}\right) - \frac{H^2\gamma\sin\psi}{2\tan\psi}}{\sin\psi - \cos\psi\tan\phi}$$

$$L = \frac{\frac{(5)(15)}{\sin(50)} + \left(\frac{(15)^2(2.7)\cos(50)\tan(35)}{2\tan(50)}\right) - \frac{(15)^2(2.7)\sin(50)}{2\tan(50)}}{\sin(50) - \cos(50)\tan(35)}$$

L= 55 tonnes

Exercise 03

a) Using the Limit Equilibrium Models as defined in Hoek's Practical Rock Engineering , calculate the minimum and maximum possible factors of safety for the slope under fully saturated conditions and earthquake loading. The cohesive strength of the surface was determined to range from 0.05MPa to 0.2MPa, and the friction angle from 30 to 45 degrees.
b) Under the same conditions as described in Question a, recalculate the maximum and minimum factors of safety of the slope assuming a water filled tension crack is present. What conclusions can be made about the effect of a tension crack on the forces acting on the slope?

Additional Information:

H=60m ψ_f=50° ψ_p=35° $\alpha = 0,08g$ γ_r=0.027MN/m^3 γ_w=0.01MN/m^3

Solution:

Using the equations defined on pg. 96 of Hoek's notes :

A= $\frac{H}{\sin\psi_p} = \frac{60}{\sin(35)} = 104.6m^2$

W=$\frac{\gamma_r H^2}{2}$(cot ψ_p −cot ψ_f) $= \frac{(0.027)(60)^2}{2}$(cot (35) −cot(50))=28.63 MN/m

Since the slope is fully saturated, the height of the water is equal to the height of the slope.

U = $\frac{\gamma w H_w^2}{4\sin\psi_p} = \frac{(0.01)(60)^2}{4\sin(35)}$=15.69 MN/m

FS=$\frac{104.6c + [\ 28.63\ (cos(35) - 0.08sin(35)) - 15.69 + 0\ ]tan\phi}{28.63\ (sin(35) + 0.08cos(35)) - 0} = \frac{104.6c + 6.45tan\phi}{18.30}$

FS = 5.72*c + 0.35tanϕ

Note that the value of T is equal to zero as there is no anchor system present.

When c = 0.05 and $\phi = 30$:

FS = 5.72(0.05) +0.35 tan(30) =0.286 +0.202 =0.49

When c = 0.2 and $\phi = 45$:

FS = 5.72(0.2) +0.35 tan(45) =1.144 +0.35 =1.49

Using the equations defined as

z_w = H(1- $\sqrt{cot\,\psi_f\,tan\,\psi_p}$) = 60(1- $\sqrt{cot(50)\,tan\,(35)}$)=14.0 m

$$A = \frac{H - z_w}{\sin\psi_p} = \frac{60 - 14.0}{\sin(35)} = 80.2 m^2/m$$

$$W = \frac{\gamma_r H^2}{2}\left(\left(1-\left(\frac{z_w}{H}\right)^2\right)\cot\psi_p - \cot\psi_f\right) = \frac{(0.027)(60)^2}{2}\left[\left(1-\left(\frac{14}{60}\right)^2\right)\cot(35) - \cot(50)\right] = 24.85 MN/m$$

$$U = \frac{\gamma_w z_w A}{2} = \frac{(0.01)(14)(80.2)}{2} = 5.61 MN/m$$

$$V = \frac{\gamma_w z_w^2}{2} = \frac{(0.01)(14)^2}{2} = 0.98 MN/m$$

$$FS = \frac{80.2c + (24.85(\cos(35) - 0.08\sin(35)) - 5.61 - 0.98\sin(35) + 0)\tan\phi}{24.85(\sin(35) + 0.08\cos(35)) + 0.98\cos(35) - 0} = \frac{80.2c + 13.04\tan\phi}{16.685}$$

FS= 4.807c + 0.782 tan ϕ

When c= 0.05 MPa and $\phi = 30°$

FS = 0.24 + 0.45 = 0.69

When c= 0.2 MPa and $\phi = 45°$

FS = 0.96 + 0.782 = 1.74

It can be seen that when a tension crack is present, the contribution of cohesion decreases and that of friction increases as compared to when there is no tension crack.

Chapter IV

Exercise 01

At a depth of 750 m, a 10-m diameter circular tunnel is driven in rock having a unit weight of 26 kN/m³ and uniaxial compressive and tensile strengths of 80.0 MPa and 3.0 MPa, respectively. Will the strength of the rock on the tunnel boundary be exceeded if:

(a) k = 0.3 , and (b) k = 2.0 ?

Solution
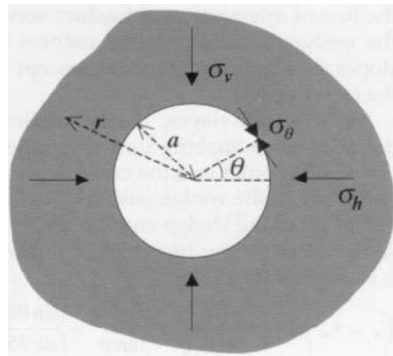
1) Since the tunnel has neither a support pressure nor an internal pressure applied to it, the local stresses at the boundary have $\sigma_3 = \sigma_r = 0$ and $\sigma_1 = \sigma_\theta$ The solution for the circumferential stress is:

$$\sigma_\theta = \frac{1}{2}\sigma_v[(1+k)\left(1+\frac{a^2}{r^2}\right) + (1-k)\left(1+3\frac{a^4}{r^4}\right)\cos 2\theta]$$

For a location on the tunnel boundary (i.e. a = r), this simplifies to:

$$\sigma_\theta = \sigma_v[(1+k) + 2(1-k)\cos 2\theta]$$

1- First, we can assume that the vertical stress is equal to the weight of the overburden,giving:

$$\sigma_v = \gamma z = 0.026 \times 750 = 19.5\ MPa$$

2- The extreme values of induced stress occur at positions aligned with the

principal in situ stresses, and so in order to compute the stress induced

in the crown and invert (i.e. roof and floor) we use $\theta = 90°$, and for

the sidewalls we use $\theta = 0°$.

For k=0.3:   Crown/invert ($\theta = 90°$): σ_θ= -1.95 MPa (i.e. tensile)

Sidewalls ($\theta = 0°$): $\sigma_\theta = 52.7$ MPa

For k=2.0:   Crown/invert ($\theta = 90°$): σ_θ= 97.5 MPa

Sidewalls ($\theta = 0°$): $\sigma_\theta = 19.5$ MPa

Exercise 02

A gold-bearing quartz vein, 2 m thick and dipping 90°, is to be exploited by a small cut-and-fill stoping operation. The mining is to take place at a depth of 800 m, and the average unit weight of the granite host rock above this level is 29 kN/m³. The strike of the vein is parallel to the intermediate stress, and the major principal stress is horizontal with a magnitude of 37.0 MPa. The uniaxial compressive strength of the vein material is 218 MPa, and the tensile strength of the host rock is -5 MPa. What is the maximum permissible stope height before failure occurs?

Solution :

a.We can assume that, in 2-D cross-section, the stresses induced in the sidewalls (tensile) and the crown (compressive) of the stope can be approximated using the equations for an elliptical excavation

$$\frac{\sigma_{sidewall}}{\sigma vertical} = 1 - k + 2\left(\frac{w}{h}\right)$$
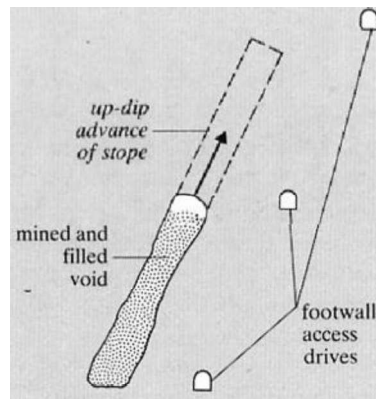
$$\frac{\sigma_{crown}}{\sigma_{vertical}} = k - 1 + k\sqrt{\frac{2h}{p_{crown}}} = k - 1 + 2k\sqrt{\frac{h}{w}}$$

1-Rearranging the given equations, we can solve for the height of the excavation as the minimum of:

$$h = \frac{2w}{\frac{\sigma_{sidewall}}{\sigma_{vertical}} + k - 1} \quad \text{or} \quad h = \frac{w}{4k^2}\left(\frac{\sigma_{crown}}{\sigma_{vertical}} + 1 - k\right)^2$$

2 The maximum stress that can be sustained by the crown and the sidewall are 218 and −5 MPa, respectively. Note that the sidewall stress is negative because this represents the tensile strength.

3 The vertical stress is:

$$\sigma_{vertical} = \gamma \cdot z = 0.029 \times 800 = 23.2 \text{ MPa}$$

And hence the ratio of horizontal to vertical stress is:

$$K = \frac{37.0}{23.2} = 1.59$$

4 The maximal height of a stope such that the compressive strength of the rock in the crown is not exceeded is given by:

$$h = \frac{w}{4k^2}\left(\frac{\sigma crown}{\sigma_{vertical}} + 1 - k\right)^2$$

$$= \frac{2}{4\times1.59^2}\left(\frac{218}{23.2} + 1 - 1.59\right)^2 = 15.3 \text{ m}$$

The maximal height of a stope such that the tensile strength of the rock in the sidewall is not exceeded is given by:

$$h = \frac{2w}{\frac{\sigma_{sidewall}}{\delta_{vertical}} + K - 1} = \frac{2\times2}{\frac{-5}{23,2}+1.59-1} = 10.7 \text{ m}$$

Thus we see that sidewall failure is the limiting condition if no stress-induced failure is acceptable in the stope design.

<u>**Exercise 03**</u>

A circular tunnel with an opening of 12 m is built in a soil mass at a depth of 85 m.

The geotechnical characteristics of the soil are: E=1550 MPa, Poisson's ratio 0.26, cohesion 500 kPa, friction angle of 32 °, the volumetric weight of the soil equal to 25 kN / m3. The support is placed at a distance equal to 3.5 m from the working face.

The support consists of:

- TH sliding arches with a section of 36.5 cm² with a minimum spacing of 1.5 m, the admissible stress of the steel is estimated at 190 Mpa, Es=200000 Mpa.

- Shotcrete 30cm thick with a deformation modulus equal to 10000 MPa, ν=0.2 and a compressive strength fc28 equal to 32MPa.

1- Plot the convergence curve.

2- Determine the rigidities and pressures in the support.

3- Plot the confinement curve.

Solution

The initial constraint

$$\sigma_0 = \gamma.h = 2125 \, kPa$$

The compressive strength of the massif

$$\sigma_c = \frac{2.C.\cos\varphi}{1 - \sin\varphi} = 1804,04 \, Kpa$$

Checking the behavior of the soil mass

$\frac{\sigma_c}{2} = 902.02 Kpa$ donc $\sigma_0 \geq \frac{\sigma_c}{2}$ → The soil has an **elastoplastic behaviour**

1. The convergence curve

The deconfinement rate at the end of the elastic phase

$$\lambda_e = \frac{1}{K_p + 1}\left(K_p - 1 + \frac{\sigma_c}{\sigma_0}\right) = 0,72$$

$$K_p = \frac{1 + \sin\varphi}{1 - \sin\varphi} = 3,254$$

$$\mathbf{u_{Re}} = \boldsymbol{\lambda_e}.\mathbf{u_{R0}}$$

$$u_{R0} = \frac{1+v}{E}.\sigma_0.R \quad \boldsymbol{u_{R0}} = \mathbf{10,36} \boldsymbol{mm}$$

$$u_{Re} = 0,72.10,36 = \mathbf{7,46} \boldsymbol{cm}$$

The radial stress at the end of the elastic phase σ_{Re}

$$\sigma_{Re} = (1 - \lambda_e)\sigma_0 = (1 - 0,72).2125 = \mathbf{595} \boldsymbol{Mpa}$$

- **Plastic displacement**

Determination of the plastic radius

$$\frac{R_p}{R} = \left[\frac{2.\lambda_e}{(1-\lambda)(k_p - 1) + \frac{\sigma_c}{\sigma_0}}\right]^{\frac{1}{(K_p - 1)}}$$

For $\lambda(x) = 1$

$$K_p = \frac{1 + \sin\varphi}{1 - \sin\varphi} = 3,25$$

$$\frac{R_p}{R} = \left[\frac{2.0,72}{(1-1)(3,25-1) + \frac{1804,04}{2125}}\right]^{\frac{1}{(2,46-1)}} = 1,26$$

$$R_p = 1,26.R = 7,\mathbf{61}\mathbf{m}$$

With ψ : *the dilatancy angle*

$$\psi = \varphi = 32°$$

$$K = \frac{1 + \sin 32}{1 - \sin 32} = 3.25$$

$$G = \frac{E}{2(1+v)} = \frac{1550}{2(1+0.26)} = 615.08 Mpa$$

$$u_{pl\infty} = \frac{\lambda_e \sigma_0.}{2.G}\left(\frac{R_P}{R}\right)^{\alpha+1} = 0,01992 m$$

$$u_{pl\infty} = \mathbf{19,92mm}$$

$\lambda(x)$	$\dfrac{R}{R_p}$	$R_p[m]$	$\sigma_R[MPa]$	u_R [mm]
0,8	1,05	6,31	425	9,17
0,85	1,095	6,57	318,75	10,97
0,90	1,14	6,84	212,5	13,00
0,95	1,20	7,2	106,25	16,19

2. Confinement curve

Evaluation of the displacement at the support setting by the similarity method (Panet's formula)

$$\xi = \frac{u_{\infty el}}{u_{\infty pl}} = \frac{7,46}{19,92} = 0,37$$

$$u_{S0} = \frac{1}{\xi}[\alpha_0 + (1 - \alpha_0)\alpha_d]\frac{\sigma_0 R}{2G}$$

$$\alpha_0 = 0,25 \text{et } m = 0,75$$

α_d : Form Function

$$\alpha_d = 1 - \left[\frac{m.R}{m.R + \xi.d}\right]^2$$

$$\alpha_d = 1 - \left[\frac{0,75.5,7}{0,75.6 + 0,32.3,5}\right]^2 = 0,39$$

$$u_{S0} = \frac{1}{0,37}[0,25 + (1 - 0,25)0,39]\frac{2,125.6}{2.615,08}$$

$$u_{S0} = 0,01519m = \mathbf{15,19mm}$$

3. Stiffness and Pressures in the Supports
- **Stiffness of a cylindrical shotcrete shell**

R>10.e

$$K^{shotcrete} = \frac{E(R^2 - R_i^2)}{(1+v)[(1-2v)R^2 - R_i^2]} \quad \text{With } R_i : \text{ Intrados radius} = R - e$$

$$R_i = 6 - 0,30 = 5,7m$$

$$K^{shotcrete} = \frac{11000(6^2 - 5,7^2)}{(1 + 0,2)[(1 - 2.0,2)6^2 + 5,7^2]} = \mathbf{594,84Mpa}$$

- **Pressure in the shotcrete support**

$$P_S^{shotcrete} = 0,5.\sigma_a\left(1 - \frac{R_i^2}{R^2}\right)$$

$$\sigma_a = f_{c28} * F_{sb} \qquad f_{c28} = 32Mpa$$

$$\sigma_a = f_{c28} * F_{sb} = 0,56.32 = 17,92Mpa$$

$$\mathbf{P_S^{shotcrete}} = 0,5.17,92.\left(1 - \frac{5,7^2}{6^2}\right) = \mathbf{0,8736Mpa}$$

- **Stiffness of the lattice girders (TH)**

$$K^{lattice} = \frac{E_a.A}{e.R}$$

$$\mathbf{K^{lattice}} = \frac{200000.36,5.\,10^{-4}}{1,5.6} = \mathbf{81.11}Mpa$$

- **Pressure in the lattice girders**

$$\mathbf{p_s^{lattice}} = \frac{190.36,5.10^{-4}}{1,5.6} = \mathbf{0,0770Mpa}$$

$$\mathbf{p_S = min\ (p_{S\ max}, (u_R\text{-}u_{S0})K_s\ /R)} \qquad \text{pour } \lambda > \lambda_8$$

K_s: Stiffness of all supports

p_{Smax}: Maximum pressure of all supports

$$P_{smax} = \mathbf{P_S^{shotcrete}} = \mathbf{0,873MPa}$$

$$\mathbf{K_s} = \mathbf{K^{shotcrete}} + \mathbf{K^{lattice}} = \mathbf{675,95MPa}$$

$$(U_{PL\infty} - U_{s0})K/R = \frac{(19,92-15,19)675,95}{6.10^3} = \mathbf{0,532MPa}$$

$$\mathbf{P_s} = \min(0{,}873, 0{,}532) = \mathbf{0,532Mpa}$$

La courbe convergence - confinement
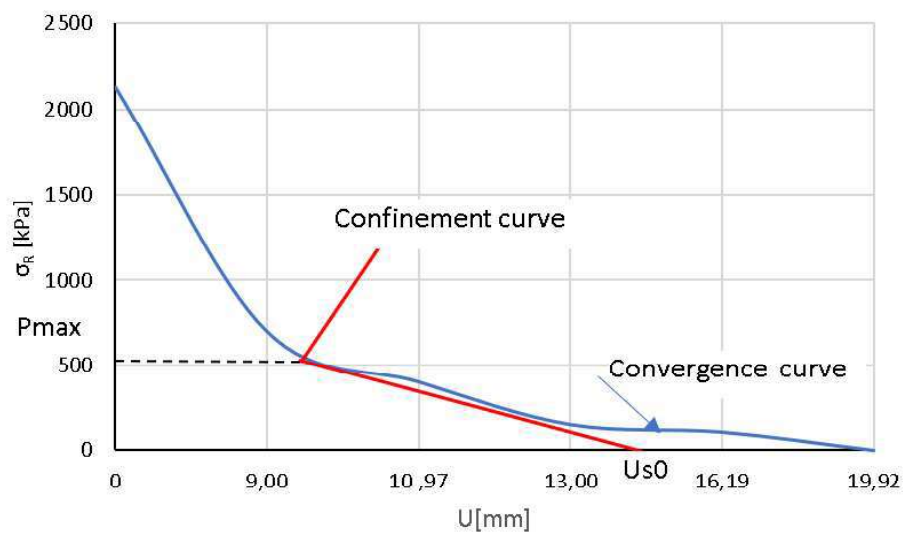
convergence- confinement curve

LIST OF TABLES

LIST OF FIGURES

Symbols and abbreviations

List of symbols

σ_R : Radial stress

σ_θ : Ortho radial stress

σ_0 : The initial stress in the massif

σ_a : Permissible strength of steel

$\sigma_{e\ acier}$: Yield strength of steel

σ_{yb} : Yield strength of bolts

F_{sa} : Safety factor taken from the yield strength of the steel

H : The height of coverage

A : Section d'acier.

B : Gallery width.

C : The cohesion of the field.

D: Diameter of the tunnel.

d : La distance non soutenue.

a_d : Shape Function

d_1: Bolt diameter.

D_e : The equivalent size of the excavation.

E: Mean elastic modulus of the massif.

E_i : Module de déformabilité de la roche intacte.

E_a: The modulus of elasticity of steel.

E_T: Le module d'Young dans la direction transversale.

E_b: Le module d'Young du matériau constituant la tige du boulon.

$E_{vousoir}$: Module des voussoirs

EI: Rigidité flexionnelle et normale.

EA: Normal stiffness.

f_{c28} : Characteristic strength of concrete at 28 days

F: Charging Function.

G: The Shear Modulus.

K_0: The pressure coefficient of the land at rest.

$K_{cintres}$: stiffness of the supports formed by the arches

e : Longitudinal Hanger Spacing

p_s^{cintre}: Permissible pressure in the support (hangers)

$P_s^{boulons}$: Pression admissible dans le soutènement (boulons)

K_{sb} : The stiffness of the concrete support

K_{SF} : Module de rigidité flexionnelle du soutènement.

K_p : Thrust coefficient.

K : The Volume Compressibility Module.

K_s: Stiffness of all supports/linings.

$K_{boulons}$: Stiffness of the support/lining consisting of all the point anchor bolts.

H_p : Hauteur de la surcharge de terrain uniformément répartie suivant l'horizontale.

H_t : Height of the gallery.

I : The moment of inertia of the profile.

I_s : The resistance index.

I_c : The discontinuity index.

L: The length of the bolts.

Q : Quality index (Tunnelling Quality Index).

$P_S^{béton}$: The permissible pressure in a concrete shell

$p_{S\,max}$: Maximum permissible pressure of all supports/linings.

R : Radius of excavation.

R_p : Plastic Spoke

R_i : Rayon intrados.

$e_l\ et\ e_t$: Bolt spacing in the transverse and longitudinal directions of the tunnel.

T_b : Charge admissible dans le boulon.

v_L: Le coefficient de Poisson dans la direction longitudinale.

v_T: The Poisson's Ratio in the Transverse Direction.

v_b: The Poisson's Ratio of Concrete.

λ(x) : The containment rate at a distance x from the face

γ : Le poids volumique.

φ : Angle de frottement exprimé en degrés.

Ψ: Angle de dilatance.

τ : Shear strength.

v : The Soil Poisson's Ratio.

λ_e : Rate of deconfinement at the end of the elastic phase.

$R_c,,\ \sigma_c$: Simple compressive strength of the ground

σ_1 : Major main constraint.

σ_2 : Minor main constraint.

σ_{Re} : Radial stress corresponding to the end of the elastic phase

σ_a : Permissible strength of steel

u_0 : Radial displacement at the face.

J_n : Characterizes the number of seal families.

J_r : Characterizes the roughness of joints.

J_a : Characterizes joint weathering by specifying the degree of erosion, weathering, and filling.

J_w : Hydraulic Seal Reduction Factor.

SRF : Stress Reduction Factor.

GSI: The Geological Strength

ESR : Excavation Support Ratio

List of abbreviations

R.Q.D : Rock Quality Designation.

RMR : Rock Mass Rating.

SFR : Stress Reduction Factor : specifies the state of the stresses in the massif.

ESR : Excavation Support Ratio.

AFTES : Association Française des Travaux en Souterrain.

NATM : New Austrian Tunnelling Method.

References

1   AFTES, Recommandations relatives à la caractérisation des massifs rocheux utile à l'étude et la réalisation des ouvrages souterrains, TOS, (2003).

2   *A. Marache, Comportement mécanique d'une fracture rocheuse sous contraintes normale et tangentielle, Thèse de l'École Centrale Paris, (2002)*

3   B. Damjanac., C.Fairhurst, Evidence for a long term strength threshold in crystalline rock. *Rock Mechanics and Rock Engineering,* 43, 513-531, (2010).

4   CFMR, Fondements, vol. 1 de Manuel de mécanique des roches, Presses de l'ENSMP, Paris, (2000).

5   CFMR, Les applications, vol. 2 de Manuel de mécanique des roches, Presses de l'ENSMP, Paris, (2004).

6   C. Plumelle. Théorie et pratique de la géotechnique. Exercices et applications de mécanique des sols, Le Moniteur, Paris, (2015).

7   *D.C Wyllie., Rock Slope Engineering : Civil Applications, 5th ed., CRC Press, (2017)*

8   D.M. Cruden, A theory of brittle creek in rock under uniaxial compression, *Journal of Geophysical Research,75,* 3431-3442, (1970)

9   E. Hoek, P. Marinos, Predicting tunnel squeezing problems in weak heteroge- nerous rock masses », *Tunnels and Tunnelling International,* November- December, (2000)

10 E. Hoeck Practical Roek engineering , Capilano CrescentNort h Vancouver, British Columbia

11 E. Hoek., Bray J., *Rock Slope Engineering,* 3rd ed., Institute of Mining and Metallurgy, London, (1981)

12 E.Hoek, and E.T. Brown, *Underground Excavations in Rock*, The Institution of Mining and Metallurgy, London. (1980)

13 F.D. Patton, Multiple modes of shear failure in rock, *1er Congrès de la Société Internationale de Mécanique des Roches,* Lisbonne, (1966), p. 509-513

14 F. Martin. Mécanique des roches et travaux souterrains : cours et exercices corrigés. Ed. BG Ingénieurs Conseils, ENS Cachan, France. (2012)

15 GS. Gundewar, SP. Sinha, Application of Rock mechanics in surface and underground mining.controller général indian bureau of mines, india (2014)

16 J.A Franklin, Suggested methods for determining water content, porosity, density, absorption and related properties and swelling and slake durability index properties. Int. J. Rock Mech. Min. Sci. & Geomech. Abstr., Vol. 16, No.2, pp. 141-156.4 (1979)

17 J.L. Durville et H. Héraud, Description des roches et des massifs rocheux (c352), Techniques de l'Ingénieur, Traité de Construction (1995).

18 M. Gasc Barbie et D. Huntz. La mécanique des roches appliqué au Génie Civil, Dunod, Paris , (2019)

19 M. Panet, Mécanique des roches appliquée aux ouvrages de génie civil, Presses de l'ENPC , Paris, (1976).

20 M. Panet, Le calcul des tunnels par la méthode convergence - confinement, Presses de l'ENPC, Paris, (1995).

21 M .Panet, J-P, Rotheval., Stabilité des masses rocheuses , La *mécanique des roches appliquée aux ouvrages du Génie Civil,* ENPC, (1976).

22 N. Barton , F. Løset,, R.Lien, and J. Lunde, Application of the Q-system in design decisions. In *Subsurface space,* (ed. M. Bergman) 2, 553-561. New York:Pergamon. (1980).

23 R.E Goodman., *Introduction to rock mechanics,* John Wiley & Sons, 1989.

24 Y. Guéguen, V. Palciauskas, Introduction à la physique des roches*, Hermann, (1992)

25 Z.T.,Bieniawski, *Engineering Rock Mass Classification,* Wiley, New York, (1989).

26 https://www.appstate.edu/~abbottrn/rck-id/ignchrt.html

27 https://www.studysmarter.co.uk/explanations/environmental-science/geology/rock-textures/

28 https://byjus.com/physics/igneous-rocks/

29 https://www.pinterest.com/pin/333266441194679777/

30 https://www.facebook.com/photo/?fbid=2895033333866771&set=a.309939202376210&locale=fr_CA

31 45Citation: Vásárhelyi, B.; Narimani, S.; Davarpanah, S.M.; Mocsár, G. Modeling Brittle-to-Ductile Transitions in Rock Masses: Integrating the Geological Strength Index with the Hoek–Brown Criterion. Appl. Mech. 2024, 5, 634–645. https:// doi.org/10.3390/applmech5040036

32 https://www.researchgate.net/publication/312048403/figure/fig1/AS:960304020201479@1605965728729/Schematic-representation-of-direct-shear-test-under-constant-normal-stress-CNL-a-ASTM.gif

33 https://www.fhwa.dot.gov/clas/ctip/context_sensitive_rock_slope_design/ch_5_1.aspx

34 https://en.wikipedia.org/wiki/Sea_cave

35 Underground Structures

36 https://link.springer.com/article/10.1007/s11043-023-09633-9

37 chrome-extension://efaidnbmnnnibpcajpcglclefindmkaj/http://cavescience2-cloud.bcra.org.uk/3_CaveAndKarstScience/cks095.pdf

38 https://link.springer.com/article/10.1007/s11043-023-09633-9

39 https://sciencenotes.org/types-of-rocks-igneous-sedimentary-metamorphic/

40 https://www.amnh.org/explore/ology/earth/if-rocks-could-talk2/three-types-of-rock

41 https://www.britannica.com/science/igneous-rock

42 https://www.nps.gov/subjects/geology/igneous.htm#:~:text=by%20Eva%20DiDonato.-,Introduction,it%20then%20is%20termed%20lava.

43 https://fiveable.me/introduction-geology/unit-3/bowens-reaction-series-magmatic-differentiation/study-guide/dHHPJab6fVBJzPGP   BOWNS

44 http://www2.ggl.ulaval.ca/personnel/bourque/s2/r.ign.html   CHANBRE

45 https://www.geologyin.com/2023/12/igneous-rocks.html   Métamorphique

46 https://www2.paradisevalley.edu/~douglass/v_trips/wxing/introduction_files/rocktypes.html

47 http://www.minsocam.org/msa/collectors_corner/id/rock_key.htm tableau ignous rock

48 https://www.vedantu.com/question-answer/draw-the-diagram-of-a-rock-cycle-and-explain-it-class-10-social-science-cbse-5fe98c2ea729973d3f927387   cycle rock

49 https://link.springer.com/article/10.1007/s12542-021-00598-z process of sedimentory

50 https://pressbooks.openeducationalberta.ca/practicalgeology/chapter/6-1-metamorphism-and-plate-tectonics/

51 https://commons.wikimedia.org/wiki/File:Loose_rock_in_Karwendel.jpg

52 https://home.wgnhs.wisc.edu/wisconsin-geology/karst-sinkholes/

53 http://www.chim.lu/ech1274.php

54 chrome-extension://efaidnbmnnnibpcajpcglclefindmkaj/https://staff.univ-batna2.dz/sites/default/files/baheddi-mohamed/files/chap_4_comportement_mecanique_et_critere_de_rupture_des_roches.pdf